DEGREE PROJECT

Investigations of the Transient Luminous Events with the small satellites, balloons and ground-based instruments

Safura Mirzayeva

Space Engineering, master's level (120 credits)
2022

Luleå University of Technology
Department of Computer Science, Electrical and Space Engineering

LULEÅ UNIVERSITY OF TECHNOLOGY

Julius-Maximilians-
UNIVERSITÄT
WÜRZBURG

LULEÅ
UNIVERSITY
OF TECHNOLOGY

MASTER THESIS

OF

SAFURA MIRZAYEVA

“Investigations of the Transient Luminous Events with the small satellites, balloons and ground-based instruments”

Examiners:

Prof. Dr. Sergio Montenegro, Julius Maximilian University of Würzburg, Germany
Dr. Victoria Barabash, Lulea University of Technology, Kiruna, Sweden

April 20, 2022

Co-funded by the
Erasmus+ Programme
of the European Union

space master

Abstract

The lightning is the natural source of electromagnetic radiation. It is an atmospheric electrical discharge. However, since recent times, it was discovered that there are other types of lightning besides those that are visible to the naked eye. They are called TLEs (Transient Luminous Event) and take place above the clouds during thunderstorms. Distinct classification is applied to the various existing TLEs in compliance with their shapes, size, color, altitude, origin and duration. Thus, all Transient Luminous Events are categorized to the following types: elves, spites, halos, blue jets, blue starters, gigantic jets, trolls, gnomes, pixies and ghosts. TLE investigation missions are important for several scientific purposes. They allow to gain an understanding of the lightning creation processes, contribution on global electric circuits as well as chemical influence on the Earth's climate.

TLE observations can be performed by lightning detection and location systems which differs according to their location. They can be ground-based, space-based as well as carried on aircraft or balloon. Lightning location systems in space are usually conducted on large-, medium- or micro-sized satellites.

The main scope of this thesis is to explore and describe all possible and known methods and techniques of TLE investigation as well as discussions of gained observation results for better understanding and further analysis of more suitable instruments for TLE detection mission on LEO orbit. Analysis of suitable equipment will be done according to the conclusion made from considered lightning detection systems with similar missions and pursuant to nanosatellite requirements.

Keywords: Lightning, upper-atmospheric lightning, TLE, sprite, jet, elves, halo, Lightning detection, lightning location, nanosatellite, CubeSat

Declaration of Authorship

Hereby I declare that I completed my master thesis “Initial design of the payload for CubeSat intended to detect and locate the Transient Luminous Events (TLE)” on my own and that all the information directly or indirectly taken from other sources are specified in this document. Neither this nor a similar work has been adopted or presented to another examination committee.

Baku, 20 April, 2022 Safura Mirzayeva

Acknowledgment

I want to express my gratitude to my supervisor Prof. Dr. Sergio Montenegro for his support and help in directing me to the right track, for being always ready to help despite the condition of my distant work over the thesis, thank you for being so understanding.

I would also like to thank every lecturer and teaching assistants of JMUW and LTU. Many thanks for sharing that immense knowledge with us.

I am grateful to Mr. Eckhard Thill and Ms. Heidi Frankenberger for their help in the thesis submission process.

Many thanks to Dr. Victoria Barabash for giving me another chance and supporting me in my hard times.

Furthermore, many thanks to my family for their incredible support throughout all my study.

Table of Contents

Abstract ……2
Declaration of Authorship ……3
Acknowledgement……4
List of Figures ..……....7
List of Tables……...11
List of Abbreviations ……..12

1. Chapter 1 – Introduction……15

    1.1.Thesis objective ……...15
    1.2.Relevance of the study ……16
    1.3. Outline of the thesis ……16

2. Chapter 2 – Theoretical background ……18

    2.1.Lighting phenomenon and its formation……...18
    2.2.Types of lightning ……...21
        2.2.1. Cloud to Ground (CG) ……21
        2.2.2. Ground to Cloud (GC) ……22
        2.2.3. Cloud to Cloud (CC) …….. 22
        2.2.4. Cloud to Air (CA) …….. 23
        2.2.5. Intra-Cloud (IC) …… 23
        2.2.6. Upper Atmospheric Lightning (or TLE) ……23
            2.2.6.1. Elves……..24
            2.2.6.2. Sprites……25
            2.2.6.3. Halo ……..27
            2.2.6.4. Jets……28
            2.2.6.5. Trolls, Gnomes, Pixies and Ghosts……30

3. Chapter 3 - Lightning Location Systems……33

    3.1.Space-based Observations……...33
        3.1.1. ASIM Project ……..33
        3.1.2. The THOR Experiment……35
        3.1.3. FormoSAT-2 …….. 38
        3.1.4. TARANIS ……..…..42
        3.1.5. Russian experiment programs …… 45
            3.1.5.1. Tatiana-2 ……...45
            3.1.5.2. Chibis-M ……...48
            3.1.5.3. TUS ……...50

3.1.5.4. RELEC ……52
3.2.Aircraft Observation…….54
3.2.1. EXL98 Campaign ……...54
3.3.Balloon Observations……...58
3.3.1. Nasa SPRITES'99 Campaign……..58
3.3.2. Sprite Balloon Campaign 2002-2003……...…60
3.4.Ground-based Observations...……...61
3.4.1. TLE observations in the vicinity of Israel ….……..61
3.4.2. Infrasound observations of Sprites in Israel ……63
3.4.3. High-speed video ……65
3.4.4. VLF and TLE events correlation……67

4. Chapter 4 - Lightning Location Techniques ……...69

4.1.Ground-based techniques...……..…….....69
4.1.1. Time of Arrival…….……....69
4.1.2. Interferometer …….…..71
4.1.3. Magnetic Direction Finding ……73
4.2.Space-based techniques…….74
4.2.1. Optical (OTD, LIS, GLM) ……...74
4.2.2. Electric and magnetic ……...76

5. Chapter 5 - Analysis of suitable instruments for TLE detection by nanosatellites…….…78
5.1.FireFly ……...78
5.2.LINSAT ……...80
5.3.Summary……....82

6. Chapter 6 - Conclusion ……...91

Bibliography ……....93

List of Figures

Figure 1. Charge distribution between cloud and ground. A negatively charged bottom of the cloud polarizes the surface of the earth beneath itself so that it charges positively and when conditions for electrical breakdown appear, lightning takes place [9]……..……...…….18

Figure 2. Step by step illustration of cloud to ground lightning development with time-scaling. (Uman, The lightning discharge) [15]……..….20

Figure 3. Percentagewise distribution of lightning types (V.A.Rakov) [15]……21

Figure 4. ELVES are the highest type of upper atmospheric lightning [27]……24

Figure 5. Photo of ELVES layer [27]……...……25

Figure 6. Sprite origin [28]..……..…25

Figure 7. Gamma rays, runaway relativist electrons, X rays, EM, HF and VHF emissions as a part of sprites origin [28]…….…26

Figure 8. First Color image of a Sprite, captured from an aircraft at 4th of July in 1994 [28]…….26

Figure 9. Thomas Ashcroft photographed 'jellyfish' lightning sprite from his observations in New Mexico, 289 miles away on June 23 in 2014[30]……..26

Figure 10. Image of Sprite Halo taken by Wyoming Infrared Observatory, July 28, 1998 [35]……...27

Figure 11. A pulsating blue jet recorded from space by ESA astronaut Andreas Mogensen during “Thor experiment” in September 2015 [36]……28

Figure 12. Clear Blue jet captured by pilot and photographer Thjis Bors during a thunderstorm in Australia [37]…….....29

Figure 13. Gigantic jet photographed by Phebe Pan in China on August 13, 2016 [38]…….….30

Figure 14. A Troll alongside the Sprites above the thunderstorm in Mexico captured by astronaut on the board of International Space Center [39]……..31

Figure 15. A cumulonimbus incus cloud, or so-called anvil-top shape of the cloud [40]……..…31

Figure 16. Green Ghost over red sprites captured in 2014 from the photo archives of Thomas Ashcraft. “At the time, I did not realize what I had captured,” he says [42]……..32

Figure 17. Nadir pointed ASIM on Columbus Module, International Space Station [44]……..34

Figure 18. Consecutive frames of the pulsating blue jet filmed from ISS flying over the Bay of Bengal, India at 8th of September 2015 [50]…….….36

Figure 19. Blue discharges on the top of the cloud. Left column- discharges, right column- discharges superimposed on the image of the cloud [50]……..37

Figure 20. Spite imager (left side) and spectrophotometer (right side) of the ISUAL instrument [54]……39

Figure 21. First Sprite Image captured form Space, FORMOSat-2, 2004 [51]……..39

Figure 22. Global distribution of a different kind of TLEs in the time frame (4 July 2004- 31 May 2014) [51]..……...41

Figure 23. Dependence of elves occurrence due to the sea surface temperature. 26 degree is the point of rapid increase of elves rate. …….…….42

Figure 24. Scientific payload of TARANIS [58,59,60]……43

Figure 25. Global distribution of TLEs detected by Tatiana-2 satellite during October 2009-January 2010 [204]……...46

Figure 26 (a). Geographical distribution of the TLEs with photon energy less than 51021 [203] …….49

Figure 26 (b). Geographical distribution of the TLEs with photon energy more than 51021 [203] ……49

Figure 27. Chibis-M microsatellite detected lightning activity over the world map.[82]……..49

Figure 28. Lightning discharge accompanied by ground reflection pulse allowing to calculate the height of lighting physical origin. [205] ……....49

Figure 29. Radiation at frequency 50-60 Hz and Schuman resonances (at left), Chibis-M fly trajectory over Japan. [204]……....50

Figure 30. Double Elve measured by TUS payload on April 10, 2017. Pixel map (on the left side) and oscillogram plot (on the right side) [84]…….52

Figure 31. a) and b) Short VU and IR pulses of TLE, c) long TLE events, d) TLE waveforms with predominant UV signal over IR [87]…….54

Figure 32. Gulfstream aircraft associated for EXL98 campaign where NIR and NUV were installed in the way to have sensors FOV out of aircraft windows with 0˚ to 5 ˚ elevation angle. The NIR camera (bottom right) [61]……..55

Figure 33. Images of sprites and OH Airglow captured by visible wavelength (left) and NIR (right) cameras. Airglow structure brighter and clearer on NIR image while sprites dominate in visible wavelengths image and faint in NIR one [61]…….....56

Figure 34. Best viewing geometry to catch relation between sprites tops alignment at 87 km along with OH Airglow Layer row……. 57

Figure 35. Six images of the sprite captured by six different cameras on EXL98 [61]……..57

Figure 36. Photometer current, magnetic and electric field plots and high-speed images of an event of 21st August 1999 [65]……..……..…..59

Figure 37. CCD camera images of sprites (A)-from polluted Tel-Aviv site on October 31st, 2006, (B)- from Mizpe-Ramon site on January 14th, 2006 [71]……..62

Figure 38. Pressure pulse and frequency spectrum of the sprite observed on November 9, 2012 [73]……64

Figure39. Inverted chirp signal visualization after PMCC analysis [73]……64

Figure 40. a) Distribution of sprite development phase duration, b) Distribution of sprite luminosity phase duration, c) Distribution of sprite total duration [74]……..……..……66

Figure 41. Event 1 – sprite (top left), Event - 2 elve (top right) captured on Eurosprite-2007 mission. The geographical location of VLF transmitter-receivers (top-middle). Plots of VLF perturbations of events 1 and 2 recorded on NSC, DHO and HWU receivers (bottom) [78]…….68

Figure 42. Time of Arrival geolocation method. Trilateration [92]…….70

Figure 43. Time-Of-Arrival technique. Twofold ambiguity in the case of lightning strike locations outside the triangle of three sensors (left side). Single intersect point of sensor hyperboles indicating single solution for lightning strike location. (right side) [92]……...70

Figure 44. Broadband interferometer geometry [95]…..…….71

Figure 45. Rocket triggered lightning captured by the camera on the left panel and its VHF interpretation image on the right panel [96]……..72

Figure 46. Magnetic Direction Finding technique geometry [100]…….73

Figure 47. Two sinusoidal error function of a magnetic direction finder sensor [101]……74

Figure 48. OTD and LIS projects' short description and coverage areas [103]……76

Figure 49. Working principle of OLD instrument on board of FireFly CubeSat [109]……...79

List of Tables

Table 1. Technical characteristics of the camera used for THOR experiment [48]…….35

Table 2. Review of the achieved results in the THOR experiment' classified by target type and date [48] ……36

Table 3. Number of ELVES, Sprites, Halos, Blue Jets and Gigantic jets detected by FORMOSat-2 in 10 years (4 July 2004- 31 May 2014) [54]…….40

Table 4. EXL98 Campaign instruments carried on the board of Gulfstream II [61]..……....55

Table 5. Two winter observation review of TLE in the vicinity of Israel [71]……..……62

Table 6. Optical instruments explored in different TLE observation missions and their main parameters…….....84-85

Table 7. List of photometers, spectrometers and DUV detectors from TLE detection missions and their parameters.....88

Table 8. RF instruments used in previously described missions and their main parameters.....89

Table 9. Advantages and disadvantages of optical and RF systems [111] 90

List of Abbreviations

ASIM	Atmosphere-Space Interaction Monitor
ATD	Arrival Time Difference
AWESOME	Atmospheric Weather Electromagnetic System for Observation, Modeling and Education
CA	California
CC	Cloud-to-Cloud lightning
CG	Cloud-to-Ground lightning
CNES	National Center for Space Studies
CT	Cloud Turret
CTT	Cloud Top Temperatures
DFT	Discrete Fourier Transform
DOY	Day Of Year
DMI	Danish Meteorological Institute
DTU	Danish Technical University
EAS	Extensive Air Showers
EF	Exposure Facility
ELF	Extremely Low Frequency
ELVES	Emission of Light and Very Low Frequency perturbations due to Electromagnetic Pulse Sources
EMP	Electromagnetic Pulse
ESA	European Space Agency
ESR	Experiment Scientific Requirements
FOV	Field of View
GHOST	Green emissions from excited Oxygen in Sprite Tops
GLIMS	Global Lightning and sprIte MeasurementS
GLM	Geostationary Lightning Mapper
GOES	Geostationary Operational Environment Satellite
GRD	Gamma Ray Detector
GSFC	Goddard Space Flight Center
GW	Gravity Wave
IC	Intra-Cloud lightning
IDEE	Instrument for the Detection of the Energy Electrons
IHY	International Heliophysical year
IME-BF	Instrument for Electric field Measurements – Low frequency
IME-HF	Instrument for Electric field Measurements – High frequency
IMM	Instrument for Magnetic Measurements
INPE	Instituto Naciola de Pesquisas Espaciais
ISS	International Space Station
LDS	Light Detection System
LIS	Lightning Imaging Sensor

LLS	Lightning Location Systems
LLTV	Low-Light (Level) Television
LPATS	Lightning Position and Tracking System
LPCE	Laboratoire de Physique et de Chimie de l'Environnement
LSI	Lightning and Sprite Image
MAPMT	Multi-Anode Photo-Multiplier Tube
MCP	Micro Cameras and Photometers
MDF	Magnetic Direction Finder
MIR	Medium InfraRed
MLE	Mesoscale Lightning Experiment
MMIA	Modular Multispectral Imaging Array
MXGS	Modular X- and Gamma- ray Sensor
NASA	National Aeronautics and Space Administration
NCKU	National Cheng Kung University of Taiwan
NFS	National Science Foundation
NIR	Near InfraRed
NLDN	National Lightning Detection Network
NSPO	National Space Program Office / National Space Organization
NSBF	National Scientific Balloon Facility
NUV	Near UltraViolet
OH	Hydroxyl
OLD	Optical Lightning Detector
OTD	Optical Transient Detector
PH	Photometer
PMCC	Progressive Multi-Channel Correlation
RSI	Remote Sensing Instrument
SDM	Short Duration Mission
SFERIC	radio atmospheric signal
Sprite	Stratospheric Perturbations Resulting from Intense Thunderstorm Electrification
TAU	Tel Aviv University
TARANIS	Tool for Analysis of RAdiation from IightNing and Sprites
TGF	Terrestrial Gamma Flashes
TOA	Time of Arrival
TLE	Transient Luminous Event
TROLL	Transient Red Optical Luminous Lineaments
TRMM	Tropical Rainfall Measurement Mission
UHCER	Ultra-High Energy Cosmic Rays
UFO	Unidentified Flying Object
UTC	Universal Time Coordinates
VAFB	Vandenberg Air Force Base
VHF	Very High Frequency
VITF	VHF Interferometer

VLF	Very Low Frequency
VLFR	VLF Receiver
WWLLN	World Wide Lightning Location Network
XGRE	X-ray, Y-ray and Relativistic Electron experiment

Chapter 1- Introduction

1.1 Thesis objective

Recently discovered geophysical phenomena called Transient Luminous Events (TLE) are brief optical electrical discharges that occur in the upper atmosphere and associated with an underlying active thunderstorm. Duration of these phenomena varies anywhere from a few milliseconds up to a maximum of 2 seconds. That short-lived luminous emissions are connected with electrical discharges of "ordinary" lightning ongoing inside and under the thunderstorm [1].

There have been a number of reports about such phenomena observed by pilots for many years until it was proved photographically. At the night of July 6, 1989, when researcher Dr. Robert Franz left low-light television camera filming the sky overnight first serendipitous video record of TLE event in the mesosphere was captured [2]. Another video recording of Transient Luminous Events were taken on the board of Shuttle Mission STS-34 carrying out Mesoscale Lightning Observation Experiment in 1989, October 21. Nowadays, the global rate of recordings of TLE taken all over the globe from both ground and space observations exceeds several million events yearly [3].

Since that, a lot of optical recordings together with another different type of scientific investigations followed studying these phenomena with growing intensity. Due to that intense effort, morphology and phenomenology, as well as generation dependence of TLE, became a well-investigated phenomenon with the help of observational and theoretical literature since the mid-90s [4].

All that knowledge about TLE was gained through observations performed on Lightning Location Systems (in particular TLE Location Systems) and the researches were done on the base of the data collected there. These systems vary in compliance with the aspect of where the observations were performed: on the ground, in air, or in space. Space-based lightning detection and investigations were performed or ongoing on the boards of large, medium and at least micro-sized satellites, and even a smaller number of similar missions performed by nanosatellites.

The main objective of this thesis is to investigate and analyze different type of instruments, which were used during ground based, from air and in space-based missions necessary for TLE observation and exploration. Furthermore, discussions and analysis of existing well-known Lightning Location Systems (LLS) and techniques of TLE investigation are provided according to the obtained results.

The majority of the LLS exploited till nowadays are very expensive, complex in terms of equipment and large-scale in respect of coverage area and mission life duration projects. In addition, review of CubeSat applicable

instruments according to the low cost, low mass, low power, low volume requirements are provided. With this in mind, analyzed parameters of instruments explored in listed LLS systems are used to recommend the proper equipment suitable to CubeSat for TLE detection mission implementation.

1.2 Relevance of the study

Data collected during TLE research missions can be used in different scientific fields. TLE observations provide with a better understanding of lightning nature, like kinetic physics of processes creating the lightning discharge. Regional effects of it to the atmosphere also can be studied as well as a contribution to the global electric circuit. For example, gigantic jets and sprites are the luminous events which are highly energetic and can transfer a significant amount of negative or positive charge respectively [5].

As TLE is an electrical activity the investigation of it allows to gain an understanding of its chemical influence to the climate of the Earth. Furthermore, the concentration of greenhouse gases influenced by blue jets which prove another reason to study events occurring on the tops of the thunderstorm, as radiation balance are more effected by greenhouse gasses lying on higher altitudes rather than by near the Earth's surface gases [6].

Worldwide effect of TLE lightning can be derived from analysis of perturbations of ozone and NOx concentrations. Dust storms produced by volcano eruptions, fires in the forest and dust storms are also affects lightning [7].

1.3 Outline of thesis report

Chapter 1 introduces the thesis objectives and underlines the necessity of razing that theme. The importance of investigating of TLE and its application is emphasized.

Chapter 2 presents the theoretical background of lightning, to its formation structure as well as to its types and special attention is paid to the description of the TLE variations: sprites, elves, halos, blue jets, blue starters, gigantic jets, trolls, gnomes, pixies and ghosts.

Chapter 3 outlines different lightning location systems according to the location of the observer: space-based observations from the satellites, on the board of aircraft monitorings, observations with the help of balloon and ground-based lightning monitorings are described in detail. Moreover, the results achieved on that LLS are illustrated.

Chapter 4 highlights ground and space-based lightning locations techniques used till now in different LLS and are tent to be used in future.

Chapter 5 provides analysis of all the instruments previously used in listed similar missions for TLE investigation, as well as, emphasizes their technical requirements and necessary spectra of parameters, which are critical for fulfilling the nanosatellite mission conditions.

Chapter 6 follows with the whole thesis conclusion.

Chapter 2 - Theoretical background

2.1 Lightning phenomenon and its formation

Since ancient times, lightning has been an object of interest and nowadays it is one of the most unexplored natural phenomena. Despite the perception of lightning as a manifestation of higher forces, nevertheless, already in ancient times, certain patterns were revealed in the defeat of objects by lightning. In the middle ages, people noticed that temples located in elevated places played the role of lightning rods and so they did not build houses above this temple in order to protect them from fires. A great leap in the study of lightning was given by the development of sailing. In addition, it was the seafarers who were the first to notice that before the thunderstorm there were phenomena similar to those that arise when electrifying wool from friction [8].

Lightning is an electric spark discharge in the atmosphere which usually can occur during a thunderstorm, accompanied by a bright flash of light and thunder.

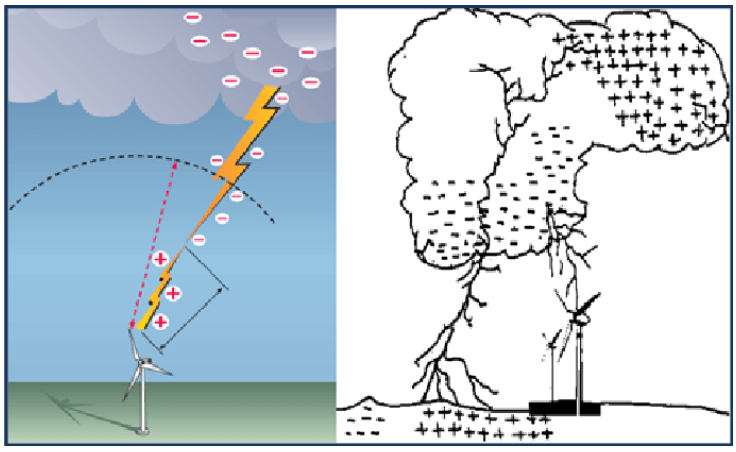

Figure 1. *Charge distribution between cloud and ground. A negatively charged bottom of the cloud polarizes the surface of the earth beneath itself so that it charges positively and when conditions for electrical breakdown appear, lightning takes place [9].*

Discharges can form only under certain conditions. Inside a thundercloud, air masses travel at great speed. They carry the particles of water that are in the cloud into motion when the air masses rub against a drop of water, static electric discharges occur. Scientists have found that the top of a thundercloud is charged positively, and in the lower part, there is an accumulation of negatively charged particles (Figure 1). The earth always has a positive charge. Negatively charged

particles of the cloud want to rush to a positively charged earth but this does not occur constantly, since the earth's surface and the cloud share a large layer of air, which isolates the discharges from each other. Charges can separate air only when they reach a certain power. When enough power is accumulated in a thundercloud of a negatively charged particle, they rush to the ground, forming huge sparks in the form of lightning. When lightning strikes the ground, we manage to notice only one flash; in fact, in this visible flash, there is a discharge of about ten strikes. Negatively charged particles fly so quickly to the ground that several lightning strikes are perceived into one [8], [10].

As it known, a lightning strikes to highest places. This is because the positive charge of the earth's surface always accumulates on the peaks, so the first lightning always hits the tallest buildings or trees that are located alone on the plain.

The lightning discharge is accompanied by the release of enormous heat, the temperature of lightning can reach 30,000 degrees. The current in the lightning discharge reaches 10-500 thousand amperes, voltage - from tens of millions to a billion volts. Discharge power - from 1 to 1000 GW.

For lightning to occur, in a large part of the cloud, there must be a field with an average intensity that will be enough to support the discharge that has begun (~ 0.1-0.2 MV / m), while in the smaller part of the cloud there must be enough tension to start electrical discharge (~ 1 MV / m) [8].

The process of forming lightning consists of several stages. The first stage is the start of impact ionization. It is created by free charges, which under the influence of an electric field acquire significant speeds and collide with the air molecules and ionize them.

The start of lightning begins from highly energetic particles which generate runaway breakdown. Thus, how the air breaks down into narrow electrical paths called **streamers**. That well-conducting channels that when merged, give start to a bright channel with high conductivity called the **stepped leader** (or bi-leader) [11].

As its titles suggest, the movement of the leader towards the Earth surface takes place in several steps with the speed approaching 50 000 km/s with the following stops and repeats of movement [8].

While the stepped leader propagating down to the Erath’s surface, the electrical field at its tip increases and reverse directed connecting discharge is generated from the high ground places right under the stepped leader. They get connected at the height of several meters above the ground. This principle is used in lightning rods to have control over the lightning hit point [12].

On the next stage after stepped leader discharged the **returned stroke** moves by the leader ionized channel with some additional branches around it. This movement is directed from the ground up to the cloud. That stroke produces the highest luminosity, thunder and containing temperature from 20000 to 30000 degree of C. It is fast enough so the human eye sees all the path brightened

simultaneously. The current of the lightning channel can reach up to 100kA. The length of the return stroke is within the range of 1 to 10 km, the diameter of the channel is several centimeters [13], [14].

However, the cloud may not completely discharge after the first leader. In that case, provided sufficient charge at high altitudes of the cloud will start a new stroke called **dart leader** moving along the channel of the return stroke. Lightning can have several repeated strokes or can reach twenty or thirty discharges while the duration of lightning can last 1-1.5 seconds. Dart leaders contain less charge than stepped leaders but they can form a new channel for one or more ground impacts [14].

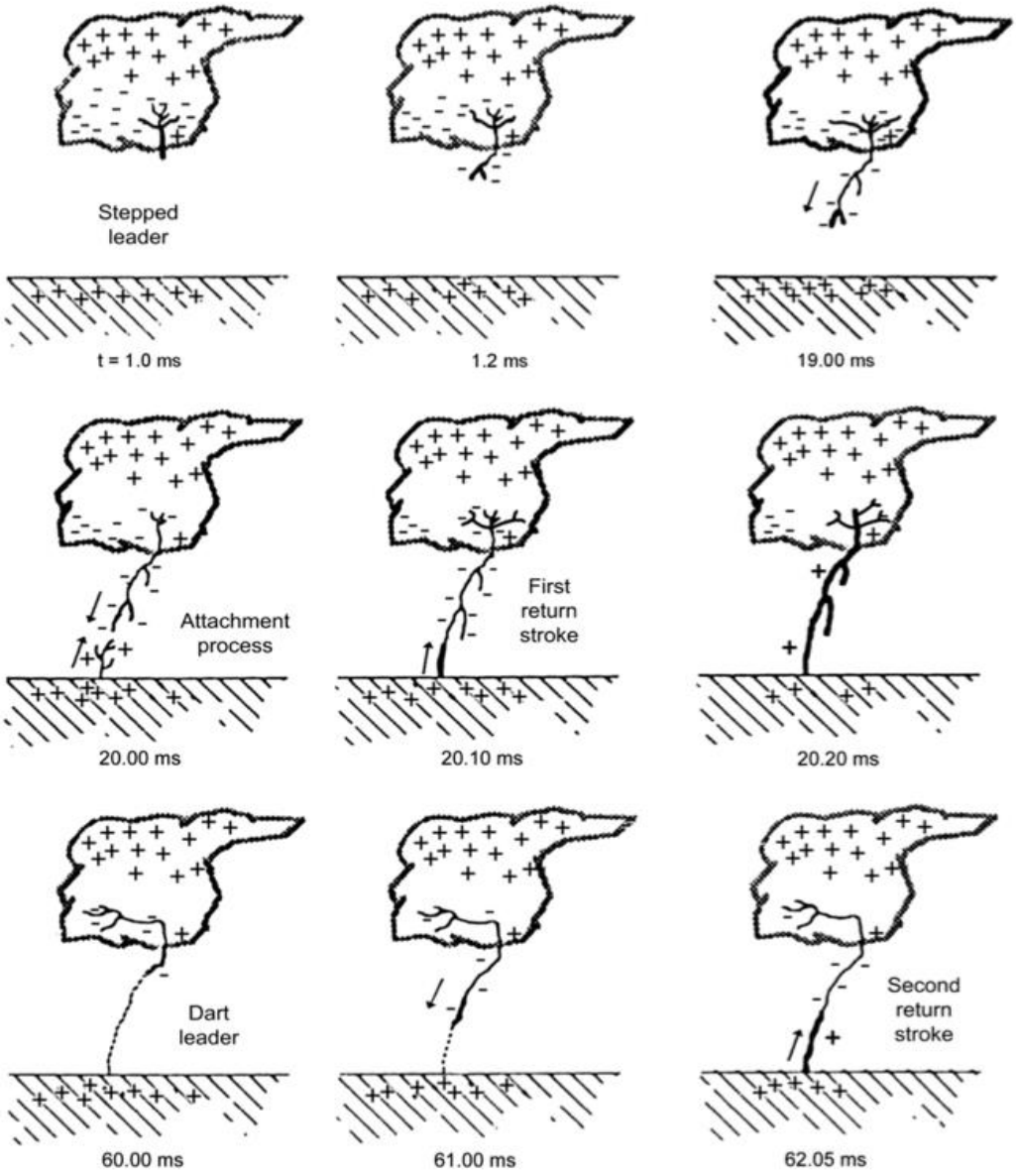

Figure 2. Step by step illustration of cloud to ground lightning development with time-scaling [15].

2.2 Types of lightning

Since the main topic of this work is the study of methods for detecting a special type of upper atmospheric lightning or so-called TLE (Transient Luminous Event), the main attention will be paid to the description of this lightning, however, TLEs are generated from “original” types of lightning occurring inside and below the clouds.

Lightning can be divided into five main large groups:

- Cloud-to-Ground lightning (CG),
- Ground-to-Cloud lightning (GC)
- Intra-Cloud lightning (IC),
- Cloud-to-Cloud lightning (CC)
- Cloud-to-Air (CA)

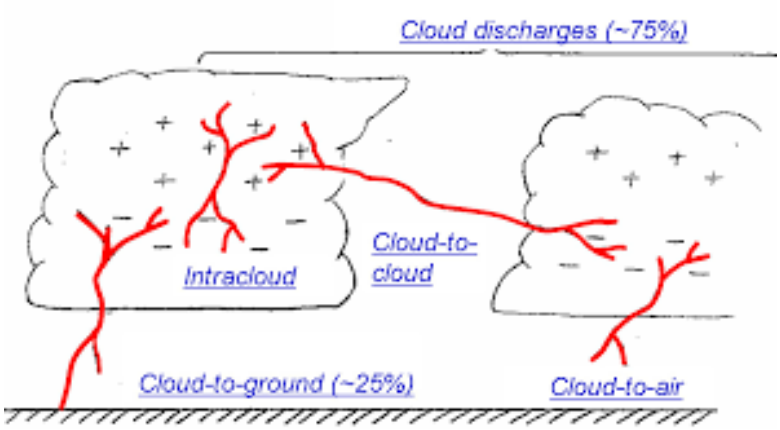

Figure 3. Percentagewise distribution of lightning types [15].

However, each of them branches into subgroups. Among all these groups the cloud-to-ground lightning (CG) is better studied and investigated group.

2.2.1 Cloud-to-Ground Lightning

It is an electric discharge originated in the cloud and ascending down to the ground. There are two kinds of cloud-to-ground lightning, negative and positive with corresponding abbreviations “-CG” and “+CG”. Negatively charged CGs lightning are more common events for everyday nature events like storms rather than the positively charged CG. The main difference in the occurrence of these two types of lightning is the opposite sign of the stepped leader passing downward from the cloud to the Earth surface.

Negative cloud-to-ground lightning has another identifying feature. When propagating downward negatively charged stepped leader has more characteristic branches also directed down, except for the close to the ground part of the leader

where branches are ascending. Whereas, positively charged stepped leaders of positive CGs determined as the leader with almost no branches around. Branches of this leader may appear at high altitudes but barely will occur near the Earth surface [16].

Negative and positive cloud-to-ground lightning also differ in the number of return strokes they consist of. Negative CGs usually have several return strokes while the positive CGs is composed of only one return stroke. These pulsing return strokes that fill the channel with the bright flashes. The return stroke of the positive charged cloud-to-ground lightning gives the brightest and the most intense flash so for the most photographers it is problematic to capture them. The only first return stroke of negative CGs has branches around and that branches illuminated just ones. Usually positive CGs accompanied by a very loud thunder which sounds like low-frequency booms. Bolt from the Blue, Bread Lightning and Ribbon Lightning are examples of CG type lightning [17], [21].

Bolt to Blue Lightning – lightning strike that starts from the cumulonimbus thundercloud, propagates horizontally for a long distance and then abruptly drops down to the Earth surface. This lightning can reach the ground in the areas where already thunderstorm is passed away and the blue sky is overhead [18].

Bead Lightning – very rare type of lightning that developed as a result of an extremely fast cooling process in different parts of the lightning channel, which forms usual lightning into dotted line [19].

Ribbon Lightning – is the type of lightning when several duplicated return strokes propagate downward strictly parallel to each other but slightly shifted to the side. It was assumed that the displacement occurs due to weather conditions, in particular, because of strong wind [19].

2.2.2 Ground-to Cloud Lightning

This is a discharge passing upward between a terrestrial object usually located on the tallest point (skyscrapers, tall towers) and a thundercloud. The tops of those objects becoming the best points where accumulated electrostatic charge can break through the air gap and reach the bottom of the cloud. The taller the object, the higher the probability for it to be struck by lightning. The polarity of Cloud-to-Ground lightning also can be either negative or positive [16], [22].

2.2.3 Cloud-to-Cloud Lightning

When lightning discharge appears between two or more separate clouds and concurrently does not reach the Earth surface it is called cloud-to-cloud or Inter-cloud lightning (not to confuse with Intra-cloud lightning) [18].

Anvil Crawler lightning (also called Spider lightning or Rocket Lightning) is a typical example of a cloud-to-cloud type of lightning. Anvil Crawlers are long-distance horizontally propagating discharges easily visible to the human eye. Too long leader of Anvil Crawler may separate to several two-directional. Its tree-like leader usually takes place in high altitudes so the sound of its thunder reaching the observer is quite soft. Occasionally, Anvil Crawlers can also appear as a part of cloud-to-ground lightning or may independently occur within a single cloud [16], [20].

2.2.4 Cloud-to-Air Lightning

Cloud-to-Air lightning can be described as a lightning flash which starts from the storm cloud as a normal cloud-to-ground strike but terminates in the air far before reaching the Earth. In general, it can be said that side branches of the leader are cloud-to-air components of the cloud-to-ground lightning [16], [23].

2.2.5 Intra-Cloud Lightning

Inter-Cloud Lightning one of the most common types of electrical discharges forming between differently charged regions of the single cloud. Usually, they appear between the upper anvil area and the bottom of the storm cloud [18].

Sheet Lightning is CC type discharge taking place too far away from the Earth surface deep inside of the cloud so for the observer it can be seen only in the form of totally either partially illuminated cloud without any sharp channels [20].

2.2.6 Upper Atmospheric Lightning (or TLE)

Upper atmospheric lightning is also called ionospheric lightning however mostly recognized as Transient Luminous Events due to the absence of some usual tropospheric lightning's characteristics. Thus, TLEs are the class of secondary phenomena of optic electrical discharges that occur in upper regions of the atmosphere above large thunderstorms.

Existing TLEs are categorized in compliance with their shapes, size, color, altitude, origin and duration into various groups: elves, spites, halos, blue jets, blue starters, gigantic jets, trolls, gnomes, pixies and ghosts. Each of these types will be separately described below [3].

2.2.6.1 ELVES

ELVES (Emission of Light and Very Low Frequency perturbations due to Electromagnetic Pulse Sources) are the type of phenomena representing fast-expanding doughnut-shaped optical and ultraviolet emission appeared as a result of the propagation of on electromagnetic pulse from a positive or negative lightning strike. The diameter of the elves may reach 400km [27].

This red hue colored conical glow occurs at the height of around 100km in the ionosphere right above the clouds of an active thunderstorm and last less than 1ms [26].

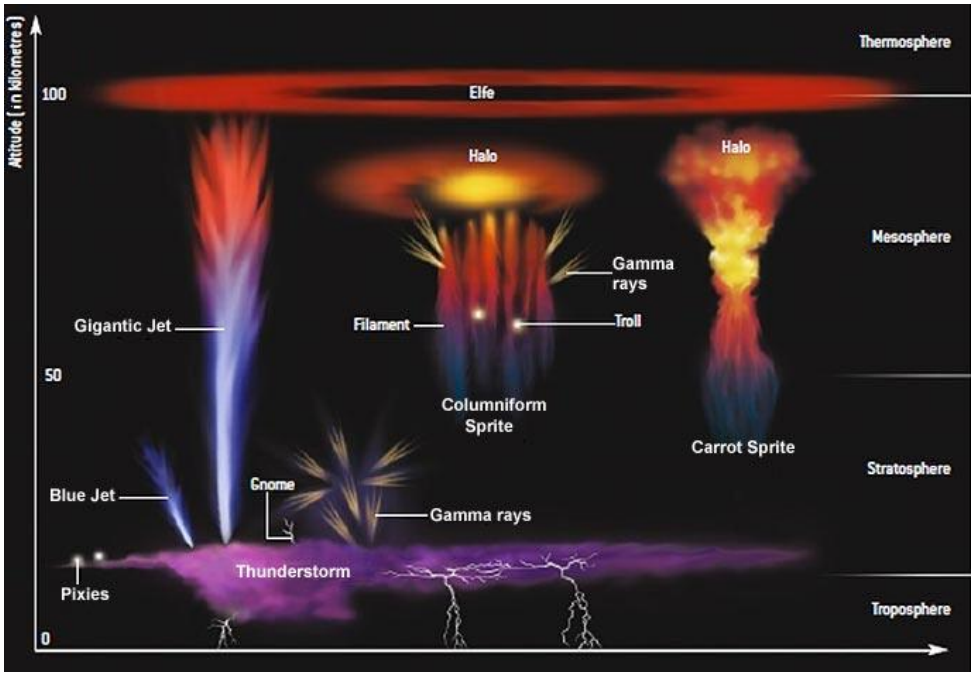

Figure 4. Elves are the highest type of upper atmospheric lightning [27].

The prerequisite condition for the Elves' visibility may be represented as the release of millisecond impulses of gamma-rays in the high electric fields produced right after the lightning leader and milliseconds before the lightning bolt [24].

Despite the differences in the process of formation of elves and sprites, the appearance of sprites may be accompanied by elves.

Unusual abbreviation of elves is associated with the process of light formation as a result of the excitation of nitrogen molecules.

The first time the images of elves were captured in the late ‘80s –early ‘90s. Later in 1992 elves was recorded with a low-light video camera as a subject of Mesoscale Lightning Experiment (MLE) on the board of Space Shuttle [3], [29].

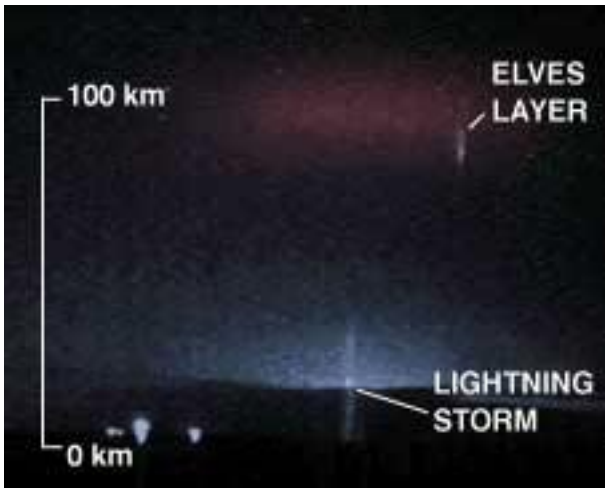

Figure 5. Photo of elves layer [27].

2.2.6.2. SPRITES

Sprites (Stratospheric/Mesospheric Perturbations Resulting from Intense Thunderstorm Electrification) are a massive luminous form of electrical discharges produced in the upper atmosphere directly above the thunderstorm system. They are generated specifically by discharges of powerful cloud-to-ground (CG) positive lightning strokes [34].

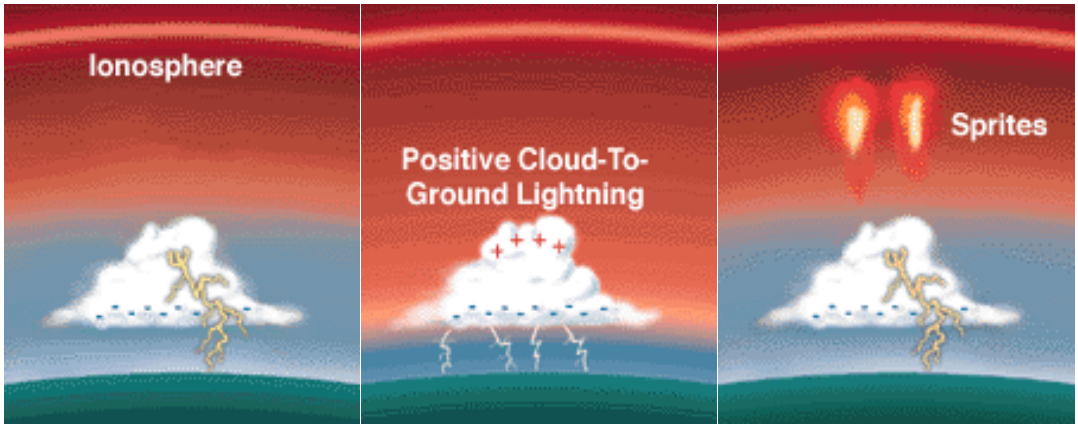

Figure 6. Sprite origin [28].

These bursts of electricity usually start at an altitude of 50 kilometers till almost 95 kilometers. The color of this phenomenon can be described as a smooth gradient from blueish to predominantly reddish streams which may be accompanied with dim red halo (see section Halo) on the top. At the range of 65-75 kilometers the sprite has its most intense glow, over which there is a usually dim red structure that spreads vertically till the edge of mesosphere while blue

fibrous structured streams of sprites extend till 30 kilometers down. [26], [28], [34].

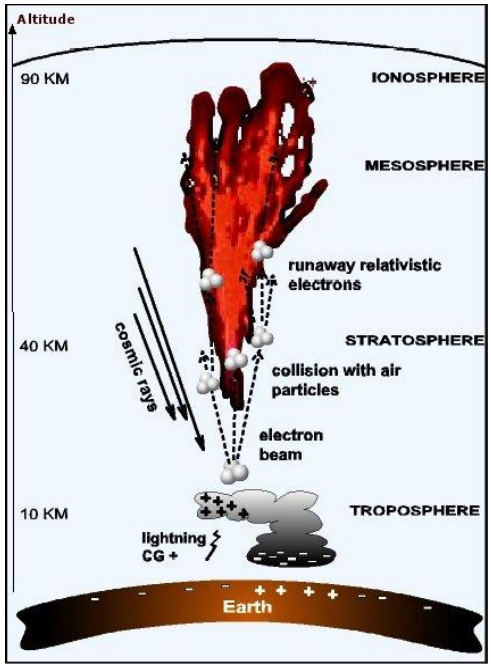

Figure 7. Gamma-rays, runaway relativist electrons, X rays, EM, HF and VHF emissions as a part of sprites origin [28].

Visual forms of sprites are differently described like giant jellyfish or like crowns of carrots or downward firework. Sprites are huge however weak flashes what makes them almost invisible at day time. High-speed red-sensitive camera and black clear sky is necessary to record them.

First photographic evidence of sprites existence was captured accidentally on low-light level television camera in 1989 by the scientist from Minnesota. [3], [34].

Figure (left) 8. First Color image of a Sprite, captured from an aircraft at 4th of July in 1994 [29].
Figure (right) 9. Thomas Ashcroft photographed 'jellyfish' lightning sprite from his observations in New Mexico, 289 miles away on June 23 in 2014 [30].

2.2.6.3. Halo

Halo (also called sprite-halo) is upper-atmospheric optical emissions which usually (but not always) precedes to the sprite formation. Sometimes Halos are mistaken for elves as they very similar visually, both are disk- shaped glow. Nevertheless, they differ in some characteristics. Halos lifetime can vary between 3 to 6 that is much longer than elves' duration (less than 1 ms) which makes them almost imposable to be observed by standard video rate but halos can be easily captured by that imagers [31]. Halo occurs on the lower altitude than elves around 80 km and has a smaller horizontal diameter of about 65km [32]. Unlike sprites, both elves and halos can be initiated with either negative or positive discharges [33]. Identical physical processes initiate sprite and halo production, however, because of weak ionization halo does not form streamers like sprite do [34]. In figure 10 below can be seen the image of sprite halo observed from Wyoming Infrared Observatory at July 28, 1998. According to the report of NLDN (National Lightning Detection Network) that image corresponds to the multiplicity of two positive lightning discharge at a distance of 762 km away from observation place [35].

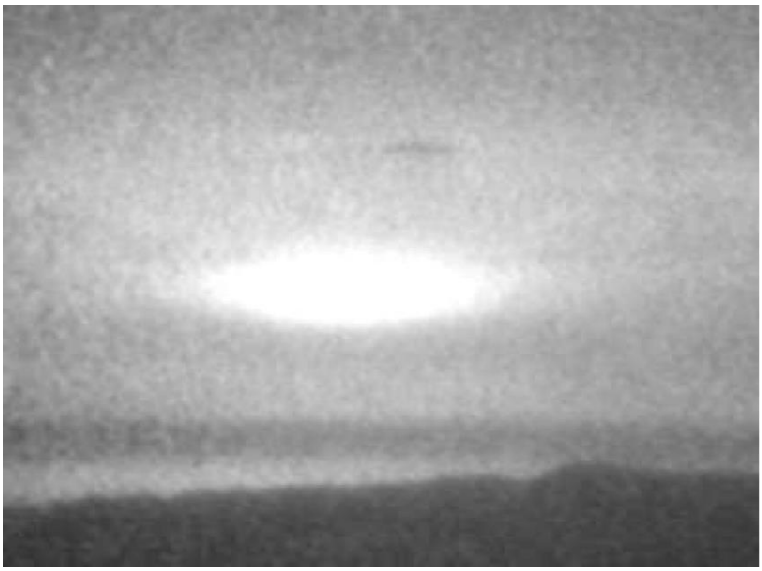

Figure 10. Image of Sprite Halo taken by Wyoming Infrared Observatory, July 28, 1998 [35].

2.2.6.4. JETS

One of the most illustrative types of transient luminous events occurring in the upper atmosphere is Jets. They can be classified into three main groups:

- Blue Jets
- Blue Starters
- Gigantic Jets

Blue Jets are optical cloud-to-air ejections initiated from the top of the tropospheric regions of thunderstorms. They were first time captured by monochrome video on the board of Space Shuttle while it was flying over Australia on 21st October 1989. [3], [26]

In comparison with the other types of TLE (even though they are generated by tropospheric lightning), jets are the only type which electrically connected to tropospheric lightning but not necessarily associated with the cloud-to-ground(CG) type of lightning.

Blue jets are generally considered to be triggered between a positively charged upper region of the thunderstorm and a negatively charged "screening layer" which lays above it. Positive leader discharges the negatively charged "screening layer" before the negative leader discharges the positively charged upper region. As a result, one can see the positive leader leaves the thundercloud and spreads upward [3], [22].

They propagate upward in the shape of conical jets of bluish tinge and near-ultraviolet light with about 15-degree inclination to the side. The altitude they reach is between 40 to 50 km [3].

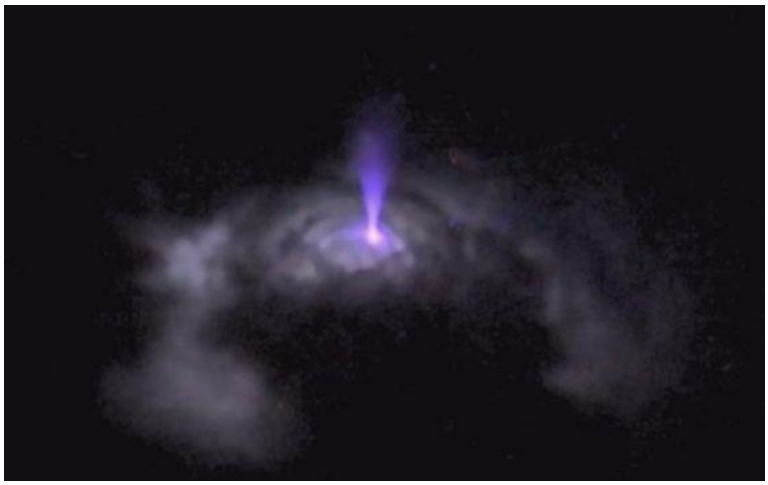

Figure 11. A pulsating blue jet recorded from space by ESA astronaut Andreas Mogensen during "Thor experiment" in September 2015 [36].

Blue Jets are much brighter than sprites however less frequent. They usually occur in the highest points of the very active thunderstorms and linked with severe weather like strong hail.

They speed up to 100-120 km/s which makes their life time very short and last only for a quarter of a second, nevertheless, jets are visible by the human eye [27].

Figure 12. Clear Blue jet captured by pilot and photographer Thjis Bors during a thunderstorm in Australia [37].

Blue starters were first time filmed in 1994 during a flight over thunderstorm. Blue starters are the shorter version of blue jets as the main difference between them is the altitude they can reach (from 17 km to 25.5 km). Another difference is brightness, blue starters are much brighter. They can even be considered as incomplete blue jets. “Blue starters appear to be blue jets that never quite make it” – quote of Dr. Victor Pasco, professor of electrical engineering [3].

Gigantic jets, as the name implies, are the huge version of blue jets. They are the rarest and at the same time the tallest (up to 80-90km) kind of lightning which ever were discovered in the world. September 14th of 2001 was the date when American researchers from Arecibo Observatory for the first time photographed the gigantic jet reaching the altitude of 70 km above the thundercloud [3], [27].

In contract to blue jets, gigantic jets initiated between positively charged upper and negatively charged lower zones of the thundercloud [3].

The color and the shape of the gigantic jets' bottoms appear similar to the blue jets' however their tops look more like red carrot-shaped sprites which propagate upward [26].

Figure 13. Gigantic jet photographed by Phebe Pan in China on August 13, 2016 [38].

2.2.6.5. Trolls, Gnomes, Pixies and Ghosts

Trolls

In the process of a detailed study of such a phenomenon as a Sprite, technological improvements were applied to the previously used video cameras. This, in turn, led to the discovery of new details of the studied area previously unknown to the science. Application of faster cameras allowed to identify a new type of TLE called TROLL (Transient Red optical Luminous Lineaments) which looks like a collection of red spots near the top of the active thundercloud and has reddish tail-shaped streamers directed upward like blue jets. The formation of TROLLs can only be observed after a very strong sprites [3].

Watching the video recording of the troll in the slow motion, it is possible to notice that the troll consists of a series of events that originate in the tendril of the sprite with a following drop-down action and each subsequent event starts above the previous one, which ultimately looks like upward blur [39].

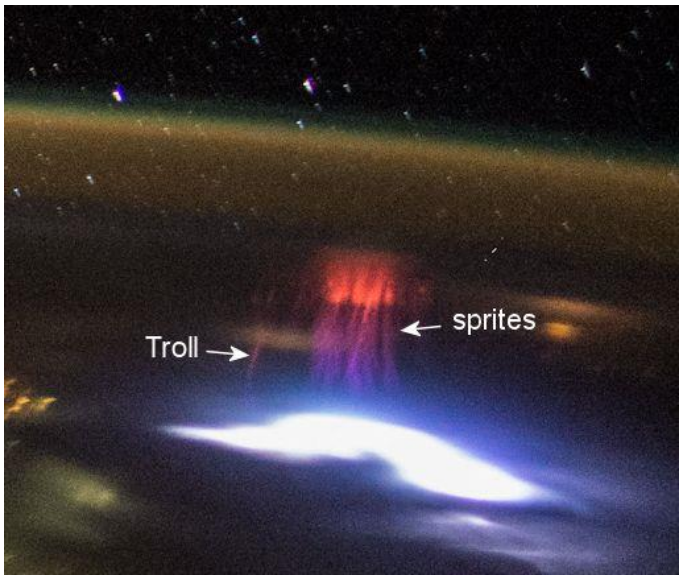

Figure 14. A Troll alongside the Sprites above the thunderstorm in Mexico captured by an astronaut on the board of International Space Center [39].

Gnomes

When the thundercloud reaches stratospheric stability level at its mature stage it forms characteristic flat shape - cumulonimbus incus also called as an anvil cloud. Small and very short spikes of light directed upward from that cumulonimbus cloud's top are called Gnomes. They are only 1 kilometer short in height, 200 meters in wide and last no more than several microseconds. The reason for their occurrence is in the process of pushed up moist air from the top of the cloud by strong updrafts [3].

Figure 15. A cumulonimbus incus cloud over Africa, or so-called anvil-top shape of the cloud , February 5, 2008 [40].

Pixies

Pixies are randomly flashing luminous events scattering at the domes of the thunderstorm. They are white colored pinpoints of light lasting no longer than 16 milliseconds each and have less than 100 meters across. (See Figure 4). Participants of the STEPS programme (field programme that exploring electrical characteristics of regions over thunderstorms) were the first who observed these lights in the summer of 2000. That was a series of lights which they witnessed for over 20 minutes [3], [29].

Ghosts

A video recording by a professional photographer of thunderstorm Pecos Hank together with TLE photographer Paul Smith on May 25, 2019, for the first time, captured another previously unexplored phenomenon that was named as Ghost (Green emissions from excited Oxygen in Sprite Tops) [41].

The Ghost is a green glow, barely noticeable even on the camera, which forms immediately after the red sprite and disappears in milliseconds. Since this discovery is very recent, the nature of Ghost phenomenon has not yet been described in any scientific work. However, there are hypotheses that the origin of it may be the same as the origin of the aurora borealis, namely, explanation of the green light glow as a result of the excitation of oxygen atoms [42].

Figure 16. Green Ghost over red sprites captured in 2014 from the photo archives of Thomas Ashcraft. "At the time I did not realize what I had captured," he says [42].

Chapter 3 - Lightning Location Systems

Last 80 years have become fundamental for the progressive development in various technological areas that have led to the creation of modern Lightning Location Systems (LLS). Lightning activity is monitored by several ground-, air- and space-based LLS in the all corners of the globe. Nowadays, there is a huge variety of lightning detection and location systems developed worldwide. In this chapter, the most valuable projects of TLE detection systems will be described.

3.1 Space-based Observations

3.1.1 ASIM Project

ASIM (Atmosphere-Space Interaction Monitor) mission was successfully launched on 2nd April 2018 by a SpaceX Falcon9 rocket in a SpaceX Dragon spacecraft from Cape Canaveral at Kennedy Space Center in Florida with further mounting on the Columbus module of the International Space Station (ISS) [43].

ASIM is an international project implemented by the European Space Agency (ESA) and a number of partners responsible for different managements. Danish Technical University (DTU) is responsible for scientific leadership. Therma (Danish Aerospace company) is the head contractor, which has constructed ASIM, leading the technical part of the mission. Danish Meteorological Institute (DMI) helping in providing a scientific interpretation of collected data. Major partners included such organizations as University of Bergen (Norway) which provides the software for instruments calibration, University of Valencia (Spain) which supplies with software calculating the TGFs' angle of arrival, Space Research Center (Poland), OHB (Italy). Eventually, the number of participants in this project exceeded 80 research associations from over 30 countries [43].

This mission pursued a long list of goals. ASIM is created to observe lightning flashes in the upper atmosphere above the violent thunderstorms and to measure X-ray high-energy radiations coming from them. Those investigations will give the new insight for better understanding of how chemical and electrical activities influence the planet's climate and how to reduce uncertainty and improve it. Also, new ASIM observations are aimed to help researchers to study stratospheric thunderstorm activity like sprites, elves and jets. Furthermore, ASIM's instruments provide an opportunity to investigate meteors, Northern Lights, water vapor, clouds and their interplay.

Figure 17. Nadir pointed ASIM on Columbus Module, International Space Station [44].

One year data from ASIM gave to the researchers a new understanding of the invisible and visible processes that create and drive the lightning above the thunderstorms, so-called terrestrial gamma flashes (TGF) and transient luminous lightning (TLE). These flashes appear as a result of the connection of gamma-ray bursts with high-energy X-rays accompanied by lightning and thunderstorm [45].

ASIM is attached outside of the ISS (400km) to the Columbus model with the nadir view to the Earth, which is the ideal place to monitor the thunderstorms up to 100 km from the Earth's surface. It catches main thunderstorm region with the latitude degree +/- 51.6 [46].

ASIM is designed with different instruments on board. One of them is intended for measuring the Gamma-ray bursts (TGFs) from a thunderstorm. ASIM is the first mission where such kind of device is used in space. The instrument is called Modular X- and Gamma-ray Sensor (MXGS) under the lead of DTU Space and is headed by DTU Space [45].

MXGX consists of two sensors which measure the photons' energy in the range from 20 keV to 20 MeV and time of their arrival (milliseconds). Angle measurement between the photon busters and the sensor gives the instrument the ability to locate the thunderstorm that is emitting these photons [45].

Another instrument is optical and dedicated for observation of visual high-altitude electrical discharges (TLEs) in the form of sprites, elves, jets and halos. MMIA (Modular Multispectral Imaging Array) is developed by Therma and measures optical emissions by two 180-250 nm, 337nm and 777nm wavelength cameras with 5nm bandwidth. Imaging can take place only at night as both cameras' CCDs are light sensitive [46].

ASIM has three photometers working at 180-777 nm to measure changes in photon flux. Continuously working instrument (100,000 counts per second) detect sudden changes in photon flux and collect the data before and after the event, save it and sent to the processing center on the Earth [46].

3.1.2. THOR Experiment

THOR is an experiment on the International Space Station (ISS) assigned by National Space Institute of the Technical University of Denmark (DTU Space). It was conducted by European Space Agency in September 2015 with the direct involvement of Andreas Mogensen (first Danish astronaut on the board of ISS) during IrISS mission [49].

The experiment holding the name of the god of thunder is aimed to image specific electrical activities taking place above the thunderstorm, namely, targets are TLEs, Gravity Waves (GW) and Cloud Turrets (CT)[48].

The scientific objective of THOR is motivated by the importance of water vapor investigation as a greenhouse gas. Cloud Turrets are formed in the process of strong and rapid upward motion of cumulonimbus cloud penetrating the tropopause. Gravity Waves are wave-like patterns generated from thunderstorm convection. They play a significant role in water, energy, momentum transfer between different layers [48].

ISS is the most suitable location for such an experiment as it offers coverage of the most regions of interest like tropical and subtropical latitudes, as well as ISS is the lowest existing observation platform. ISS allows the observations of TLE in the optical bands which are more observed when watched from the ground.

All the observations were made from the panoramic Cupola module. Instrument used for CT and TLE capturing is a light-sensitive high-resolution camera - NikonD4 with the following technical parameters [48], [49]:

ISO sensitivity	6400
Shutter speed	1/25s
Frame size	1920x1080
Frame rate	24frames/s
ISO Sensitivity Range	A12800
Lens	58 mm/f1.2
Len's field of view	34.4 x19.75

Table 1. Technical characteristics of the camera used for THOR experiment [48].

THOR was a Short Duration Mission (SDM) which was to be performed within 10 days (2^{nd} -11^{th} of September) with the onboard available equipment as weight upload capability, time and budget were limited. At the end of 2014 while preparations for experiment due to the misalignment of hardware on board with Experiment Scientific Requirements (ESR) observations of GW was canceled from THOR mission [48].

Andreas Mogensen's activity on the board of ISS was accompanied by preliminary prepared thunderstorm forecast data. Where the time of overfly,

position of the storm and pointing angles were collected by lightning systems on the ground, meteorological satellites and radars to increase the possibility of capturing events on camera [48].

THOR can be considered as a successful mission. Three successful observations were achieved, one of them (8th of September around 22:30 UTC) while ISS flying over the Bay of Bengal (India). Video recording was made at night time over the thunderstorm (See Figure 18) [50].

Day of observation	Target Type	Images Count	Video Duration
DOY 249	Time Synch	3	
DOY 250	Calibration	176	
DOY 251	CT	160	
DOY 251	Calibration	3	
DOY 251	TLE		2’40”
DOY 252	Calibration	59	
DOY 252	TLE		6’30”
DOY 254	Calibration	26	
DOY 254	TLE		6’20”

Table 2. Review of the achieved results in the THOR experiment classified by target type and date [48].

The THOR was the first mission where the blue jet was seen and successfully filmed pulsating at the top of the thunderstorm.

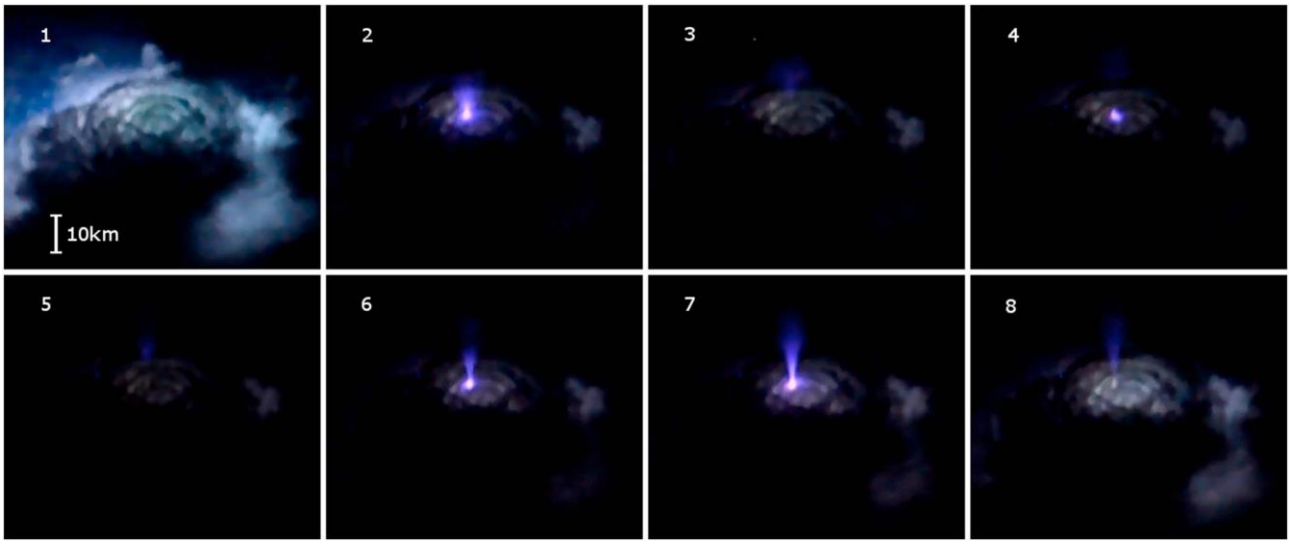

Figure 18. Consecutive frames of the pulsating blue jet filmed from ISS flying over Bay of Bengal, India at 8th of September 2015 [50].

Image 1 represents the cloud illuminated from inside.
Image 2 captured the first pulse reaching the altitude of approximately 13.25km.
Image 3 shows the process when pulse fading leaving a weak glow up to 17.5 km.
Image 4 reveals the second pulse occurring in the same place but jumping higher till ~ 10.5-20 km.
Image 5 displays the second pulse fading and emitting blue light.
Image 6 represents third bright discharge to the 18.5 km height.
Images 7-8 blue jet reaches its maxima up to ~21.5 km.

Another observation of the blue discharges was on the DAY 251 with the duration 160s captured on the top of the storm cloud. During that time 245 discharges were filmed, which means the event had the rate of 90 discharges per minute. Figure 19 left column represents blue discharges while the right column shows the superimposition of the cloud over these discharges [48,50].

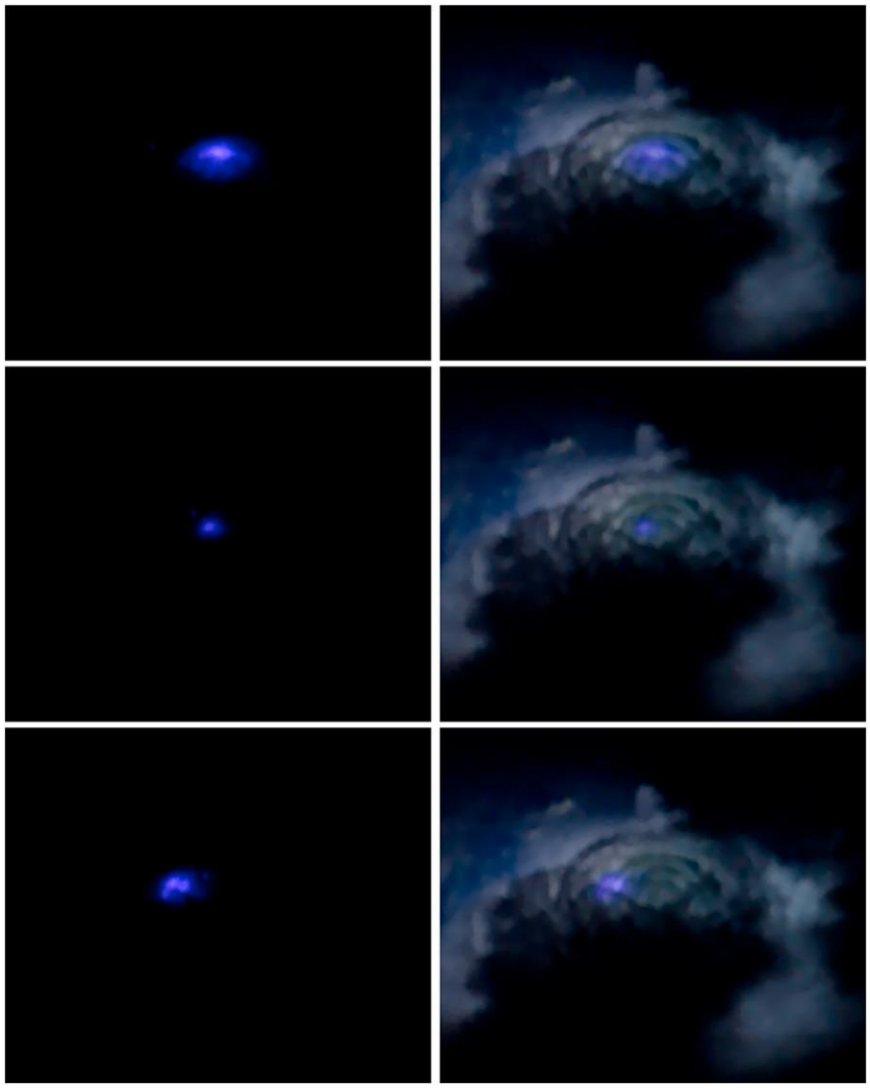

Figure 19. Blue discharges on the top of the cloud. Left column- discharges, right

column- discharges superimposed on the image of the cloud [50].

Correction of the superimposion on the image of a moving camera was carried out due to the comparison of city lights existing on the whole frame. Superimposed images give the spatial orientation of discharges regarding cloud geometry. That blue discharges appear only on the very top of the cloud but in different locations. They last longer than one frame (42ms) and have approximate spatial dimensions between 4 to 9 km^2. However, they are not related to the activity deeper inside the lightning cloud, so observed blue flashes cannot be the result of scattered lightning coming from inside of the cloud as they all have weak blue component. These blue surface discharges may resemble such a phenomenon as a pixies but there are significant differences by an 1 order of magnitude in size and longer duration (83-125ms). [50]

3.1.3. FORMOSAT-2

FORMOSAT-2 (or previously known like ROCSat-2) was the first Taiwan-owned imagery satellite developed by National Space Organization (NSPO) in collaboration with EADS Astrium SAS from France [51].

The main mission of the FORMOSAT was to provide high-resolution observations of Earth with remote sensing instrument (RSI) on a daily basis to help in monitoring a different kind of environmental changes. In the same time, satellite carried the payload (ISUAL) for scientific interest. The objectives were to provide the researches with observations that will help to understand the nature of TLEs phenomena by investigating spectral and spatial properties of the lightning discharges in the upper atmosphere [52].

The satellite was launched at 20 May 2004 on a Taurus-XL rocket from VAFB, CA. It had sun-synchronous orbit with the mean altitude of 888 km satellite allowed it to orbit Earth 14 times per day [51].

ISUAL is a research instrument designed by NSPO, UCB (University of California at Berkeley) together with NCKU (National Cheng Kung University of Taiwan, Japan). That is the first international scientific instrument in space with the purpose to observe sprites, elves and different kind of jets.

ISUAL consists of several fundamental elements:

1) Spite Imager
2) Array Photometer
3) Spectrophotometer
4) Electronics package

The staring-type CCD camera of the Sprite Imager can film at the speed of 180 frames per second with following resolution and FOV (Field of View): 512x128 pixel and 20˚x 5˚respectively [53].

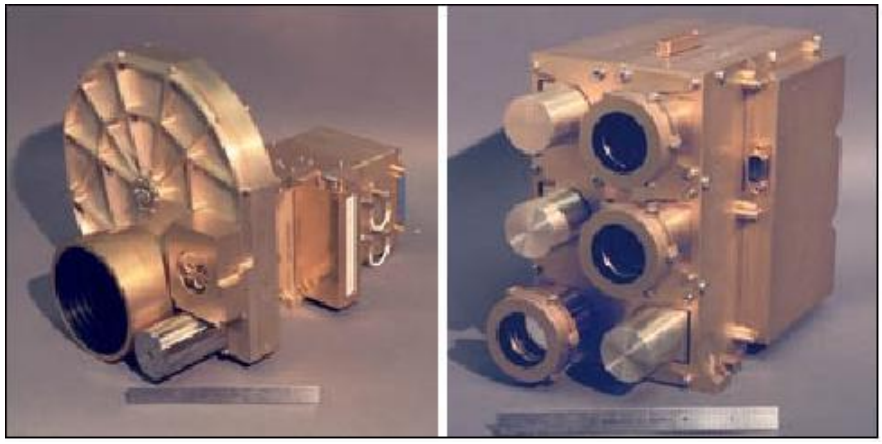

Figure 20. Spite imager (left side) and spectrophotometer (right side) of the ISUAL instrument [54].

The instrument can operate in three different modes:

1) Mode for continuous sprite imaging (sample rate of 100 Hz)
2) Sprite burst mode (sample rate 1000 Hz)
3) Aurora mode working at constant 1 sample/s rate

Sprite Imager (Figure 20) is attached to a large disk containing six colored filters. In order to measure different wavelengths of the red sprites' emissions instrument rotates the disk and changing filters. All kind of observations was possible during only night-side pass. ISUAL [53].

With a spatial resolution of 2 km, time resolution of 1–30 ms and SNR=43:1 at 30 ms sensitivity ISUAL was capable of providing detailed images of individual sprites. On July 4, 2004, the first image of sprite was recorded on the board of FORMOSat-2 flyting over the Philippines (See Figure 21).

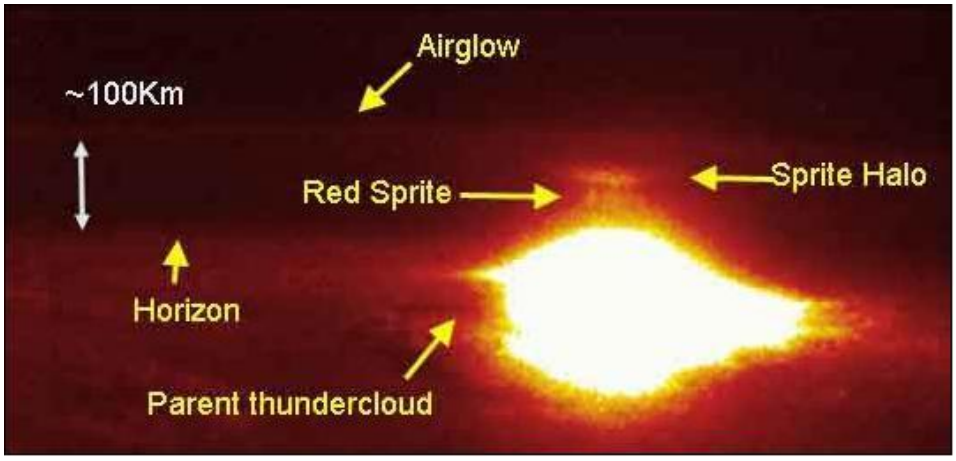

Figure 21. First Sprite Image captured form Space, FORMOSat-2, 2004 [54].

In 10 years of ISUAL function on the board of FORMOSat-2 more than 35,000 TLE events were recorded (See the Table3). In the table below the percentage distribution of a different kind of TLE is illustrated. It is clear that the largest amount of TLE occurs in the form of elves (74%) and the rarest event is Gigantic Jet (0,3 %) [54].

Year	Elves	Sprites	Halos	Blue Jets	Gigantic Jets	Total
2004 (%)	588 (77.37)	68 (8.95)	67 (8.82)	37 (4.87)	0 (0.00)	760 (100)
2005 (%)	1,420 (73.46)	217 (11.23)	165 (8.54)	124 (6.41)	7 (0.36)	1,933 (100)
2006 (%)	2,212 (75.88)	201 (6.90)	258 (8.85)	239 (8.20)	5 (0.17)	2,915 (100)
2007 (%)	2,653 (73.92)	255 (7.11)	277 (7.72)	398 (11.09)	6 (0.17)	3,589 (100)
2008 (%)	2,643 (75.15)	188 (5.35)	163 (4.63)	507 (14.42)	16 (0.46)	3,517 (100)
2009(%)	3,046 (75.19)	261 (6.44)	218 (5.38)	510 (12.59)	16 (0.40)	4,051 (100)
2010 (%)	3,195 (72.75)	250 (5.69)	234 (5.33)	697 (15.87)	16 (0.36)	4,392 (100)
2011 (%)	3,394 (72.46)	300 (6.40)	258 (5.51)	718 (15.33)	14 (0.30)	4,684 (100)
2012 (%)	3,016 (73.98)	217 (5.32)	190 (4.66)	718 (15.33)	15 (0.37)	4,077 (100)
2013 (%)	2,795 (73.23)	244 (6.39)	162 (4.24)	612 (16.03)	4 (0.11)	3,817 (100)
2014 (%)	1,036 (72.45)	99 (6.92)	51 (3.57)	239 (16.71)	5 (0.35)	1,430 (100)
Total (%)	25,998 (73.93)	2,300 (6.54)	2,043 (5.81)	4,720 (13.42)	104 (0.30)	35,165 (100)

Table 3. Number of Elves, Sprites, Halos, Blue Jets and Gigantic jets detected by FORMOSat-2 in 10 years (4 July 2004- 31 May 2014) [54].

With the closer look to the table 3 within that 10 year, it can be noticed that percentage of blue jets continuously increasing from 5 % to near 17 % , in contrast the percentage of halos decreasing from around 9% to about 4%. As well as minor changes in the percentage of elves, sprites and gigantic jets occurrence can be seen from 2004 till 2014. [113]

In Figure 22 green dots correspond to observed elves, red dots for Sprites, orange dots - for Halos, blue dots - for Blue Jets finally black dots states for the occurrence of Gigantic Jets.

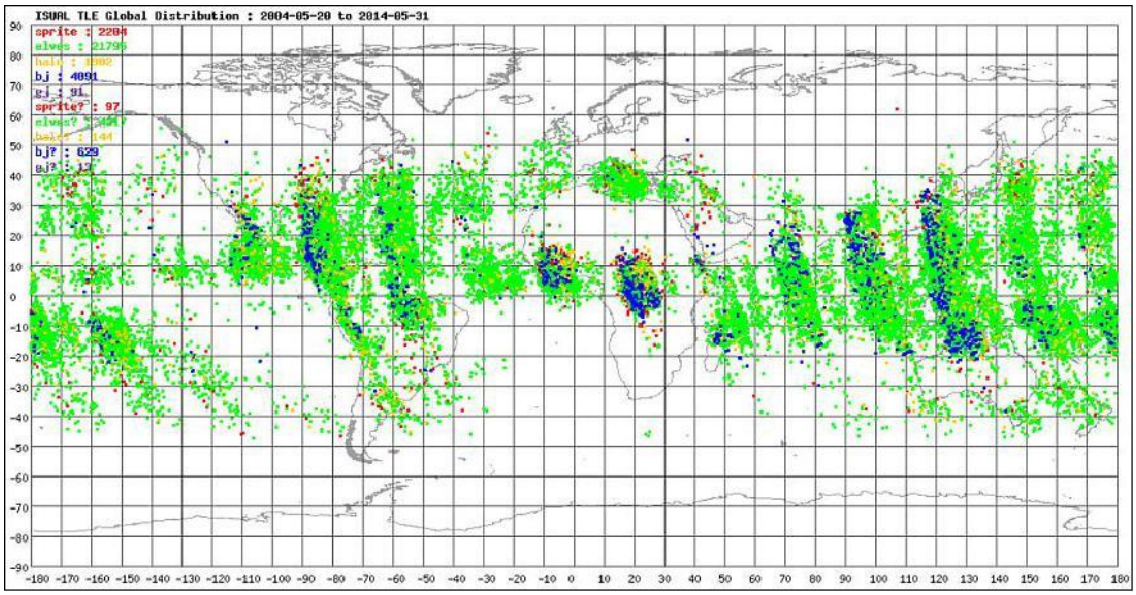

Figure 22. Global distribution of different kind of TLEs in the time frame (4 July 2004- 31 May 2014) [53], [54].

The most frequent zones of occurrence of elves are over the Caribbean Sea, Central Pacific Ocean, South China Sea, Southwest Pacific Ocean, West Atlantic Ocean and East Indian Ocean.

Whereas sprites tend to be originated over land and coastlines rather than over the ocean. The distribution of halos over land and water is intermediate between elves and sprites. The concentration of sprites and halos has been found in Central Africa, West Atlantic ocean and Japan Sea .

Areas such as the Arctic Ocean were almost devoid of TLE and none of any type of TLE were observed over deserts. [114]

According to observations collected, around 60% of all elves appeared over oceans, which proves that lightning with high peal current is more likely to occur over the ocean than over the land.

The warm surface of the tropical oceans is the most favorable heat reservoir and an important condition for the formation of vertical conventions contributing to the occurrence of such natural phenomena as tropical storms, hurricanes and even typhoons.

Based on this fact, the relationship between the temperature of the sea surface and the frequency of occurrence of elves was investigated. Figure 23 shows this pattern with a significant increase at a threshold temperature of 26 degrees. This explains why elves appear more often over warm water than over colder sea surfaces, and even less often over land. [114]

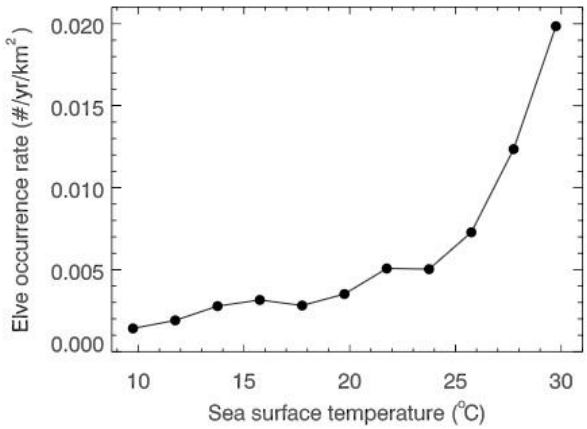

Figure 23. Dependence of elves occurrence due to the sea surface temperature. 26 degree is the point of rapid increase of elves rate.[114]

3.1.4. TARANIS

One more satellite in the name of mythological god of thunder is TARANIS (Tool for Analysis of RAdiation from Iightning and Sprites). It is a microsatellite developed by French government space agency CNES (National Center for Space Studies) together in collaboration with several institutions and international laboratories from Denmark, Poland, USA, Japan and the Czech Republic [56].

TARANIS is planned to be launched in September 2020 by VEGA rocket from Kourou, New Guiana to the sun-synchronous orbit. Scientists await its launch since 2015. It will orbit an Earth on the altitude of 700 km with 98˚ inclination for at least 2-4 years [55].

The main research objectives of the TARANIS mission are including the following paragraphs:

- Studying the physical correlation between luminous (TLE) and radiative (TGF) signatures through their detection and recording with high spatial resolution instruments [57].

- Revealing the generation mechanisms of TLEs and TGFs and environmental conditions like lightning activity, thermal plasma variations, atmospheric showers [56].

- Discover the effects of the transient Lightning-induced Electron Precipitations (LEP), electromagnetic perturbations and energy transfers on the space environment, radiation belt and on the Earth atmosphere regardless if they related with TLEs or not [56].

Scientific instruments on the board of TARANIS are intended to be capable of identifying optical, electromagnetic, electron-beam and X-Gamma signatures simultaneously.

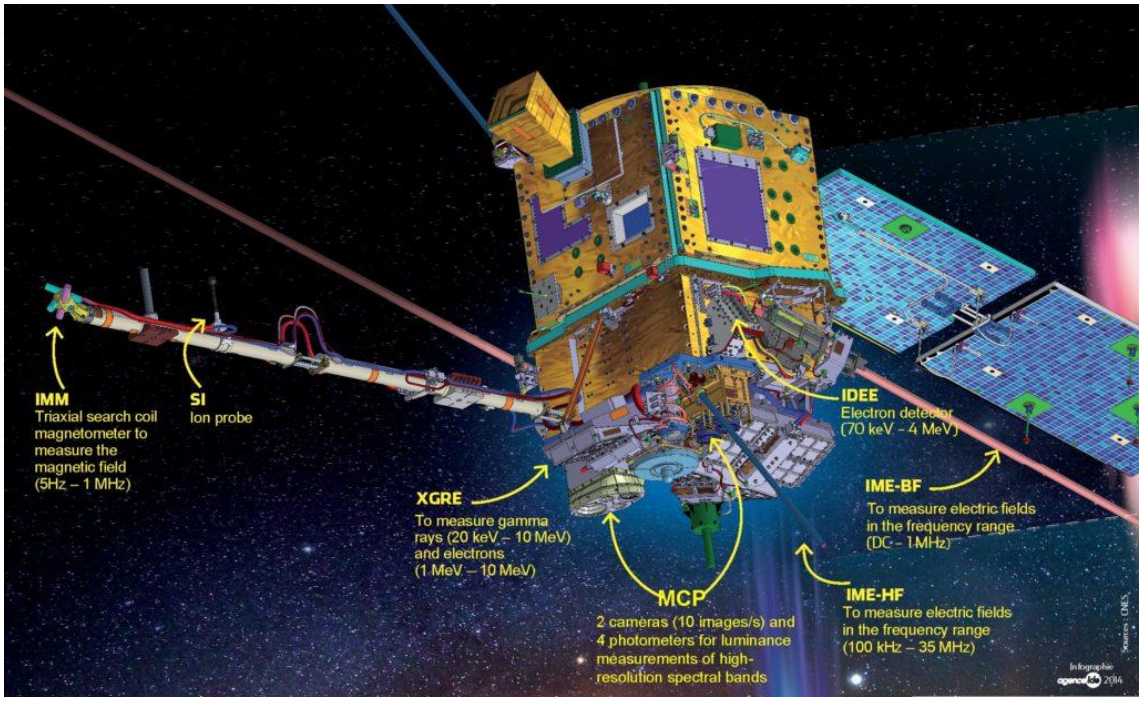

Figure 24. Scientific payload of TARANIS [59].

TARANIS payload consists out of six instruments and is operated as a single element for data return maximization [58], [60].

1. MCP (Micro Cameras and Photometers) – consist of 2 cameras and 4 photometers dedicated for identifying the TLEs' brightness, wavelength, size and relative location.

2. XGRE (X-ray, Y-ray and Relativistic Electron experiment) – is a set of 3 sensors necessary for measuring high energy photons and relativistic electrons are released after each event.

3. IDEE (Instrument for the Detection of the Energy Electrons) – involves 2 spectrometers measuring high energy electrons (between 70 keV to 4Mev). Each spectrometer has a side axis, the first axis is located in an angle of 60˚ with nadir direction, the second axis makes 30˚ angle with opposite nadir direction. (see Figure 24)

4. IME-BF (Instrument for Electric field Measurements – Low frequency)- consist of low frequency antenna measuring electric field in the range from DC to 3.3 MHz and BF-Analyzer.

5. IME-HF (Instrument for Electric field Measurements – High frequency)- consist of high frequency antenna measuring in the range from 100kHz to 30 MHz and HF-Analyzer. IME-HF has an objective to identify HF electrostatic or electromagnetic signatures of TLEs.

6. IMM (Instrument for Magnetic Measurements)- "search-coil" type tri-axis magnetometer consisting of 2 magnetic and 3 electric antennas. IMM is instrument detecting 0^+ whistlers (specific kind of electromagnetic waves) - information bringing clarity to TLEs' and TGFs' generation mechanisms. IMM identify sources of heating, perturbations of VLF signals [58], [60].

On November 17, 2020 at 01.52.20 UTC Arianespace commercial launcher Vega Light Rocket was launched with 2 satellites carried on board: SEOSAT-Ingenio and TARANIS. It was planned to deploy them on slight different orbits, after which the stage of returning the upper stage to the Earth's atmosphere was to follow. [115]

Unfortunately, it was announced that 8 minutes after the lift-off the rocket had failed and whole mission was lost. Purported reason could be in ignition of the engine of the 4^{th} stage at the Vega launcher, which entailed the trajectory deviation. According to the initial analysis of Arianespace mission was lost due to "human error". [116]

3.1.5. Russian experiment programs

Russia as the country with advanced space exploration programs also investigate the TLE phenomena as well as energetic particles in the upper atmosphere. With that purpose, there are several space missions and experiments were launched since 2000.

3.1.5.1. Tatiana-2

Tatiana- 2 is a microsatellite launched on September 17^{th,} 2009 on the board of Fregat rocket from Baikonur Cosmodrome to the sun-synchronous orbit as a part of Meteor- program on the altitude of 825km [79].
Main mission focus is observations of TLE emissions measured in 8 bands of wide spectrum and on millisecond scaled images. Furthermore, NUV flashes and high-energy charged particle investigations are a high priority part of the mission [80].

Instruments used for that mission are the following [79]:

- MTEL or MEMS Telescope. It is WFOV (Wide Field Of View) telescope with the objective to image and track the TLE (with an operational wavelength range 300 to 400 nm).

- NUV+R Radiation Detector working in NUV range (300-400nm) and in red radiation range(600-700nm) with 32˚ of FOV. Objectives are to monitor luminescence and measure flash radiation.

- Scintillation Flux Detector –measuring high-energy charged particles flux on the 400 cm^2 detector area.

- BCU (Block of Central University) designed by NCU National Central University and NCKU (National Cheng-Kung University) in Taiwan is a block out of two devices: Electron Temperature Probe (ETP) and MRM (Magneto-Resistance Magnetometer) for measuring temperature, electric potential and density of Earth's magnetic field and of ionosphere's electron plasma [79].

During 3 months of its operational time from October 20, 2009 till January 17, 2010 Tatiana-2 detected more than 2000 lightning fast flashes with duration between 1 to 128 ms. 2628 events were selected after analysis out of 360 operational hours data gathered in shadowed "night" periods.

Due to duration and structure selected events can be distributed to 3 groups: short (1-5 ms) single flash, multiple short flash and longer flash. Strong correlation was found to be between profile structure of transient events and their number of photons: large photon numbers $Q_a>10^{24}$ generally are inherent to longer flash, while short single pulses mostly have photon number less than $Q_a<3\cdot10^{21}$.

The global distribution of all the detected transient events from Tatiana-2 is demonstrated on the figure 25 below. It can be seen that mostly detected TLEs are concentrated above equatorial regions of America, Indo-China and Africa and regions like Australia and Sahara shows absolute absence of events. [117]

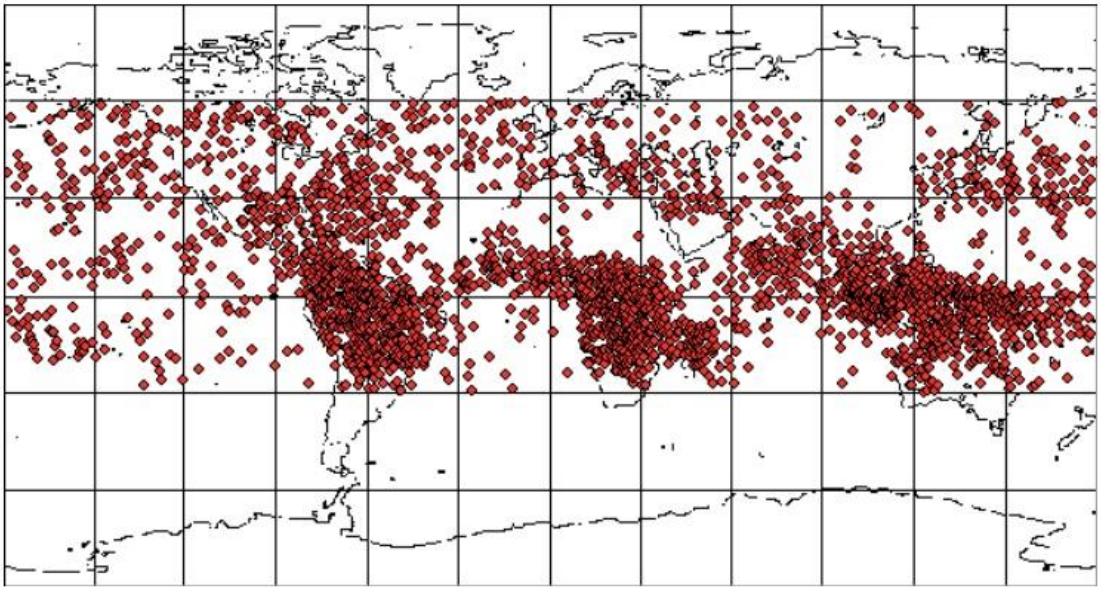

Figure 25. Global distribution of TLEs detected by Tatiana-2 satellite during October 2009-January 2010. [117]

The results of the attempt to identify the pattern of the global distribution of events showed that transients with photon numbers higher than $5\cdot10^{21}$ more evenly distributed between 0° to 30° N and S latitude, at a time when transient with photon numbers less than $5\cdot10^{21}$ concentrated above equatorial continents (figure 26 a,b). [118]

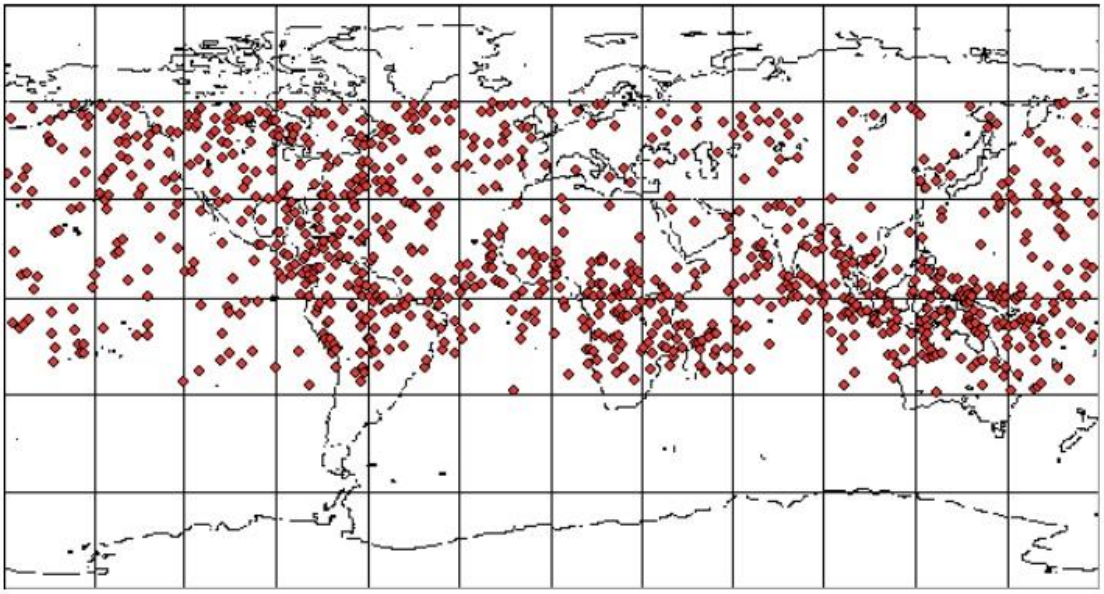

Figure 26 (a) Geographical distribution of the TLEs with photon energy less than $5 \cdot 10^{21}$ [118]

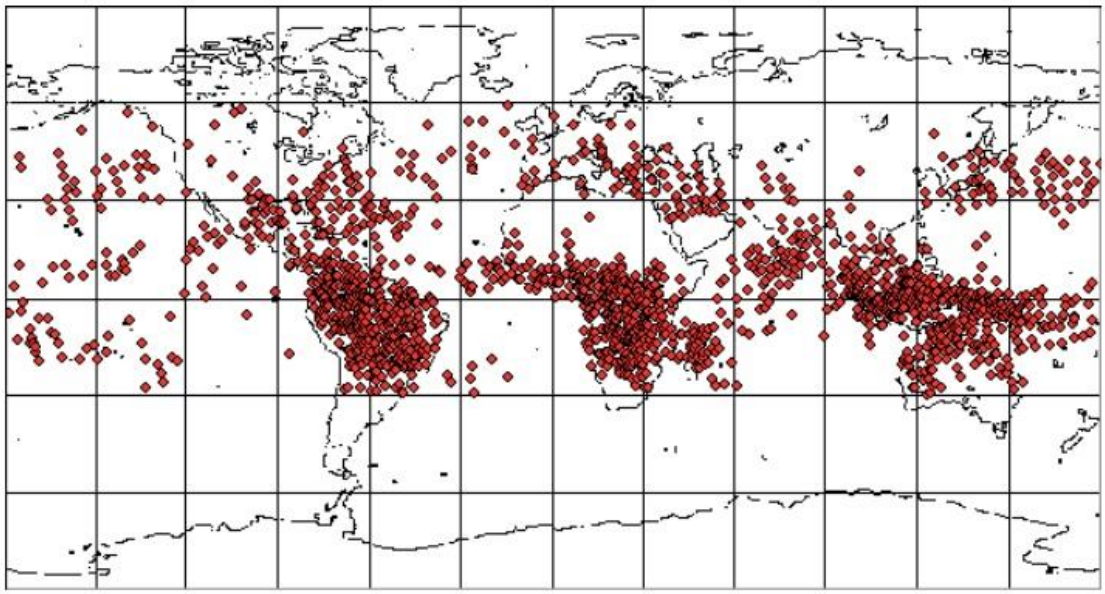

Figure 26 (b) Geographical distribution of the TLEs with photon energy more than $5 \cdot 10^{21}$ [118]

Another serious phenomenon seen in the analysis of 1354 events collected by Tatiana-2 is that 627 of them were detected far away from thunderstorm areas in absolute cloudless regions. Despite the well-known fact that TLEs are consequences of lightning (event-to-event), it can be assumed that TLEs can by triggered by electric excitation of the upper atmosphere caused by electromagnetic pulse transferred to the thousand km away from the epicenter of lightning. [118]

Data collected by Universitetsky-Tatiana-2 also showed a new feature of TLEs appearing multiple times per minute ($N_s \geq 3$). They were called “series”. 1519 (58 %) out of all detected TLEs (2628) were identified as series.

The further analysis of the single and series of transient events showed serious differences between them in numerous parameters like geographical distribution, photon number, brightness, duration and structure. Serial TLEs shows equatorial concentration above continents essential in cloudless regions while single transients uniformly spread. Single TLEs predominantly are short pulses (90%) but series has much less of them (60%). On the other hand, serial transients much brighter than single ones which proves the correlation between photon number and the temporal profile of TLEs. [118]

According to the NUV energy distribution, flashes with middle energy y˜ -1 associated with TLE. Also, was investigated that low energy events with E< 1 kJ have a larger variation of IR/UV ration than other groups of flashes [81].

3.1.5.2. CHIBIS-M

Chibis-M is a 40 kg microsatellite with a mission to measure EMR (Electro -Magnetic Radiation) in near-Earth space, to study TLE and TGF generation mechanisms and to explore fluctuations of electric and magnetic fields.

Chibis-M was delivered on November 2nd, 2011 to the ISS by cargo spacecraft Progress M-13M from Baikonur. The satellite was equipped with the next scientific instruments [82]:

- RGD (Roentgen (X-ray) and Gamma-ray detector) with 50-500 keV energy range of X-ray
- DUV (UV Detector) with 300-450 nm wavelength range
- DPC (Digital Photo Camera) in visual range.
- RFA (Radio Frequency Analyzer) in 20-50 MHz frequency range. This instrument measures the intensity of the radio emissions with 20ns time resolution.

Chibis-M registered several hundreds of upper-atmospheric events related with short lightning discharges and performed UV, IR, X- and Gamma-ray spectrum radiation measurements during its approximately 3 years of mission life (2 years and 8 months).

Figure 27 below represents the distribution of lightning detections data registered by Radio Frequency Analyzer in the range from 26 to 48 MHz. Equatorial regions of high lightning activity are pointed with blue dots [82], [83].

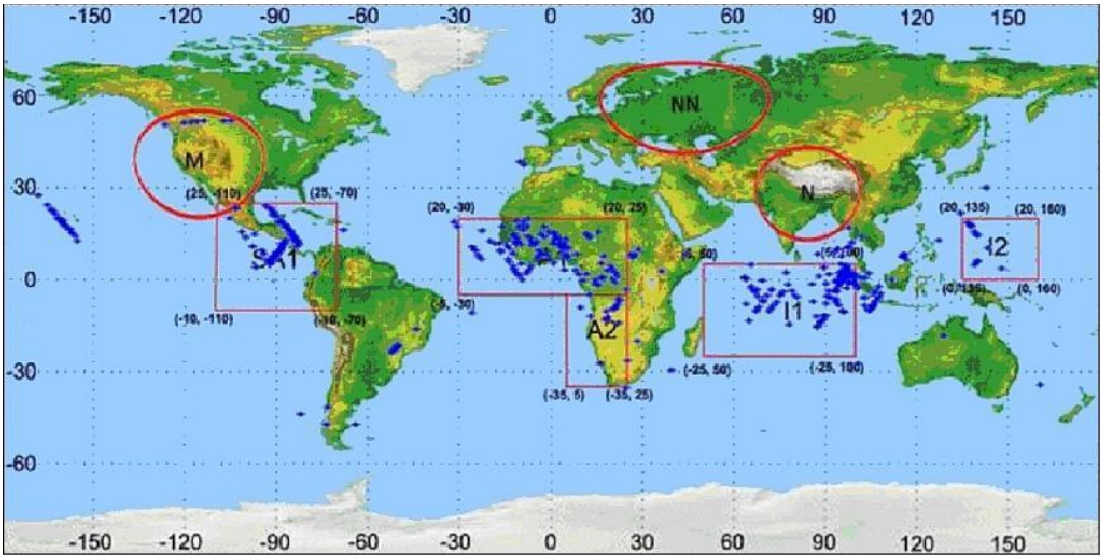

Figure 27. Chibis-M microsatellite detected lightning activity over the world map [82].

Example of the VHF type powerful pulse registered on Chibis-M is illustrated below (figure 28). Run-away breakdown generates pules accompanied with the secondary pulse which is a reflection from the ground surface. According to the difference between two pulses it is possible to determine the altitude of the origin of the lightning discharge.

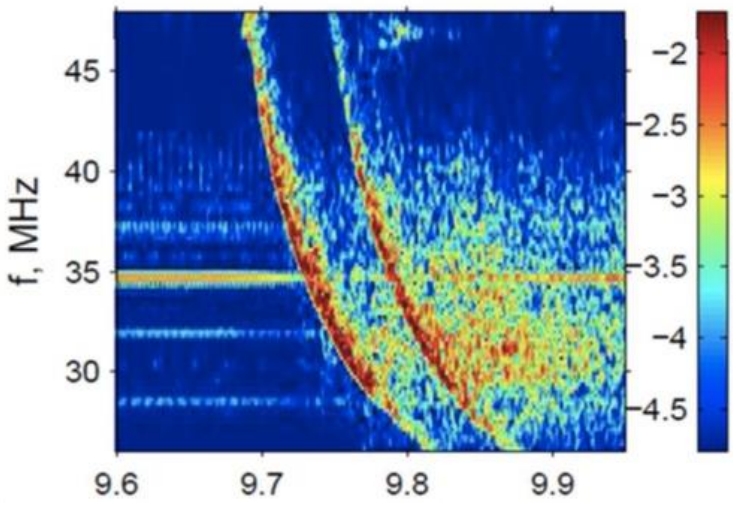

Figure 28. Lightning discharge accompanied by ground reflection pulse allowing to calculate the height of lighting physical origin. [119]

There is only 1% occurrence frequency of “solitary” VHF pulses. In fact, solitary pulse still has its almost indistinguishable pair appearing right after the first one (only 6mcs) so that they look integral. While the time lap between the usual ground reflected pulses are around 150 mcs which corresponds to the 22km altitude of discharge origin, the origin of the solitary VHF pulse is equivalent to the 2.6 km. [119]

Unexpected results of data analysis of Chibis-M flight over Japan proved the existence of LF (100 Hz) radiation in upper ionosphere (figure 29). These intensive radiation at both 50 and 60 Hz and also the Schuman resonance modes clearly registered by satellites’ high sensitive electric channel. [82]

Also, LF electromagnetic structures in the range from 0.5 Hz till 5 Hz called ionospheric Alfven resonances were detected. Possibility of leakage of them above the layer F2 in ionosphere still reminds hypothetical. Radiation at 50-60 Hz frequency was observed regularly at day and night time of the orbit and Schuman resonance phenomenon only at night time. [120]

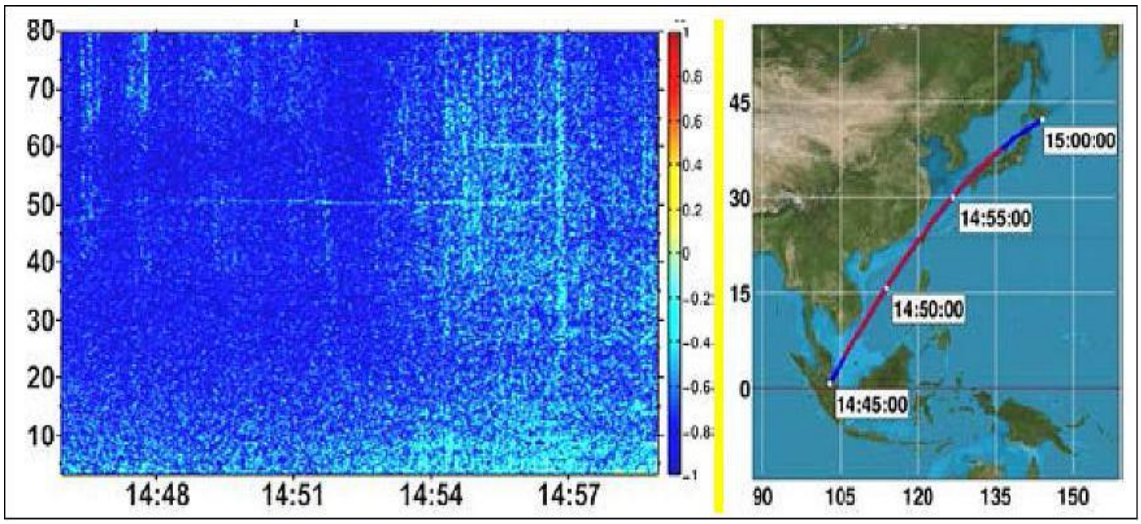

Figure 29 . Radiation at frequency 50-60 Hz and Schuman resonances (at left), Chibis-M fly trajectory over Japan. [82]

3.1.5.3. TUS (Tracking Ultraviolet Setup)

TUS is a 60kg scientific payload of “Michail Lomonosov” satellite developed in Moscow State University. The mission goal of that payload is to detect UV fluorescence generated by ultra-high energy cosmic rays (UHCER) which produce extensive air showers (EAS) and by TLEs of the upper atmosphere [84].

For that purpose, 2 m^2 mirror concentrator with 256 pixels on it takes an image of fluorescence on the 4000 km^2 coverage area in 300-400nm wavelength range. Further sampling of pixel signals at 0.8μs rate help to detect EAS particles

disc movement. The number of particles identify the EAS energy and proportional to UV fluorescence radiation.

To detect TLE on early phase TUS need to see UV flashes at bright stages. Mirror-concentrator pixels get saturated on that point. For this goal, TUS use two pinhole cameras each containing multi-anode photo-multiplier tube (MAPMT) for distinguishing TLE from UHCER [85].

The TUS detector can operate in four modes according to the different time sampling windows. The main interest of TUS mission is concentrated on the first mode for detecting extensive air showers generated by extreme energy cosmic rays with 0.8 μs sampling time. The other three modes were dedicated for observation of various optical phenomena with 25.6 μs sampling time (TLE-1 Mode), 0,4 ms sampling time (TLE-2 Mode), and the last (METEOR Mode) made it possible to discover space debris and micro-meteors at 6.6 ms sampling window [84,124].

In total 17345 events were recorded in the time interval from August 16, 2016 to November 4, 2016 obtained with TUS during the nighttime of orbits. Preliminary results were divided into four groups due to the temporal structure of waveform.[124]

- Illuminations with noise-like waveform

More than 80% of all registered events are concentrated in this group. they have a noise-like structure due to non-uniform illumination of the focal plane which takes place mainly in full moon nights or above industrial centers. This can be explained like; the relative position of the moon and the satellite contributes to the direct arrival of the moonlight to the focal surface without preliminary reflection from the atmosphere. Conclusion made: For further sensor protection from the direct moon and sun light to use the Schmidt camera, which has a deeply positioned photodetector in the telescope. [84,124]

- Instant flashes - type of flashes observed in nearly 14% of gained results which are extremely brief and produce a track like a trajectory on the surface of the focal. One of the hypotheses explains it as direct Cherenkov radiation of EAS.
- Slow spatially extended flashes - a group of events (typically lightning effects) with slow rising signals. This kind of flash is an expanding light spot. Some of them leads to total illumination of the focal plane. However, the positions of that slow flashes were far away (more than 500km, 600km, and 1600km) from +/- 1s lightning registered by WWLLN. It can be explained by the uniform registration of the detector of the UV light that is spreaded in all directions. Gigantic jets and blue jets theoretically can be detected by TUS in the form of these slow spot illuminations. [84,124]
- Flashes with complex spatial-temporal structure

One of the most illustrative results of TLE observations from TUS is the detection of doubled elves detected in this operational mode. Pixel map and corresponding oscillogram plot of doubled elves are shown in figure 30 below. Two clear separated rings are visible on the pixel map and on oscillogram plot, they appear as two picks. The brightness of the first ring is explained by the direct influence of the ionosphere to the EM wave of lightning. The second elve slightly faints as a result of emissions reflection from the ground [86].

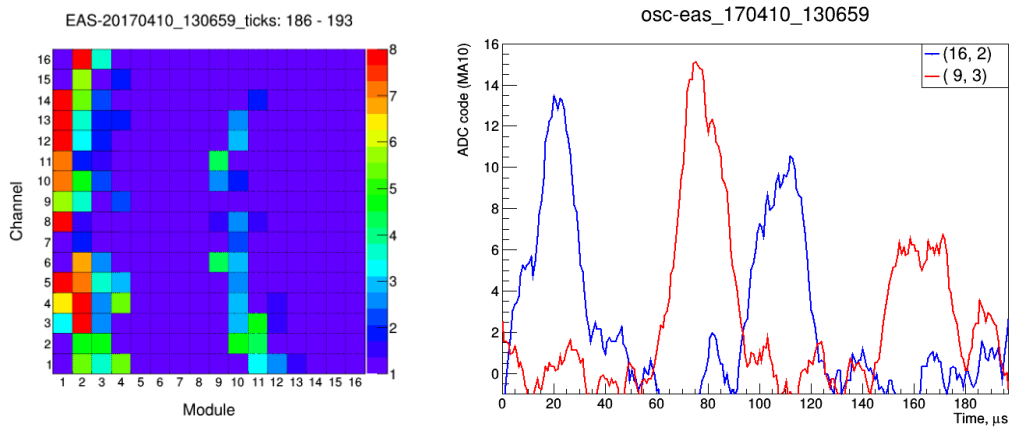

Figure 30. Double Elve measured by TUS payload on April 10, 2017. Pixel map (on the left side) and oscillogram plot (on the right side) [84].

In addition to this case, there were recorded events that can presumably be called elves. The first event was detected over the Pacific Ocean on September 7, 2016, at 09:51:35 UTC, the second event above Chad on September 18, 2016, at 22:06:48 UTC, and the third over the Northern Mariana Islands on October 18, 2016, at 13:20:11 UTC. According to the data of the ground lightning detection services (ISUAL, WWLLN, GLD 360 respectively) in all three cases, half of the registered TLEs identified as elves. This confirms the conjecture of TUS capability to detect TLE events [84].

3.1.5.4. RELEC Mission

RELEC payload is developed by S.A. Lavochkin Space Aerospace Corporation and installed on board of the Vernor spacecraft. This small satellite was launched to sun-synchronous orbit on 8th of July 2014. RELEC mission pursued the goal of observing Transient Luminous Events and Terrestrial Gamma Flashes in the wide EM spectrum range including investigation of magnetosphere relativistic electrons: their precipitation, acceleration and impact on the upper atmosphere [87], [88].

Following six equipment allowed RELEC to measure X/gamma radiation, charge particle fluxes and EM fields radiation simultaneously with high-resolution UV optical observations.

- DRGE 1 and 2 – X- and gamma-ray detectors with an energy range of 0.01 to 2.0 MeV.

- DRGE 3 – 3 Cartesian axis energetic photons (with an energy range of 1 to 100 MeV) and electrons (with an energy range of 0.01 to 10.0 MeV) directed detector.

- Telescope-T (MTEL-2 RELEC) –optical imager with WFOV (Wide Field Of View) to track the TLE working on an operational wavelength ranges 300 to 400 nm and 600-700nm.

- DUV (Ultraviolet detector) – UV flash detector. Radiation Detector working in NUV range (300-400nm).

- NChA (Low-frequency analyzer).

- RChA (Radio-frequency analyzer).

- BE – command and data collecting electronic unit with DOSTEL dosimeter module. [89], [90].

RELEC payload achieved important results. Predominantly detection of TLE was carried out using two instruments DUV and Telescope-T. Around 10 000 flashes in the UV and IR range were recorded. The temporal structures of detected bursts varied significantly from single pick flashes to complex multi-pick structures, where single-pick flashes are apparently associated with single lightning discharges while multi-pick bursts possibly associated with glow due to high concentration of excited Nitrogen and Oxygen [125].

The main regional concentration of short UV and IR bursts is observed over thunderstorm areas as a series of flashes. This conclusion was first obtained by the similar to the DVU instrument during Tatiana experiment, then later in Tatiana-2 and in the results of Chibis-M [125].

Isolated atmospheric gamma-ray bursts were also detected as well as solar and astrophysical origin space gamma-ray bursts. Detections of different magnetosphere electron and photon precipitations and low latitude electron fluxes were obtained [87].

Below is the variety of TLE waveforms detected by RELEC is illustrated in figure 31.

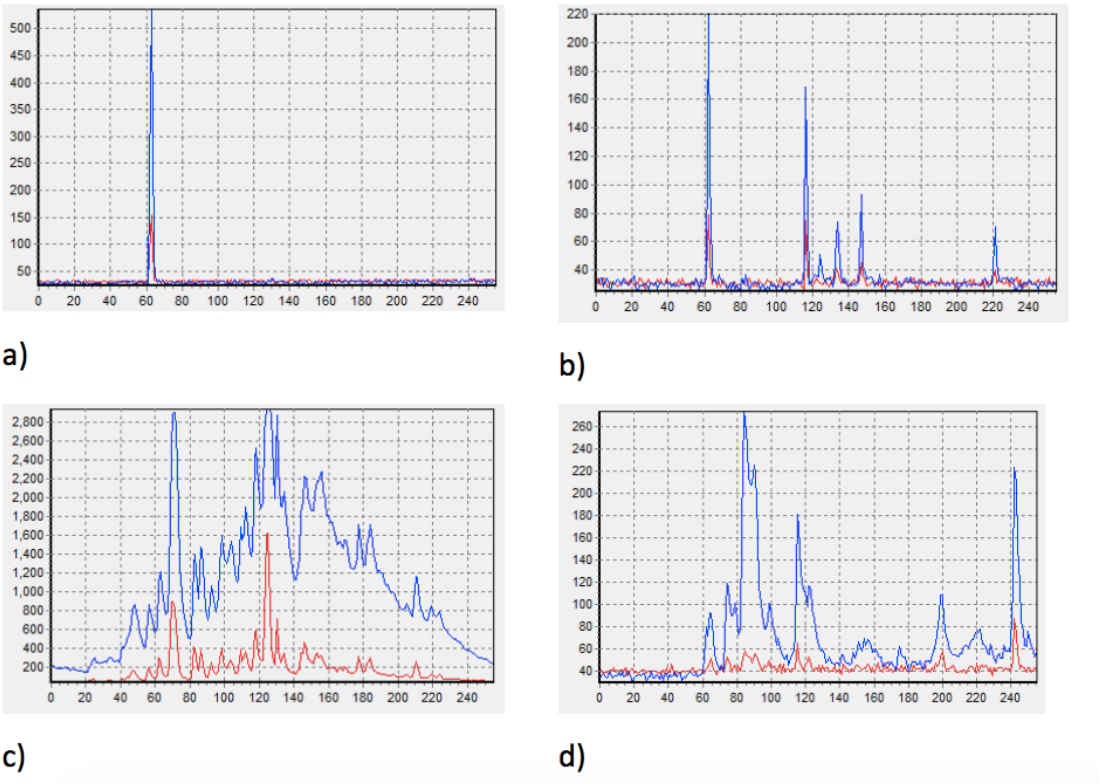

Figure 31. a) and b) Short VU and IR pulses of TLE, c) long TLE events, d) TLE waveforms with predominant UV signal over IR [87].

3.2. Aircraft Observations

3.2.1. EXL98 Campaign

Energetic of Upper Atmospheric Excitation by Lightning (EXL98) campaign was led by University of Alaska in the summer of 1998. That was the mission aimed to perform air observations of sprites, elves, blue jets by instruments on the board of jet aircraft, Gulfstream II (Figure 32). Within two weeks (July 15-29) of campaign observations were taken during night time over the Great Plains.

The main goal of the project was to obtain knowledge about energetic characteristics of the sprites through remote sensing its emissions with NIR (Near InfraRed), NUV (Near UltraViolet), MIR (Medium InfraRed) and visible wavelengths measuring equipment.

Weather forecast systems, as well as NLDN information, were used in help for ground site operations to notify about large storms location and occurrence time.

Low-light level system consisted out of eight co-aligned imaging instruments providing simultaneous observations of sprites in the wavelength range between 340-4.3 microns [61].

In the Table below all instruments with their technical specifications are listed.

	Instrument	Optical Range	Wavelength	Emissions Observed
1	Broadband wide FOV scene camera	visible	400-740 nm	Sprite N_2, blue starters
2	Color camera	visible	400-740 nm	Sprite N_2, blue starters
3	Broadband narrow FOV camera	visible	400-740 nm	Sprite N_2, blue starters, OH airglow
4	N_2^+ first negative filtered narrow FOV camera	Blue	427.8 nm	N_2^+ first negative from sprites and blue starters
5a	N_2 second positive filtered NUV spectrograph	NUV	337 nm	N_2 second positive from sprites and blue starters
5b	NUV spectrograph	NUV- visible	300-460 nm	N_2 second positive and N_2^+ first negative sprite spectra
6	NIR imager	0.9-1.7 μm	0.9-1.7 μm	Sprite N_2 first positive, OH airglow, blue starters
7	MIR radiometer	2.7 μm	2.7 μm	none
8	MIR image AMBER	4.3 μm	4.3 μm	none

Table 4. EXL98 Campaign instruments carried on the board of Gulfstream II [61].

Figure 32. Gulfstream aircraft associated for EXL98 campaign where NIR and NUV were installed in the way to have sensors FOV out of aircraft windows with 0˚ to 5 ˚ elevation angle. The NIR camera (bottom right) [61].

Aircraft observations have advantages in comparison with ground-based monitoring of TLEs, as scattering and atmospheric absorptions are much more intensive on the ground.

Observations obtained only at first night (Jule 15th) allowed to get visible evidence of the correlation between sprites and OH (hydroxyl) airglow. During that night, well-structured strong airglow and a series of sprites were filmed.

From Figure 33, it can be seen that on the same altitude of 85 km the tops of the sprite align with one of the hallows of acoustic-gravity waves generated by the OH airglow structure [61].

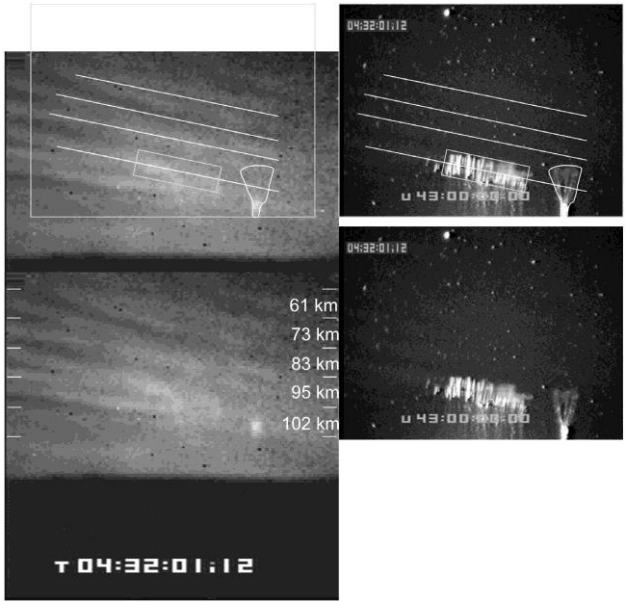

Figure 33. Images of sprites and OH Airglow captured by visible wavelength (left) and NIR (right) cameras. Airglow structure brighter and clearer on NIR image while sprites dominates in visible wavelengths image and faints in NIR one [61].

On the Figure 33 it can be seen that OH Airglow layers are tilted and sprites columns aligned with one of these rows. The tilt of acoustic gravity wave is explained by the ratio between vertical and horizontal wavelengths. Gravity waves could be reasonable explanation of some features related with sprites: such as repeating occurrence in almost the same place, similar tilt inherent for the series of sprites, displacement of sprites' appearance with respect to the charge center. So, possibly gravity waves liable for these phenomena. The main theoretical explanation of OH airglow and sprites correlation is claimed to be avalanche breakdown process in sprite formation. Nevertheless, further observations after July 15th didn't show that clear correlation. Another experiment (Sentman [2003]) with similar instruments and measurements taken from ground showed that OH airglow concentric rings occur from severe thunderstorm and gravity waves ubiquitous near them, but also didn't find precise relation between sprites formation and OH airglow. [61]

One of the important factors required to observe correlation between these two phenomena is favorable monitoring geometry. Observations should be taken far away from the sprites (500-800 km) so the airglow is bright enough and the sprites tops are in FOV, otherwise if observations taken closer, camera should be tilted in order to see the sprites top's at approximately 87 km which in turn causing faint airglow (illustration on the figure below).

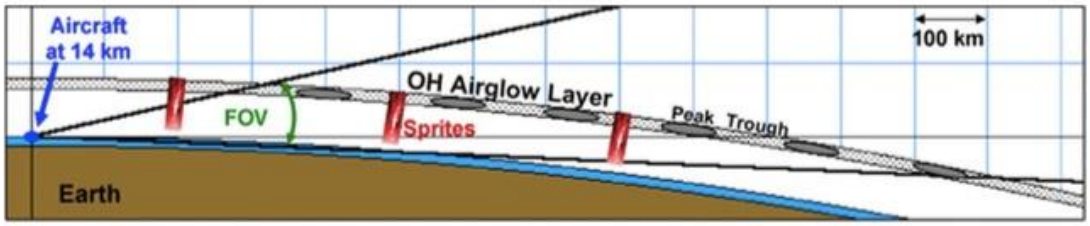

Figure 34. Best viewing geometry to catch relation between sprites tops alignment at 87 km along with OH Airglow Layer row[61].

EXL became the first mission obtaining NIR observations of sprites. and OH airglows. The next Figure 29 illustrates how different result images of the same event captured by six cameras of the EXL98.

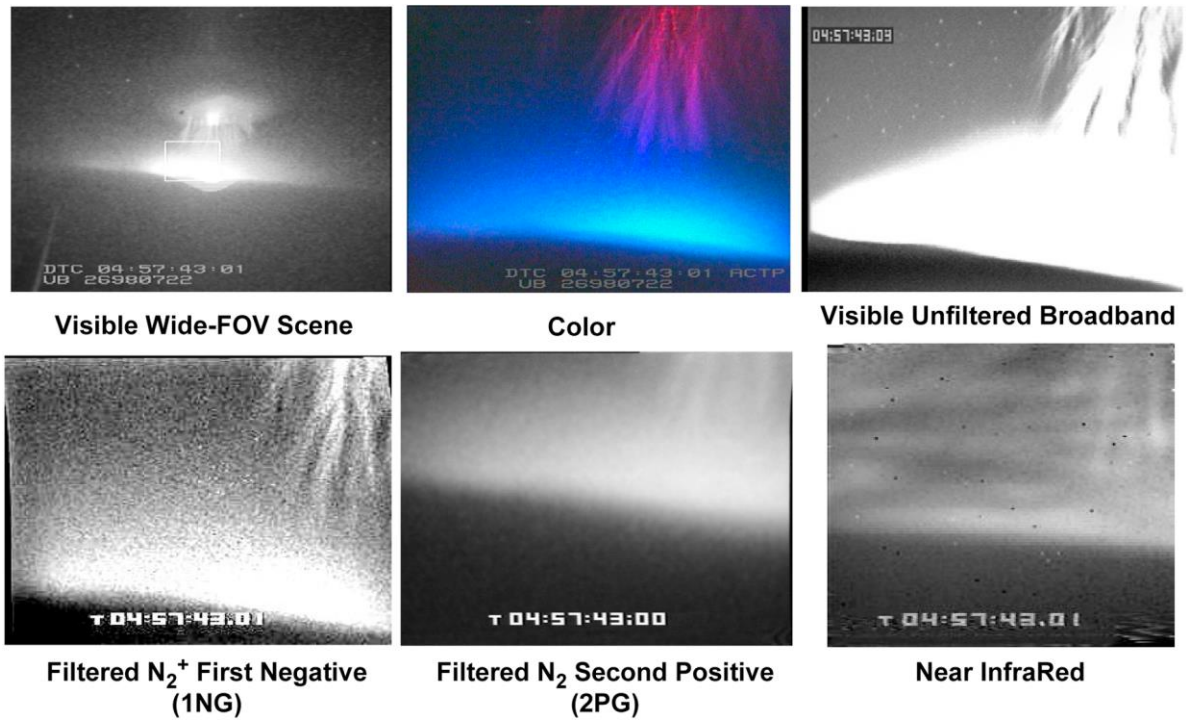

Figure 35. Six images of the sprite captured by six different cameras on EXL98 [61].

In the top left part figure 35 represents broadband wide FOV scene camera (55˚H x 43˚V) which captured large sprite with tendrils and halo. N_2^+ negative emissions can be seen in the top right corner of figure corresponding to the unfiltered broadband camera image. The color camera image on the top middle part of figure shows very clear tendrils of the sprites. Bottom left and bottom middle images of figure 35 are taken by NUV cameras. The last right bottom image of figure is taken by NIR camera and shows more dominant airglow behind the sprite and very faint tendrils [61].

3.3. Balloon Observations

3.3.1. Nasa SPRITES'99 Campaign

SPRITES'99 Campaign is a balloon-based observation mission conducted by University of Houston and sponsored by NASA and launched by NSBF (National Scientific Balloon Facility) in summer 1999 [62].

Missions were focused on detecting the stratospheric electromagnetic field signatures of lightning that initiate sprites above thunderstorms. Two out of three flights became successful in collecting data over the USA. First one was taken over Palestine on 6th of July, Texas while second and third flights were performed by balloons launched from Ottumwa Industrial Airport, Iowa.

During last flight on 21st of August two thunderstorms were observed by balloon over Minnesota and Kansas. Achieved results counted 26 (+CG) and 17(-CG) associated sprite halos with additional 88 of (-CG) TLEs later found on the recorded data. All the (-CG) and some of (+CG) strike associated halos were not followed by the appearance of sprites.

Balloons which were intended to fly near the storms but not above them were not the only site in that mission, three ground observation stations were providing monitoring of the balloon and necessary information support [63]:

1. YRFS (Yucca Ridge Field Station) in Ft. Collins, Colorado
2. WIRO (Wyoming Infrared Observatory) in Jelm Mtn., Wyoming
3. Bear Mtn. in South Dakota

Due to the location of that sites, it was possible to perform triangulation of the events video recorded by low-level light imager (LLTV) on the stations. The ground sites were also using: Dage-MTI VE-1000 SIT monochromatic camera, intensified CCD Fairchild, pointing photometers, VLF Receiver and ELF/Schuman Resonators.

The balloon itself carried following instruments estimating flash emissions (1), current density (2), conductivity (3), counting rate of X-ray photon (4), energetic particles (5), magnetic and electric fields of events (6) as well as balloon's temperature (7), time (8) and location (9) [64]:

- Photomultiplier tube – Hamamatsu R374 (1)
- One axis Split Probe Sensor (2-3-7)
- Geiger-Muller Tube and Scintillation Counter (4-5)
- 3 axis Double Probe electric and magnetic field detector (Dc -20kHz) (6)
- MTS -102 Thermistor (7)
- GPS receiver (8-9)

One of the very successful observation were captured on 17ms long NF video frame from the WIRO station after corresponding data discovery from the

balloon (see Figure 30) (-CG). It was a combination of an elve, a halo and two columnar and one carrot type sprite. In the figure below Label A indicates the pick of light intensity at 0955:36.982. The dashed line corresponds to the stroke time provided by NLDN (National Lightning Detection Network). Gain control causes small dip on the trace of photometer as a response to the sprite pulse. Label B states the burst of a pulse of very low frequency (VLF) spheric and emerges in all fields. An elve can be noticed in the bottom panel, second subpanel from left. The photometer line includes short spike (Label B, top panel) and then most intensive light flash of sprite (Label A) follows it. [65]

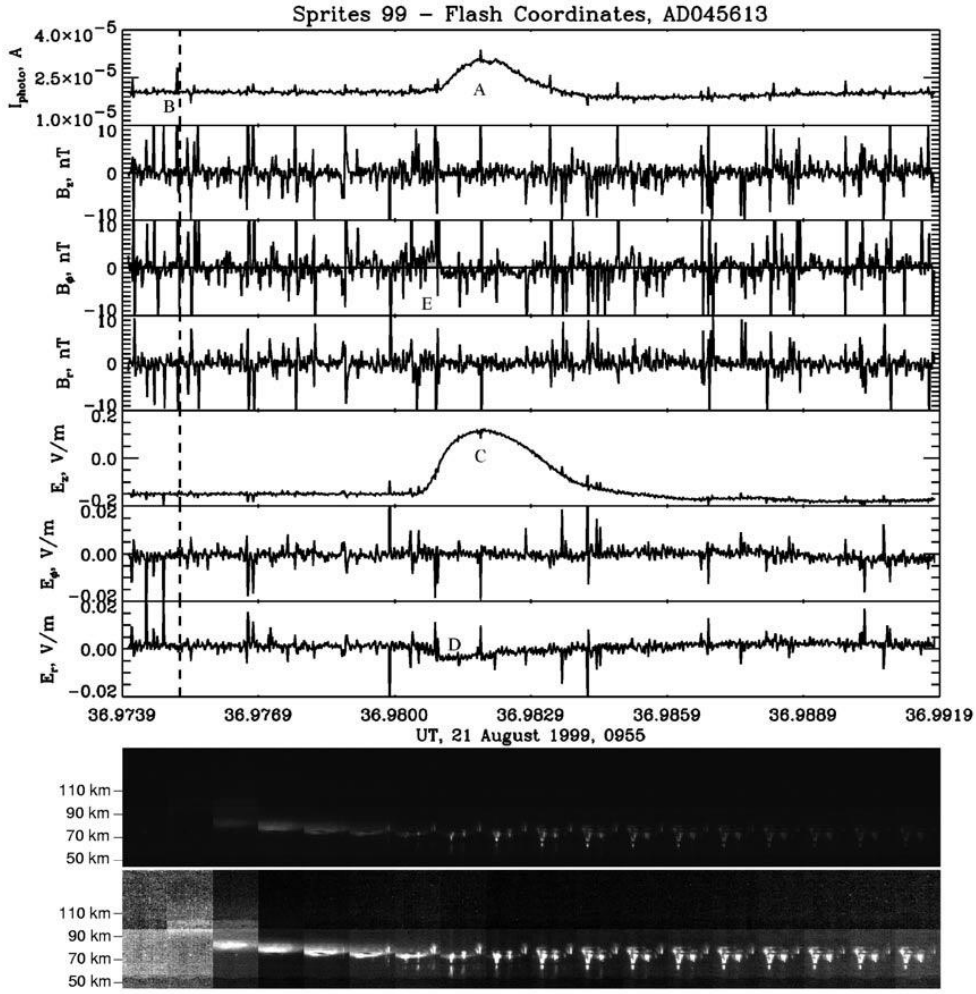

Figure 36. Photometer current, magnetic and electric field plots and high-speed images of an event of 21st August 1999 [65].

Preliminary modeling of a sprite with a start at a height of 40 km and a radius of 50 km, which is formed 4 ms after lightning, gives an almost matching Ez pulse profile with pulse profile of the event registered at 21st August 1999 (Figure 36). It gives reason to imply that this charge originated in sprite transferred from mesosphere to about 90 km. [65]

3.3.2. Sprite Balloon Campaign 2002-2003

The primary focus of that campaign was to investigate characteristics of the electromagnetic signatures and to collect them in the stratosphere above the thunderstorms which are capable to produce sprites.

For that purpose, two balloon flight were organized: one on the night of 6/7 December 2002 another on the night of 6/7 March 2003. Brazil is one of the ideal places for that mission as every year intense thunderstorms occur above the Southeastern part of Brazil during November-December. Balloons were launched from Balloon Launch Sector, Cachoeira Paulista (22˚44'S, 44 ˚56'W) [66].

Balloons of Sprite campaign carried payload consisting out of following instrument:

- 3 Low Voltage (LV) electric field detector specified for E-field vector measurements
- 2 High Voltage (HV) electric field detector. One for horizontal axes and one for vertical
- 3 Magnetic search coils for magnetic field measurements specifying the direction of the current related with sprites
- 2 X-ray detectors, up and down pointing. Helps to build a sprite generation model through investigation of the accelerated electrons.
- 2 Optical Lightning detectors, one pointed up to observe sprites and another pointed down to identify lightning. Used for timetabling of appearing events [67].

The balloons were accompanied with nearby flying Embraer airplane with an optical video camera on the board for sprite and jets presence confirmation operated by INPE (Instituto Naciola de Pesquisas Espaciais) [68]. In addition, the campaign was supported with the information provided by ground-based lightning detection systems measuring sprites appearance and their locations [69].

During this campaign, electric and magnetic field characteristics of a large amount of lightning were observed. Within those observations first largest electric field vector above 30 km was ever observed and measured. Unfortunately, due to weather conditions, optical observation from the airplane was not possible and lead to prevention of further observations.

3.4. Ground Observations

3.4.1. TLE observations in the vicinity of Israel

The Mediterranean Sea and its eastern and western coasts regions are one of the few places which contrast with particularly active thunderstorms in winter season and very rarely in summer season in comparison with other areas of the Northern hemisphere.

Nevertheless, specifically TLE observations during the winter storms in Japan [70] became the proven platform for Mediterranean researchers to start TLE observations in Israel (ILAN campaign - Imaging of the Lightning And Nocturnal flashes), as synoptically winter weather conditions in these two regions are similar. The mission focus was on imaging as much as possible TLEs in the Mediterranean region.

Ground-based TLE detection observations in the vicinity of the Israel were performed every winter from two sites [72]:

1. Tel-Aviv University (TAU) campus.
2. Wise Observatory in Mitzpe-Ramon located in the Negev desert (170 km from Tel-Aviv).

For those observations were used two cameras:

- Main camera - Panchromatic CCD camera Watec 100N with the following technical characteristics:
  Lens: 12 mm f/0.8
  Frame rate: 25 frames/s
  FOV: 31.5˚ of horizontal direction and 23˚ of vertical direction.

- Second camera – Panchromatic CCD camera Watec 902H with the following technical characteristics:
  Lens: 25 mm f/1.4
  Frame rate: 30 frames/s
  FOV: 14˚ of horizontal direction and 10.5˚ of vertical direction [72].

For determining camera's azimuth pointing and center activity location the data from BOLTEC lightning location system were applied. Further, real-time video stream data from these cameras go through UFO detection system analysis for effective data compression. Radar data from Mekorot Rain Enhancement project weather radar (with 200km range) as well as cloud top temperature information (CTT) taken from images of the GSM satellite, radiosonde information obtained from Bet-Dagan, Israel and Adana, Turkey were also applied into analysis [72].

In two winter seasons 2005/6 and 2006/7 most of the nights out of 31 selected for observations there had unclear line-of-sight in the thunderstorm regions and TLE observations were not possible, thus only 10 nights provided successful images of TLE over the storms. All of them were made over the sea between Israel and Cyprus. In total, 66 TLE observations were obtained during 2 winters: 32 for 2005/6 and 34 for 2006/7. On Figure 37 different examples of sprites observations illustrated, taken from (A) Tel-Aviv site on October 31st 2006, (B) from Mizpe-Ramon site on January 14th 2006. Below is the table classifying observed TLEs according to the location, date and type, elves or sprite [71].

Winter	Location	Date	# of sprites	# of elves	Total	Total
2005/6	MR	12-13 Jan 06	2	1	3	**32**
	MR	14-15 Jan 06	15	3	18	
	TA	6-7 Feb 06	7	2	9	
	TA	18-19 Mar 06	2	0	2	
2006/7	MR	27-28 Oct 06	3	0	3	**34**
	TA	30-31 Oct 06	2	2	4	
	TA	31Oct-1Nov 06	4	0	4	
	TA	5-6 Dec 06	3	0	3	
	TA	19-20 Jan 07	15	1	16	
	TA	12-13 Feb 07	3	1	4	
Total		**10**	**56**	**10**	**66**	**66**

Table 5. Two winter observation review of TLE in the vicinity of Israel [71].

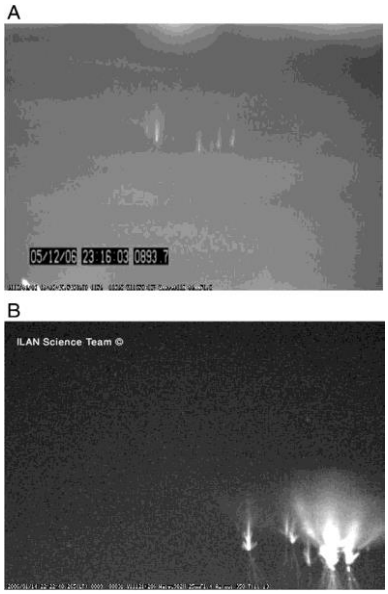

Figure 37. CCD camera images of sprites (A)-from polluted Tel-Aviv site on October 31st, 2006, (B)- from Mizpe-Ramon site on January 14th, 2006 [71].

Based on the results obtained in this study, numerous scientific assumptions and conclusions were made. It was found that sprites are formed only from positive cloud to ground lightnings (+CG). The pattern was also derived in how often sprites appear (with a maximum gap of half an hour and a minimum of

1.57 minutes). It was also noticed that most frequently sprites appear in the columnar form in groups of 4 to 9 elements. It was revealed that the sprite elements are arranged in a circle (or ellipse form depending on the viewing angle) around the parent lightning with no columns inside of it. Furthermore, 55ms was found to be mid-range time delay between ELF transient of parent lightning +CG and its sprite. [71]

3.4.2. Infrasound observations of Sprites in Israel

French Atomic Energy Commission was the first organization who have performed the infrasound observations of the sprites during Nuclear Test Ban Treaty (NTBT) and came up with the detection of "chirp" and "inverted chirp" infrasound signatures of the sprites.

First theories of the pressure produced by sprites were proposed by Bedard [121]. The definitions "chirp" and "inverted chirp" belongs to Liszka [122] who have measured infrasound data and revealed tens of seconds long pressure pulses in the range from 0.01Pa to 0.1Pa. An interesting moment was in fact that lower frequencies were arriving first, these phenomena were called "chirps". Explanation of it was related to sprites generation variety in altitude and size. When sprites are generated at height of 400km its infrasound get reflected from upper altitudes leading to increase of sound speed, waves damping and attenuation of higher frequencies. That explains why upper-frequency signals of the high-altitude parts of the sprites (80 km) arrive depleted to the infrasound arrays. While the lower parts of the sprite (50 km) produce signals reflecting from the lower altitudes. Signals get reflected and arrive at the infrasound arrays delayed, however with the complete frequency spectrum, starting from low frequencies and ending with the higher ones. The frequency range varying from 2 Hz till 10Hz also depend on the distance till observation point and on the size of the sprite [73].

In the cases, when the higher frequencies arrive before lower frequencies content is called "inverted chirps", which is intuitively explained as sprites occurred on the closer distances where infrasound signatures are direct (with no reflections), thus higher altitude signals arrive after lower ones.

Thus, the main purpose of that project, granted by Israel Science Foundation and supported by (TEA-IS) was to investigate sprite observations data collected by ILAN project during 8 years (2011-2013) over the Mediterranean Sea, in order to identify similar "chirp" and "inverted chirp" patterns [73].

ILAN project provided sprite observations data collected by equipment described in the section (3.4.1. TLE observations in the vicinity of Israel) during winter seasons.

Main equipment used for the project was Israel Infrasound array with MB 2000 micro-barometers connected to Quanterra Q330 digitizers.

This array was chosen out of two available arrays in Israel Infrasound network. First array (with 1 km aperture) located in Meron town has five

elements, another array (with 5km aperture) in the Dimona (Negev desert) has four elements. Small aperture array is more suitable for sprite detection due to appropriate wavelengths, so the data from Meron array were more suitable for the project [73].

Using ILAN data approximate infrasound arrival time interval was calculated by subtracting the distance travelled by sound at max speed 340m/s (at sea level) and min speed 250 m/s (at 90 km altitude). Thus 10 minutes time window was estimated for infrasound to reache arrays. Then waveform analysis was made using Progressive Multi-Channel Correlation (PMCC) algorithm. Last step was comparing obtained results with WWLLN (World Wide Lightning Location Network) lightning activity observations.

That process was performed for all sprites detected by ILAN. Out of 330 sprites by infrasound pressure were detected only whose sprites which had 8 or more structural elements. Infrasound arrays are not able to identify any pressure from average single-sprite which emits only less than hundred MJ, as it requires at least 0.1 Pa pressure, which can be produced by sprite depositing hundreds of MJ [73].

For example, on November 9, 2012 at Meron, station infrasound array detected pressure pulse corresponding to the sprite optically observed by ILAN. Figure 38 illustrates the frequency and pressure parameters of that pulse aligned along the timeline. Next figure 39 shows “inverted chirp” signal of the same event after PMCC analysis, which proves intuitive explanation of “inverted chirp” origin because that sprite was detected from the distance fewer than 200 km [73].

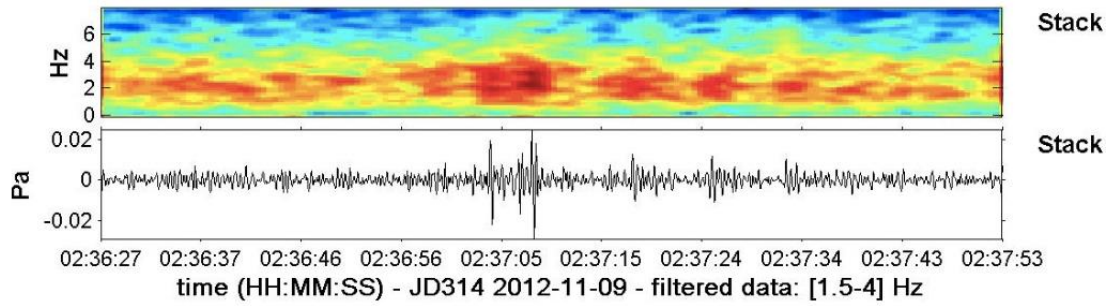

Figure 38. Pressure pulse and frequency spectrum of the sprite observed on November 9, 2012 [73].

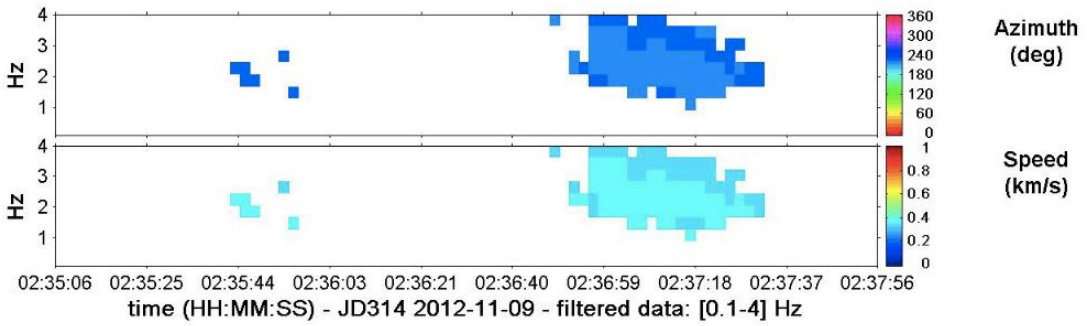

Figure39. Inverted chirp signal visualization after PMCC analysis [73].

3.4.3. High-speed video recording of TLEs over Europe

History of ground observations of upper atmospheric lightning in Europe starts from summer 2000, where usually optical cameras with frame rate no more than 25-50 frames/s were used as the main instruments. However, the USA has embedded the high-speed camera in its TLE investigations. For the first time, high frame rate video was recorded over Europe in December 2008.

Observations were made over the Mediterranean Sea region during three nights in winter to obtain recordings of the sprites and elves over thunderstorms [74].

The instrument used for high-speed recording was Phantom v7.3 CMOS camera which was attached to a gated image intensifier with phosphor persistence (1μs). The wide-angle lens with 50 focal length and f/1.4 aperture allowed to see close events while far events were recorded with 85 mm focal length and f/1.4 aperture lens. High-speed camera was aligned with another 25 frames/s LLS (low-light sensitive) recording camera and with GPS in order to be triggered and time-synchronized respectively. That assembly provided the video recordings at the frame rate starting from 6888 to 15037 frames/s according to the selected mode (standard or turbo) and picture resolution [74].

December 2nd (4 sprites and 14 elves) and 10th (12 sprites and 8 elves) and 20th of January (2 sprites and 3 elves) during that mission were the most successful nights for TLE observations. During those three nights, observations represented halos preceding the sprite. Halos were not recorded alone, only with sprite and elves. Conversely, each halo was preceded with elve 2ms before.

High frame rate video recording camera allowed to analyze development, luminosity phases of the sprite according to its timing distribution as well as total duration. According to the analyzes, regular development phase duration of the sprite differs from 7.5 ms to 80 ms, persisting luminosity phase lasts for 30 ms and the average total duration is approximately 40 ms. (see figure 40) [74].

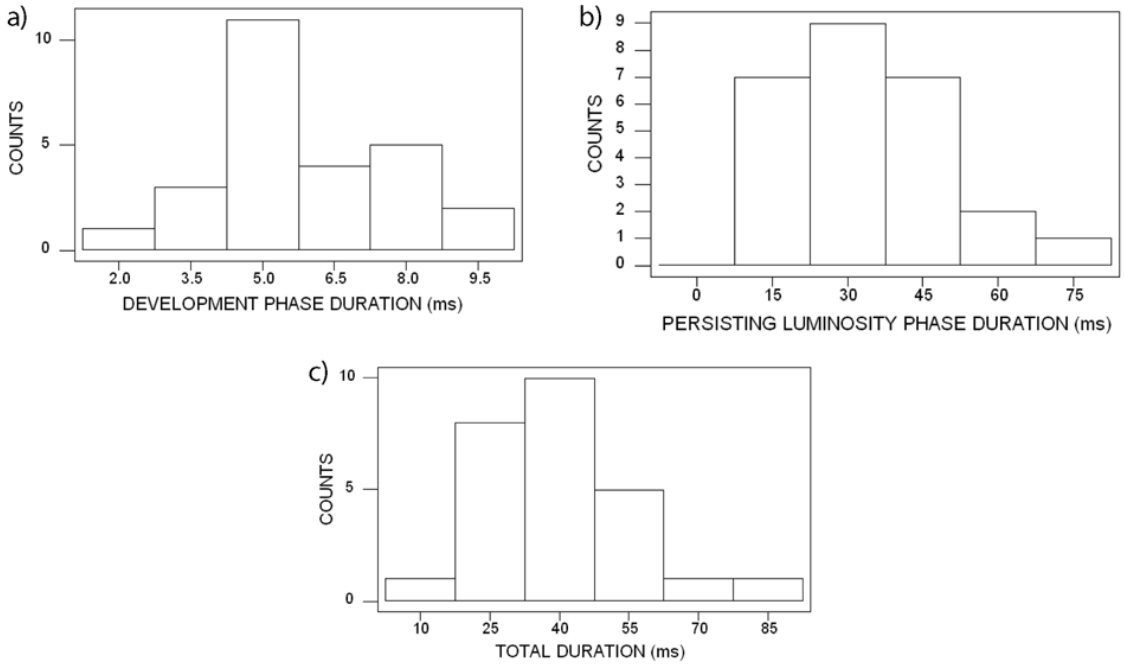

Figure 40. a) Distribution of sprite development phase duration, b) Distribution of sprite luminosity phase duration, c) Distribution of sprite total duration [74].

3.4.4. VLF and TLE Correlation

VLF (Very Low Frequency) remote sensing it is a powerful diagnostic tool for investigation of disturbances in the lower ionosphere. A large number of natural phenomena like aurora, solar frames, meteors, Gamma-rays and even seismic activity were studied with the help of VLF remote sensing system [75].

Earlier it has been represented theoretically [76] and even practically [77] that VLF signals perturbations while propagating through the ionosphere are also coincide with sprite halo occurring above the thunderstorms.

In order to prove relation between VLF perturbations and TLEs occurrence two AWESOME (Atmospheric Weather Electromagnetic System for Observation, Modeling and Education) VLF remote sensing systems were used which can record narrowband and broadband GPS synchronized data and store it. One AWESOME system locates in Algiers, Algeria and another in Sebha, Libya. That systems are part of International Heliophysical Year (IHY) with a long-term foundation from Stanford University. Each of AWESOME system consists out of following elements:

- North-South oriented magnetic loop antenna
- East-West oriented magnetic loop antenna
- Preamplifier
- Line-receiver
- GPS antenna

In that project, the data collected during Eurosprite-2007 campaign was used for analysis. Eurosprite-2007 is one more mission of capturing images of the TLEs during October and November over the Mediterranean Sea with the low-light cameras from different areas of France and Spain [78]. 16 sprites and 1 elve were detected by Eurosprite observations on 12^{th} to 13^{th} October passing night. On figure below Event 1 (top left) illustrates the sprite image taken above the receiver. In the middle of figure 41 map of transmitter-receiver locations named as DHO, NSC, ICV, HWV and HWU is shown [78]. Value 0.2 dB was taken as the minimum in the perturbation amplitude detection range. Top right shows the image of an elve appeared far from DHO. VLF perturbations on NSC of event 1 has 200ms onset duration and 3db amplitude on DHO. Onset duration of elve (event2) recorded in NSC signal is 120ms and 180ms in DHO signal. HWU receiver shows only sferics as it is distant receiver for both events [78].

Those recordings were done for all events of Eurosprite-2007 and showed similar results which proves that time of the VLF signal perturbation and a sprites' occurrence times match within 100ms, thus VLF perturbations may occur in relation with TLEs.

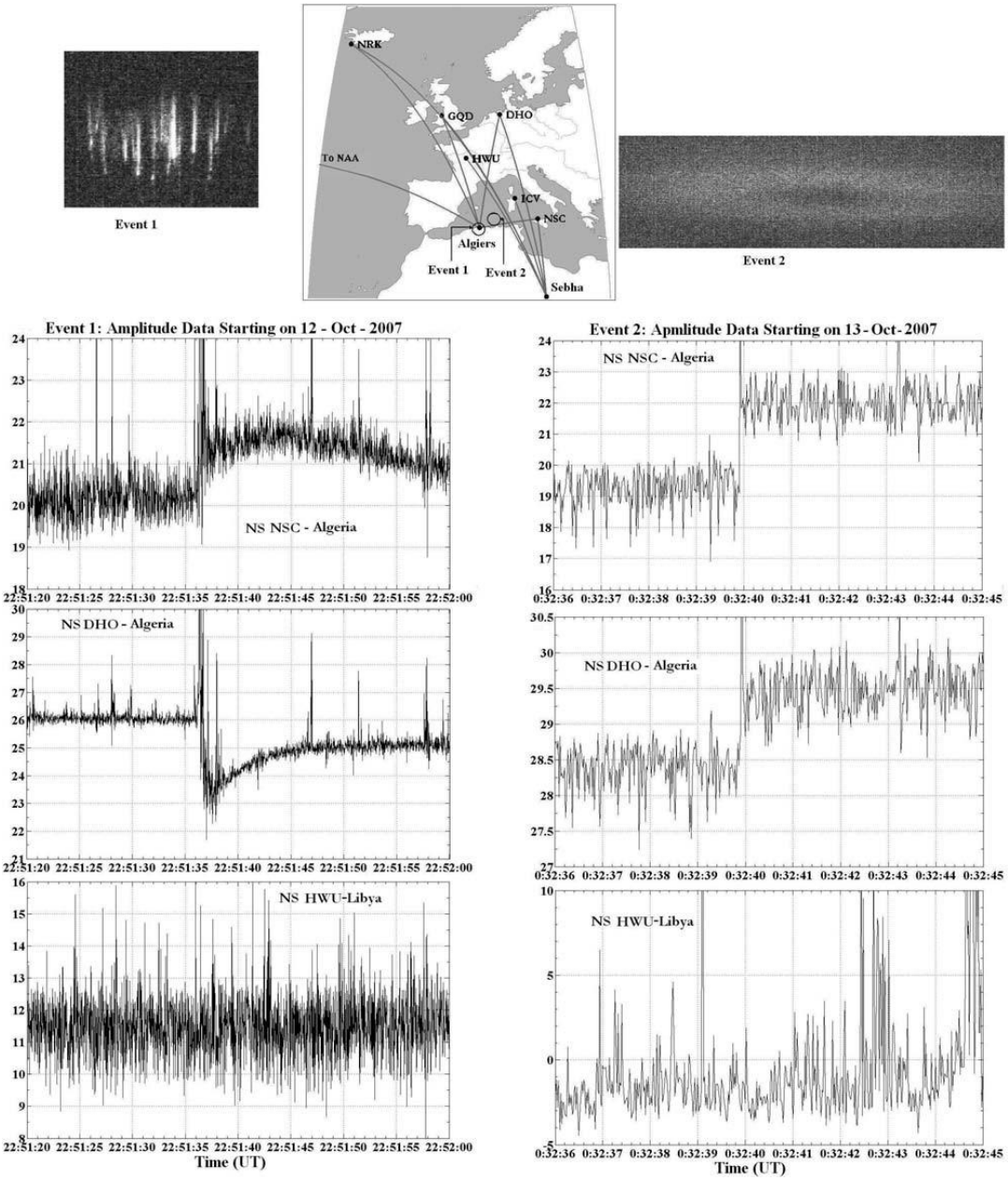

Figure 41. Event 1 – sprite (top left), Event - 2 elve (top right) captured on Eurosprite-2007 mission. Geographical location of VLF transmitter-receivers (top-middle). Plots of VLF perturbations of events 1 and 2 recorded on NSC, DHO and HWU receivers (bottom) [78].

Chapter 4 - Lightning Location Techniques

4.1. Ground-based techniques

The majority of the ground-based Lightning Location Systems are constructed on one of three fundamental Lightning location techniques or on their combination.

4.1.1. Time of arrival.

Time of Arrival is a well-known low-cost technique to determine an object's position using several distributed receivers at known locations. The main idea of TOA system is to measure the arrival time of the received signal at the GPS synchronized detection stations and calculate the signal's position from the delays. Time detection accuracy does not exceed 300 ns. This operation is also called multilateration [123].

Time of Arrival method is applied to the several lightning detection systems, for example, ATDNET is Thunderstorm detection system used by Met Office since 1986. Also, Florida LPATS (Lightning position and Tracking System) and British ATD (Arrival Time Difference) networks apply this method [91].

The electromagnetic field generated by lightning discharge in the Very Low Frequencies (VLF) range mainly around 10 kHz to 14 kHz can be detected at stations with different time-shift. Receivers recognize each specific lightning according to their unique waveform.

Due to low atmospheric attenuation, low frequency electromagnetic waves (SFERIC) can be received over thousands of kilometers away from their source, therefore TOA systems have large detection area. Fast neutralization of radiation emitted from lightning discharge occurs in the lower atmosphere. That is the reason for TOA system's sensitivity to cloud to ground (CG) strokes and low accuracy for detection of intra-cloud (IC) lightning discharges at long range from the station. Furthermore, strong errors detected in the positioning of distant flashes due to their location over the ocean, ionospheric height and soil conduction characteristics [91].

Generally, three TOA measurements from three stations are required to calculate the location (Trilateration).

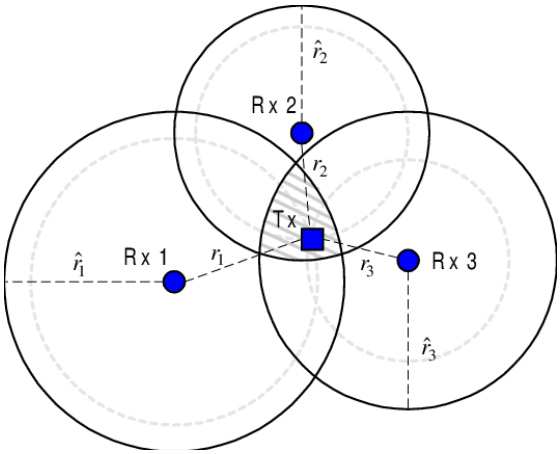

Figure 42. Time of Arrival geolocation method. Trilateration[92]

Sensors from every location provide hyperbolas representing potential locations of the detected lightning strike. Thus, lightning strike location is indicated by the intersection point of all hyperbolas. In the case when lightning strike takes place not inside the stations' triangle hyperbolas given from these three sensors results in two intersections (two possible locations of the lightning strike) which leads to an ambiguity. Nonetheless, to solve twofold ambiguity, it is preferable to have at least four receiver locations, where one of them filters out the noise (See figure 43)

In order to obtain the altitude calculation of the lightning strike, simultaneous sensor measurements of at least five stations are required [93].

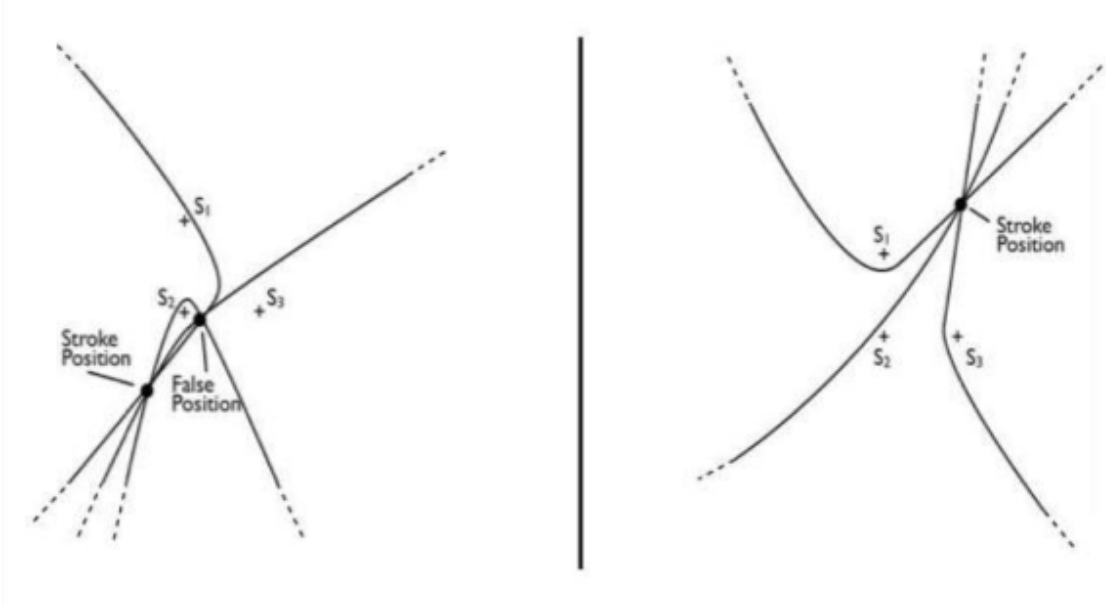

Figure 43. Time-Of-Arrival technique. Twofold ambiguity in the case of lightning strike locations outside the triangle of three sensors (left side). Single intersect point of sensor hyperboles indicating single solution for lightning strike location. (right side) [92].

4.1.2. Interferometer

The fundamental principle of the interferometer is the estimation of the phase difference of the electromagnetic Very High Frequency (30-300 Mhz) band emissions detected between closely spaced pair of broadband antennas.

VHF band is one of the most popular frequency bands used for lightning location techniques because electromagnetic emissions produced by lightning discharges propagates in wide frequency spectrum (near DC to gamma-ray), however, signals in VHF band are most intense and considered to with negative breakdown process. These techniques based on the calculation of the phase or time difference of signals between two or more antennas [93].

Among other methods, the broadband interferometer technique can derive lightning images by recording microsecond scale electromagnetic wave impulses emitted by the negative stepped leader [94].

The first step is to identify the phase difference of detected pulses at used antennas by implementing the discrete Fourier transform (DFT). Next step is to calculate the cosines of the angle between the radiation source and the antennas baseline. After that, the last step is to derive the azimuth and the elevation angles of the source of electromagnetic wave radiation. Interferometer geometry is illustrated in figure 44.

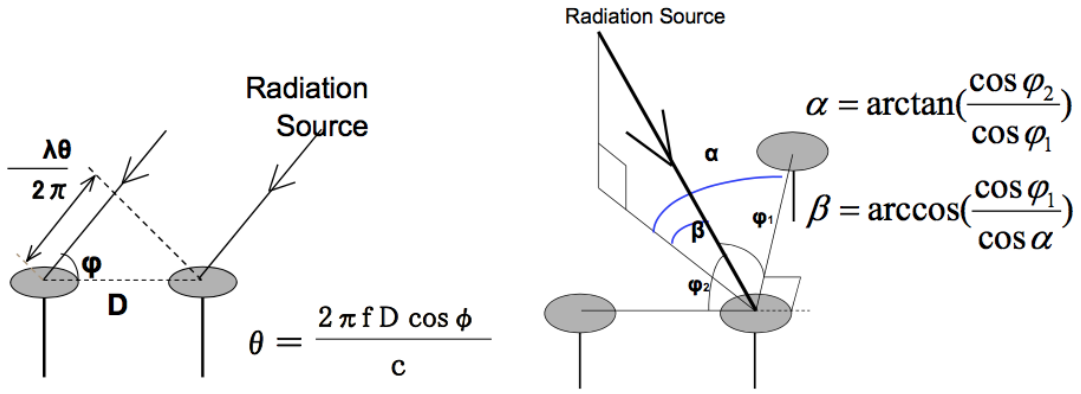

Figure 44. Broadband interferometer geometry [95].

In order to get two-dimensional lightning mapping, it is sufficient to have one broadband interferometer observation station, which provides the azimuth and the elevation angles of the radiation source. While for the determination and visualization of the light propagation in three dimensions it is necessary to have multi-station system (at least two).

First time interferometer system was applied for lightning location during the experiment of rocket triggering lightning in Hokuriku, Japan in November 1996.

In figure 45 below, the optical image of the rocket triggered lightning captured from the 50 m distance is illustrated on the left side. On the right side it is the plot representing the elevation and the azimuth angle of that lightning obtained via interferometry technique from the 36 km away located observation station [96].

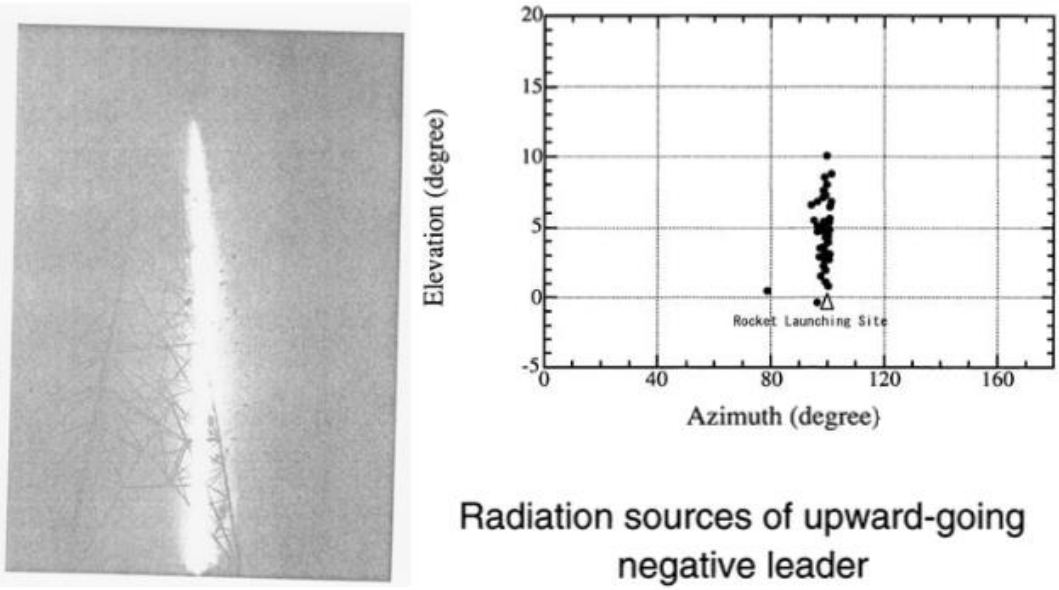

Figure 45. Rocket triggered lightning captured by a camera on the left panel and its VHF interpretation image on the right panel [96].

Despite the fact, that the interferometry technique is the system mostly applied on the ground it was also practiced for lightning source location from the space within the framework of GLIMS (Global Lightning and sprIte MeasurementS) mission due to its very high efficiency.

GLIMS was launched by H-IIB rocket on July 21st , 2012 and located as the payload at the Exposure Facility (EF) of Japanese Experiment Module (JEM) on the board of International Space Station (ISS). The main focus of GLIMS is TLE, TGF and usual lightning observations, clarification of their occurrence conditions, global distribution and rates of TLE as well as the location of VHF radiation sources emitted by lightning discharges. Lightning and Sprite Image (LSI), VHF Interferometer (VITF), Photometer (PH) and VLF Receiver (VLFR) are primary instruments for TLE and lightning detection and location on GLIMS. VITF became the first instrument launched to space with the purpose to locate VHF band lightning source [97].

4.1.3. Magnetic Direction Finder

Another approach for lightning discharge location is magnetic direction finder (MDF) system which is capable to identify the direction of upward-propagating wideband return stroke in its first few microsecond time of field incidence peak [98].

The basic idea of the MDF is a system built out of two wideband vertical orthogonal antennas with North-South and East-West oriented planes, each of them measuring the magnetic field of vertical radiator with a purpose to identify the direction of the lightning location source. In order to achieve this goal, at least two sensors are required, as one antenna station can only define the azimuth angle of the lightning source.

According to the technique the azimuth angle is calculated between the lightning source direction and Source-North plane of the antenna. It is the first step for determining the line going through the sensor and lightning strike. Then the same process applied to at least two other sensors and the intersection of these lines identify the exact location of the lightning strike as illustrated on figure 46 [99].

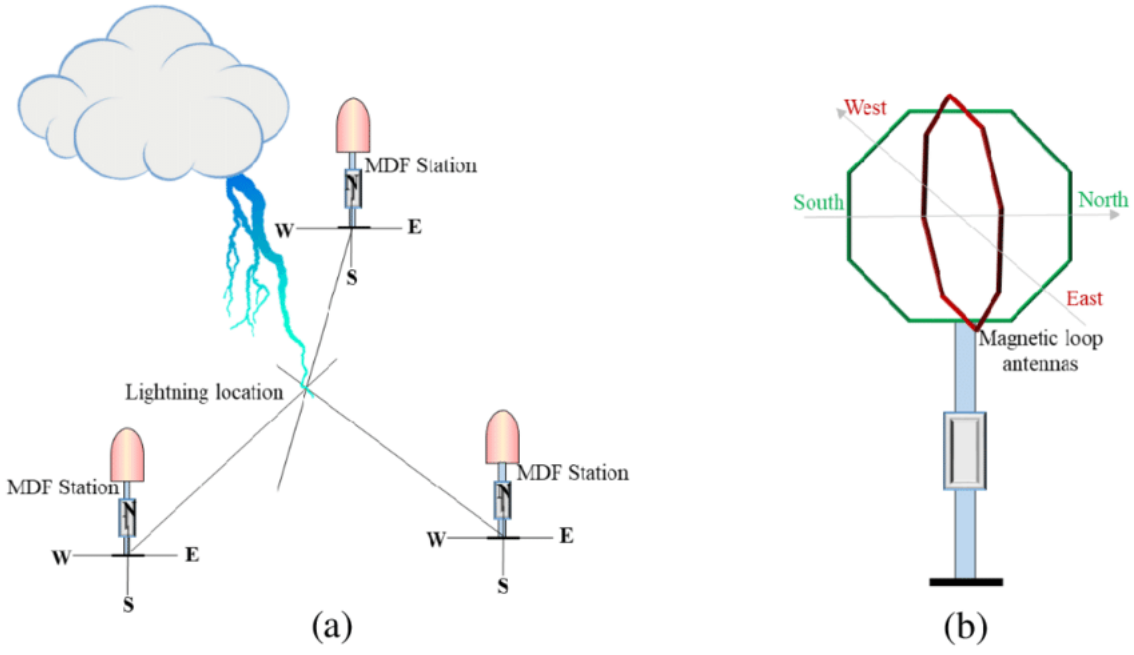

Figure 46. Magnetic Direction Finding technique geometry [100].

The main reason for the multiplicity of the sensors is a minimization of an estimation error or so-called “angle disagreement”. Metal objects, buried cables and other conducting-type side conditions are provoking up to 10 ˚ serious change in the magnetic field incidence. For the purpose of obtaining accurate lightning location results “site error correction” implementation need to be applied to the

MDF sensors. These “site error correction” in the form of correction function can be derived from the regular site errors from the historical data of every sensor and taken into consideration in the algorithm. Classic “site error correction” function applied for MDF sensor is illustrated in figure 47 below [101].

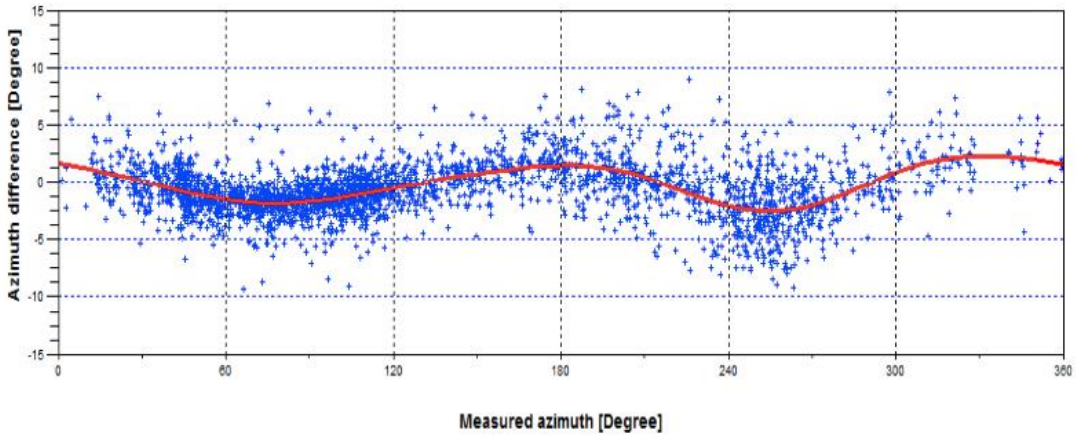

Figure 47. Two sinusoidal error function of a magnetic direction finder sensor [101].

4.2. Space-based techniques

The concept of high-quality observations of the lightning on a global scale directly from space is based on two fundamentally different research techniques, namely, the technology of optical observation of lightning discharges emitted in different frequency ranges with the help of high-resolution modern instruments and the method of detecting and analyzing the electromagnetic signatures of lightning radiation. As well as the third possible variation of observations’ method is the combination of the two above mentioned techniques.

4.2.1. Optical (OTD, LIS, GLM)

Lightning discharge propagates in a wide spectrum of electromagnetic signals which includes VLF, LF, MF HF, VHF, NIR, UV and visual spectrum as well as Gamma and X-Ray emissions.

Regardless of how technically advanced are parameters of the optical instruments used on the ground stations, due to limited line of sight from Earth surface, none of them can compete for the opportunities that are opened for observations from satellites in near-earth and geostationary orbits. In the previous chapter, lightning location systems mainly oriented on TLE type lightning were described in detail. While here the special attention will be paid to the optical

lightning detection instruments used for global lightning mapping oriented for all type of discharges, ground-to-cloud, cloud-to-ground and intra-cloud.

The significant role in global lightning mapping and lightning flash distribution identification from 1995 till 2013 were obtained as a result of collected data from two major projects.

First of them is Optical Transient Detector (OTD) instrument developed by NASA which were launched on board of MicroLab-1 microsatellite in 1995 with the capability to collect lightning data during both daytime and nighttime. That instrument represents the optical type of technique, to be precise the camera with 100˚x100˚ FOV, used for detection of optical scene momentary changes which indicate the appearance of the lightning discharge [102].

Data obtained from the OTD confirmed the scientists' understanding that lightning can be a key indicator of changes in atmospheric processes. OTD contributed to the improvement of the recognition of lightning indicators in forest fire detection systems, in systems for recognizing the dynamics of storms as well as in precipitation processes. The OTD compiled a five - year worldwide lightning report from 1995 to 2000. Moreover, between 1995 and 1996, the it recorded about 1 million lightning flashes. The OTD provided a wealth of information, collected in 3 minutes observation intervals, sufficient to compile a global map of lightning propagation. With a swath surface of 1300x1300 km, the OTD lightning imagery provided full coverage of the earth's surface in 2 days. Using these data, the annual number of lightning on Earth was calculated (1.2 billion), as well as the global frequency of flashes per second (40 flashes/s).

Another project is Lightning Imaging Sensor (LIS) instrument launched on the board of Tropical Rainfall Measurement Mission (TRMM) in 1997 which were operational till 2015. That was a collection of calibrated
instruments with the ability to detect and locate lightning discharges on the storm-scale resolution at millisecond timing. Staring imager in LIS consisted out of sensor with wide field-of-view lens and narrow-band filter along with high-speed CCD detection array [103].

As well as OTD, LIS has served as a successful tool of space-based lightning observations for more than 17 years measuring the amount, radiation energy, and rate of flashes worldwide. Data collected by LIS were used for further research in thunderstorm climatology, atmospheric chemistry, microphysics and dynamics of lightning, latent heat releases, rate of distribution of precipitation and presence of ice. Daytime and nighttime observation capabilities of LIS as well as 4 km spatial resolution and millisecond timing, and the main factor of improved sensitivity by a factor of 3 have resulted in a significant increase in detection efficiency to 90 %. This is a substantial improvement compared to the detection efficiency of the OTD (40-65%), although the LIS had a smaller coverage area with 600x600 km footprint. A critical advantage of TRMM was the possibility to compare the LIS data simultaneously gathered with four instruments onboard providing infrared, radar, microwave, and visible observations. This benefit

provided an opportunity to specifically test a series of scientific hypotheses related to the relationship between lightning over tropical clouds and updrafts [103,127,128].

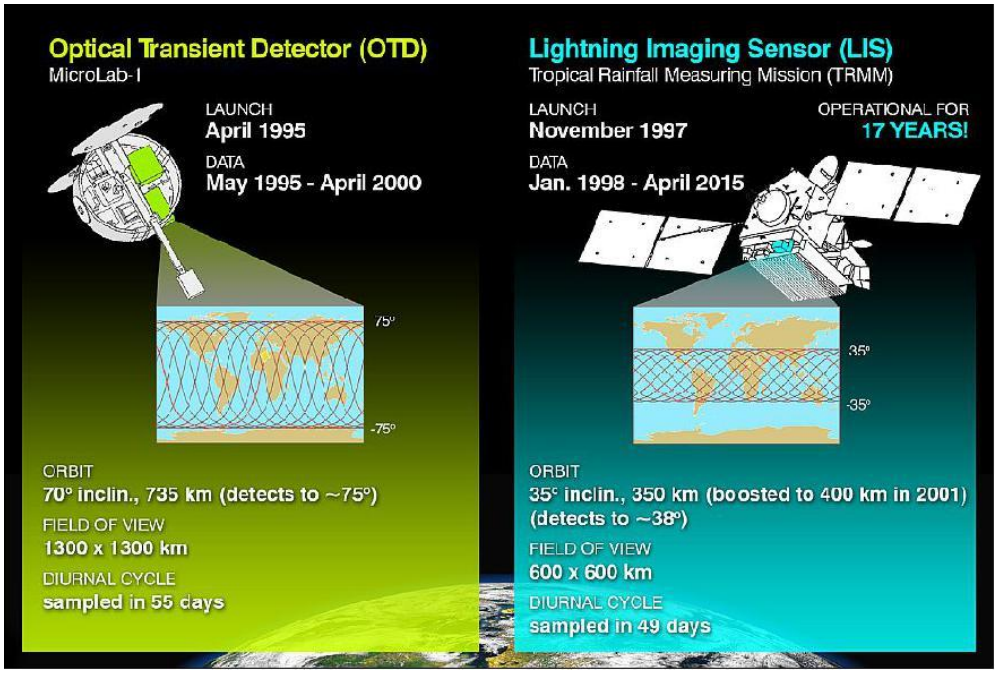

Figure 48. OTD and LIS projects' short description and coverage areas [103].

All previously mentioned satellites were operating on the near-earth orbits. Thus, GOES-16 (Geostationary Operational Environment Satellite) became the first geostationary satellite from the GOES-R series developed with the purpose to serve as weather satellite providing imagery of the Earth in 16 spectral bands. It carries first Geostationary Lightning Mapper (GLM) on its board as the main instrument. GLM is the single-channel and NIR transient optical detector which captures short-lived emissions of light since 2016 and still operational. That includes both CG and CC type lightning detection under day and night time conditions [104], [105].

4.2.2. Electric and magnetic

All types of lightning discharges consist of different stages and each of them has a characteristic and unique electromagnetic field signature.
Thus, another principle of lightning investigation from space is the magnetic field and the electric field measurements. Typically, those measurements are gathered with the help of antenna type sensors and analyzer. The frequency range of the instrument can vary with an emphasis on the type of lightning. [106]

A prime example of the satellite carrying instruments which are capable to investigate both the magnetic field and the electric field characteristics of lightning discharge is TARANIS. The device called IME-HF (Instrument for Electric field Measurements – High frequency) responsible for identification of HF electrostatic or electromagnetic signatures of TLEs and consisting out of high-frequency antenna measuring and HF- Analyzer. While instrument IMM (Instrument for Magnetic Measurements) is dedicated to detect 0+ whistlers (specific kind of electromagnetic waves)- information bringing clarity to TLEs' and TGFs' generation mechanisms. IMM identify sources of heating, perturbations of VLF signals [106].

Chapter 5 - Analysis of suitable instruments for TLE detection by nanosatellites.

Nanosatellite or so-called CubeSat is the typical research class of spacecraft. They are defined to weigh less than 10 kg and can vary in size of 1U, 1,5U, 2U, 3U or 6U where 1U is the standard CubeSat Unit with the cube-shaped structure in 10x10x10 cm. The popularity of the CubeSat in comparison with other types of satellites is defined by the relatively low cost of the development process and access to space.

In conjunction with low cost, low mass and compactness CubeSat should also meet technical requirements of low power, low instrument complexity, short ground contact as well as be considered for a short mission as it has a limited on-orbit lifetime with no service.

Thus, instruments for TLE detection on the board of CubeSat flying on Low Earth Orbit (LEO) should comply with above-mentioned requirements.

For an overall view of a typical equipment applicable for CubeSat conditions previously applied and tested two different nanosatellite projects FireFly and LINSAT will be considered.

5.1. FireFly

FireFly is 4kg CubeSat mission with 3U (10x10x34 cm) configuration directed by NASA/GSFC (Goddard Space Flight Center) funded by National Science Foundation (NSF). Firefly's circular orbit is on the altitude of 400 to 600km with the inclination more than 50°.

The main goal of that project is to study the nature of TGFs (Terrestrial Gamma-ray Flashes), exploring the origin of high energetic electron beams generating them, TGFs' effect on the inner radiation belt as well as their effect on the space weather and upper atmosphere. With the help of varying type of instruments used on board, Firefly is targeted to origin the high energetic electron beams generating TGFs, to investigate the TGFs' frequency of occurrence and its dependence on TGF's physical parameters (size), degree of illumination, energy flux, and other characteristics of TGFs. Among the questions that scientists investigate with the help of Firefly, they also hope to find a relation between TGFs and different types of TLEs. Firefly

To achieve the stated objectives CubeSat is equipped with the following instruments:

- GRD (Gamma Ray Detector) – with the goal to measure energy and time of arrival of X- and Gamma-ray photons (in the range between 100 keV to 10 Mev) and energetic electron flux (in the range between 100 keV to 2

MeV) over thunderstorm. It consists of scintillator crystal in 76x65 cm^2 x 1.5 cm volume.

- OLD (Optical Lightning Detector) – capable of time tagging (within 1μ) the optical signal of the lightning discharge. That instrument includes four Hamamatsu S9195 overlapping PIN photodiodes considered for lightning localization on one out of twelve areas. (Figure 49) There three of the photodiodes have filters in wide/ visible band while the last photodiode has filter in the specific 777.4 nm band. Since the FOV on each photodiode increases by +/-22.5 °, then at a flight altitude of 500 km, the furthest observation point will be flash at a distance 500km*cos(22.5°)=541 km.
- VLF (Very Low Frequency) Receiver with 3m BeCu Gravity Gradient Boom (GGB) performing the role of monopole antenna - working in the range of 500 Hz to 500 kHz to evaluate signature of the single-axis electric field of lightning for every TGF observed [108], [109].

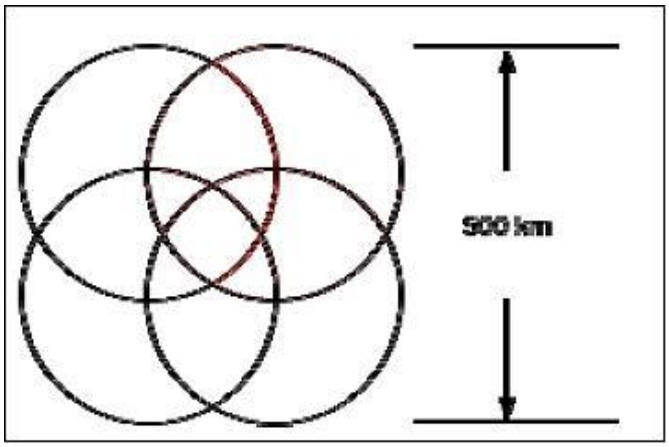

Figure 49. Working principle of OLD instrument on board of FireFly CubeSat [109].

In 2013, November 20 Firefly was launched to the near-circular orbit (500 km) on the board of ORS-3 by Minotaur I. First contact with CubeSat was performed on January 6, 2014, and all systems' healthiness was validated. From the next contact, the team was planning to switch the satellite to science mode. The total lifetime of Firefly was expected to be a minimum of 3 months and a maximum of 1 year. The status of the mission to the 2017-11-01 was still operational [109, 129].

5.2. LINSAT

LINSAT (Lightning Nano-Satellite) is an Austrian planned project consisting out of three nanosatellites constellation. CubeSat in the size of 20 cm and 5 kg mass is dedicated to identify signatures caused by electromagnetic phenomena called Sferics, locate them by flash rate and differentiate according to the lightning type. For that purpose, the satellite needs to be launched to the LEO around 800 km altitude. Observations of Sferics on the board of LINSAT planned to be measured by a broadband radio-frequency receiver in VHF range. That frequency range choice is explained by source mechanism dependence of Sferics' wave power peak frequency variation (from Hz to GHz). Thus, for terrestrial power peak frequency of Sferics occurs at VLF and HF range, while the trans-ionospheric Sferics propagating till LEO peak at VHF range. RF Receiver also investigates transient EM waves in the range of 20 to 40 MHz. Another reason to select VHF is the fact that LF radio emissions often are not capable to penetrate the ionosphere, so may not reach the LEO orbit [110].

Payload instruments of the satellite is a combination of the following units:

- Gravity Gradient Boom (GGB) performing the attitude control and acting also like the lightning detection antenna.
- Three orthogonal antennas.
- HF and VHF Electronics.
- Event detector and adaptive filtering.

In high voltage chamber of Graz University of Technology and in the laboratory of Space Research Institute of Austrian Academy of Science measurement experiments of the LINSAT productivity were successfully performed. In order to test LINSAT payload, two different measurement operations were performed in terrestrial and in a simulated environment for lightning type discrimination and its geolocation. One of the measurement operations was for artificial lightning (from 700 kV to to 1.8 MV) generated in the HV chamber in the laboratory and obtained results showing similarities of natural lightning and captured images. Another campaign was performed for natural lighting detected in an urban environment in Austria on June 30, 2010, using a digital oscilloscope and broadband antenna. Special emphasis was placed on time series, narrowband carries, and noise features to obtain specific parameters of the payload. It was statistically found how unique signature of lightning signal is respective to specific rise or fall time of that stroke. According to the achieved results, LINSAT payload is capable to receive MF, HF, and VHF

lightning signals on the ground. Pre-selectors are dedicated to avoiding detection of false signal. All LINSAT electronics were tested on Matlab, as well as adaptive filters which are intended to separate ionospheric and magnetospheric impulses from terrestrial EM signals [110, 111].

5.3. Summary

From numerous examples of satellites studying the TLE phenomenon or similar types of events, it can be concluded that all possible variation of payloads used on them can be divided into the following types: optical (these are telescopes, cameras), devices that measure the energy coming from various radiations (such as photometers), instruments that study spectra of received signals - spectrometers, equipment for measuring the level of radiation of signal and instruments fixing the electromagnetic signature of events. Analysis of the requirements for potential devices which are necessary for the detection of TLE on board of the nanosatellite will be carried out based on the collected data. This analysis will consist out of the following sub-items.

1) Spatial requirements for TLE detection.

Based on the previously studied examples, there are 3 methods for detecting lightning of thesis interest, namely, from the ground using ground stations, from the air using an airplane or balloon, and the third from space. Since the main goal of this work is the detection of TLE lightning using a nanosatellite, the focus is on the spatial requirements for the conditions of detecting TLE from space, which, first of all, is the choice of the most suitable orbit. Based on the collected data from space, the detection of lightning is possible from LEO, from MEO and GEO orbits. However, the advantage is given to the LEO orbit (500-1500 km) for the following reasons; the satellite is closer to the source of the TLE and therefore able to take clearer images and measurements than from a farther distances. LEO is the most suitable and convenient orbit for launching nanosatellites and the third reason is better protection from radiation through the Earth's magnetic field.

2) Physical requirements for equipment.

The physical requirements for the instrumentation are strictly limited by the regulations for meeting the needs of nanosatellites, namely; size (dimensions), respectively low weight, limited budget, limited duration of the mission, since there are fewer opportunities to install spare equipment due to restrictions in weight and dimensions, endurance of materials to a sharp temperature drop corresponding to low orbits.

While little-known phenomena like TLE are studied sometimes simultaneously with such phenomena as TGFs, auroras, UHECRs, gravity waves, OH airglows, their identification occurs in the subsequent process of analyzing the data obtained during the observations.

The requirements for the detection of specifically TLE will be derived empirically by the most frequent and most successful application of certain parameters of the tools used in the systems described in the previous chapters.

Thus, the next step will be to parse and select each instrument in regarding to known (since not all instruments have information about their technical parameters in the public domain) and required parameters. The first stage will consider the analysis of optical devices used in the missions listed above, the next stage is the analysis of photometers, spectrometers and DUV detectors, and the last analysis of the RF type instruments. X and Gamma ray detectors is not considered as potential type of instrument for TLE detection as they were predominantly designed for TGF detection and were used in combination with other type devices. For this purpose, a table has been compiled showing the most important parameters typical for optical devices.

Satellite	Model	Type	Pixel Resolutin	(FPS)	ISO	Temperature	Power	S/N ratio	Shutter speed	Lens	Weight	Size	Wavelength	FOV (deg)	Spatial Resolution
ASIM	MMIA	CCD	1024x1024	12fps	camera 1 - $3.2x10^6$ camera 2 - $4.2 - 10^7$	op	200 W	N/A	N/A	N/A	314 kg	122x134x99 cm	N/A	20x20 ram, 80x80 nadir	300-600 m 300-400 m
THOR	NIKON D4	CMOS	1920x1080	25fps	A 12800 (max)	0-40 C (op)	10.8 V	N/A	1/25 s	58 mm nocturnal lens	1340 g	160x157x91 mm	N/A	N/A	N/A
FORMOSAT-2	ISUAL RSI	CCD CCD	512x80 N/A	180 fps N/A	N/A	op	161 W	N/A	N/A	N/A	N/A 114 kg	N/A	RSI- For Pan: 450-900 nm For MS: B1 = 450-520, blue B2 = 520-600, green B3 = 630-690, red B4 = 760-900, NIR	ISUAL - 20x5 RSI - (+/- 45 degree)	RSI: 2 m for PAN 8m for MS
TARANIS	MC-U	CCD	512x512	N/A	N/A	op	N/A	N/A	N/A	N/A	N/A	N/A	N/A	N/A	N/A
Tatiana-2	MTEL	T1- Pin-hole trigger camera T2-Zoom-in camera T3- Spectrophotometr	N/A	N/A	N/A	op	6 W	N/A	N/A	N/A	4,5 kg	150mm x 144.5mm x 120 mm	50-400 nm (UV PMT Hamamamtsu R5900M64) 500-800 nm (Red CCD Hamamatsu S9736)	11	T1 - 160x160 km T2 - 5x5 km
CHIBIS-M	DCP		1000x1000	15 fps	N/A	op	N/A	N/A	N/A	N/A	N/A	N/A	N/A	N/A	300 m
TUS	2 pin-hole camera		256	N/A	N/A	op	N/A	N/A	N/A	N/A	N/A	N/A	300-400 nm (256 PMT Hamamatsu)	N/A	5x5 km
RELEC	MTEL-2		N/A	N/A	N/A	op	8 W	N/A	N/A	N/A	3,9 kg	500mm x 123mm x 77mm	300-400 nm (Hamamatsu H7546A) 600-700 nm	N/A	160x160 km2
EXL-98	1- WFOV camera 2-Color camera 3- NFOV camera 4-N2 (-) NFOV camera 5-N2 (+) NUV imager 6- NIR imager		N/A	N/A	N/A	N/A	N/A	N/A	N/A	N/A	N/A	N/A	1- 400-740 nm 2- 400-740 nm 3- 400-740 nm 4- 427.8nm 5- 337.0 nm 6- 0.9-1.7 μm	55x43 15x12 9.3x7 9.3x7 10.8x 8 11x11	N/A

Israel	Watec 100N	CCD	811x508	25 fps	N/A	(-10)-40 C	10.8-13.2 V	50dB	1/250-1/100000 sec	12 mm, f/0.8	125 g	42x44x53 mm	N/A	N/A	N/A
	Watec 902H	CCD	811x508	30 fps	N/A	(-10)-40 C	10.8-13.2 V	46dB	1/250-1/100000 sec	25 mm, f/1.4	90 g	35.5x36x58 mm	N/A	N/A	N/A
High-speed	Phantom v7.3	CMOS	800X600 32x16	6688 fps 500000 fps	4800 ISO/ASA monochrome 1200 ISO/ASA color	0-40 C	24 VDC/1.5 Amp	from 2 ms to 1µ	N/A	N/A	3.18 kg	10.9x10.16x24.13 cm	N/A	N/A	N/A
MicroLab 1	OTD		128x128	N/A	N/A	op	3 W	N/A	N/A	N/A	2 kg		777.4 nm	1300x1300 km	10 km
TRMM	LIS		128x128	N/A	N/A	op	35 W	N/A	N/A	N/A	25 kg	20x37 cm	777.4 nm	600x600 km	N/A
FireFly	OLD		N/A	N/A	N/A	N/A	0.18 W	N/A	N/A	N/A	N/A	N/A	777.4 nm Hamamatsu S1995	+/- 22.5	541 km

Table 6. Optical instruments explored in different TLE observation missions and their main parameters. (op-operational)

Based on the above illustrated table 6, conclusions can be drawn regarding the most common indicators for the detection of TLE using optical instruments. One of the most important parameters is the spectral range of signals to which the device will respond. According to the table, the most favorable spectral bands are NUV and IFR in the ranges from 300nm till 740 nm and specifically 777.4 nm.

Almost all devices are either CCD or CMOS type optics. Pixel resolution requirements are in the middle range between 508 and 1080 pixels. Pixel resolution defines a number of pixels displayed on each inch of image. So higher the number of pixels then higher the possibility to fix a small event. This parameter is closely related to spatial resolution of instrument which also preferable to be high, as higher the spatial resolution then higher chances to resolve small flashes. Of course, this parameter depends on the exact height of the satellites' orbit and varies with the height of the observed thunderclouds, it cannot be as stable as for missions exploring the earth's surface. Spatial resolution of 160x160 km is the most common and average used value.

At the same time, there are other related parameters in the table, such as ISO, shutter time and FPS (frames per second). The higher the ISO, the brighter the image is, which is a positive factor for shooting lightning at night. On the other hand, high ISO results in a high level of noise on the image. However, if you take a low ISO value, this leads to an automatic increase in the shutter time, which is absolutely unacceptable for filming high-speed processes, in our case, fixing lightning that appears for just a millisecond. The number of frames per second must be at least 25 for lightning shots not to be blurry.

Based on nanosatellite mass limits of approximately 10 kg, optical instruments such as MMIA weighing 314 kg, RSI weighing 114 kg and LIS weighing 25 kg can immediately be excluded from this list.

Despite the fact that the temperature in low orbits varies from -65 to +125 ° degrees of C, which is a quite harsh environmental condition, the design of the satellites, as well as the thermal protection of the subsystems, provides protection against sudden drops and extremely low and high temperatures. Thus, it can be deduced from the table that the average temperature range (-10-40) in which some of ground-based cameras (Phantom v7.3, Watec902H, Watec 100N) can operate coincides with the temperature range (0-40) of the camera (NIKON D4) previously operated in space. From this fact, it can be concluded that cameras used on the ground are also applicable for work on the same orbits.

The total power that can be obtained on a board of nanosatellite comes from parameters such as the size and power of solar panels, power and capacity of the batteries used, which in turn depend on the varying size and weight limitations of the nanosatellite. In a very similar disaster monitoring experiment using nanosatellites constellation [130], the peak value of the power consumption level for the similar optical payload is 7 watts. Based on this example and the values shown in the table, and considering the many unknown factors that affect

the final value, it can be assumed that power consumption within 10 watts is acceptable.

What conclusions can be drawn regarding the choice of an optical instrument for the mission of studying TLE lightning based on all of the above analysis:

- Unfortunately, many of the technical parameters of listed instrument were not publicly available. The tools used on large satellites are distinguished by high technical properties however they are among the excluded devices due to exceeding weight and dimensions.
- Camera should be in CCD or CMOS type; the appropriate pixel size is around 508x1080. It should have a high shutter time quantity with at least 25 frame per second related parameter. ISO of the camera should be min 1200, the higher the better. The temperature range is allowed within 0-40 (like NICON D4). The desired maximum payload power consumption is 10 watts. The dimensions of the device can vary with respect to the design of the nanosatellite, which can take on a different shape depending on the number of modules, where each module is 10x10x10 cm. Particular attention should be paid to such an element as Photomultiplier tube on the base of different Hamamatsu type photodiode, which, as the study showed, was used in several missions with successful results.
- Among the instruments most suitable for the mission are MTEL from Tatiana-2, MTEL-2 from RELEC mission, Watec 100N and Watec 902H from Israel mission and high-speed camera Phantom v7.3 according to the available parameters.

Satellite	Model	Number	Spectral bands	Bandwidth	FOV	Time resolution	Power	Volume	Mass	Energy range
ASIM	MMIA photometer	3	180-230 nm 337 nm (limb) 337 nm (nadir) 391.4 nm 650-740 nm 236.6 nm 145-250 nm	5.0 5.0 5.0 5.0 90 5.0 broadband	20x20 lim or ram 80x80 nadir	100 kHz	N/A	N/A	N/A	N/A
FORMOSAT-2	Array Photometer in ISUAL	2	150-280 nm 250-390 nm 337 nm 427.8 nm 623-750 nm 777.4 nm	N/A	22x3.6 deg	2 kHz	N/A	N/A	N/A	N/A
	6-chanel spectrometer	1	150-280 nm 337 nm 391.4 nm 624-750 nm 777.4 nm 244-392 nm	140nm 5.6 nm 4.2 nm 126.7 nm 7.9 nm 148.2 nm	20x5 deg	10kHz	N/A	N/A	N/A	N/A
TARANIS	Photometer	4	PH1 170-260 nm PH 232-342 nm PH3 757-767 nm PH4 600-900 nm	N/A	500x500 km	20kHZ	3.5 W	205x125x200 mm	2.5 kg	N/A
	Spectrometer	2	N/A	N/A	60 deg (nadir) 30 deg (opposite nadir)	N/A	N/A	N/A	N/A	70kev-4Mev
Tatiana-2	Spectrometer	1	314-378 nm 600-1000 nm	N/A	160x160 km	N/A	N/A	N/A	N/A	N/A
	NUV+R detector (with R1463 Hamamatsu PMT)	1	300-400 nm (NUV) 600-700 nm (Red)	N/A	32 deg	N/A	N/A	N/A	N/A	N/A
Chibis_M	DUV	1	180-400 nm (UV) 650-800 nm (IR)	N/A	N/A	30 µs	N/A	N/A	N/A	N/A
RELEC	DUV (with R1463 Hamamatsu PMT)	1	240-400 nm (UV) 610-800 nm (Red)	N/A	N/A	N/A	2.5 W	130x95x65 mm	0.7 kg	N/A
Sprites-99	Photometer (with R374 Hamamatsu PMT)	1	185-850 nm	N/A	N/A	1kHz	N/A	N/A	N/A	N/A

Table 7. List of photometers, spectrometers and DUV detectors from TLE detection missions and their parameters.

Based on the above illustrated table 7, conclusions can be drawn regarding the most common parameters for the detection of TLE by photometers, spectrometers and DVU detectors. It can be seen that the most favorable spectral ranges for these instruments are NUV, UV and Red, IR bands, to be specific 150-280 nm, 250 - 390nm, 623-750nm, 337nm, 777.4nm. In most cases, the FOV of a photometer or spectrometer repeats the FOV of an optical instrument used on the same satellite. The parameters of power consumption, dimensions, as well as the weight indicator of used examples correspond to the ranges of allowed norms for nanosatellites. This is because, unlike optical instruments, this type of devices is more economical in resource consumption. Also, from the table it is clear that such an indicator as time resolution varies greatly from 1 kHz till 100kHz. Considering the millisecond duration of the studied phenomena, the higher the rate of re-exploring of the incoming signal, the higher the probability of event detection. Moreover, different models of Hamamatsu PMT are an integral part in most of the listed instruments as their overlapping photodiode technique provides the opportunity of not only detection but also localization of the lightning flashes. Among the examples studied, the only parameter characterizing the spectrometer was the energy rate of spectrometer on TARANIS satellite. It varies in the range between 70kev to 4Mev.

One of the principles of lightning investigation from space is the magnetic field and the electric field measurements. Typically, those measurements are gathered with the help of antenna type sensors.

Satellite	Model	Number	Power	Dimentions	Mass	Electric field
TARANIS	IME-BF	1	N/A	N/A	N/A	from Dc to 3MHz ULF 0-64 hz VLF from few Hz to 20 kHz
	IME-HF	1	N/A	N/A	N/A	from few kHz up to 37 Mhz
RELEC	RFA	RF electric unit antenna	total 10 W	192x149x91.5 mm 54x26x66 mm	1.5 kg 0.2 kg	50 kHz - 15 Mhz
CHIBIS-M	RFA	1	N/A	N/A	N/A	20-50 Mhz
SPRITES-99	3-axis Double probe EM filed detector	1	N/A	0.4 m2 antenna	N/A	Dc-20 kHZ
Fire-Fly	VLF rceiver	1	0.18 W	N/A	104 g	500Hz - 500khz
	GBB	1 anenna	N/A	3m	350 g	N/A
LINSAT	GGB	3 antennas	<6W	N/A	500 g	20-40 Mhz

Table 8. RF instruments used in previously described missions and their main parameters.

According to the table of listed RF instruments one of the most important parameters is electric field range. It can be seen that electric field range varies generally in the diapason of 20 - 40 MHz and Dc - 20kHz. The parameters of power consumption and weight indicator of used examples correspond to the ranges of allowed norms for nanosatellites. Dimensions of the RF units typically

represented by 2 -3 m long 1 or 3 Gravity Gradient Boom antennas (GGB) plus the RF analyzer unit.

Furthermore, there are advantages of RF detection over optical detection of lightning, due to its capability to distinguish the verity of signatures while optical observations are limited in that option. Additionally, all electromagnetic waves are less affected by atmosphere [112], [111].

There is also a theory about obtaining the most complete research results through the combinatorial application of different types of tools, as complementary elements of the puzzle. Below is a table illustrating the fundamental differences in the efficiency of optical and RF principles.

	Optical	RF
Detect	Light (Current)	RF/HF/VHF/LF/VLF
Geo-location technique/ Required number of satellites:	CCD array/ 1 Satellite minimum	Time-of-arrival (TOA)/ 3 satellites minimum
Atmospheric effects	Scattering/attenuation	Least (Attenuation)
Ionospheric effects	No	Frequency dependent dispersion of signal (can be mitigated)
Lightning taxonomy	Cannot distinguish	Can distinguish CG, IC, RS, L and TIPPs, etc

Table 9. Advantages and disadvantages of optical and RF systems. [111]

All of these strengths together with information gathered in table gives a base to conclude that RF instrument is fundamental requirement for Cubsat payload dedicated for TLE detection mission. According to the instruments described and to the discussed analysis of their suitability, it can be suggested to equip the future CubeSat for TLE observations with any of free possible type of instruments or their combination that will meet the above derived requirements.

In addition, it is clear that from most of above mentioned and described either aircraft-based, carried on balloon neither space-based lightning location and detection systems cannot perform TLE observations without initially provided by ground-based weather monitoring systems information about location, approximate time, and other estimations of future predicted thunderstorms. That fact leads to the outcome necessity of triggering mechanism in the CubeSat payload.

Chapter 6 - Conclusion

Transient Luminous Events are one of the most recently investigated phenomena occurring above the thunderstorms. It is the name given to the group of widely varying electrical discharge having a colored luminous glimpse of flash and originated from "ordinary" lightning at the top of the active thunderstorm.
The interest in TLE events investigation is explained by its importance for a number of scientific purposes like chemical influence on climate, explanation of the lightning creation as well as influence to the global electric circuits. All the TLEs are sorted to groups of events called elves, sprites, halos, blue jets, blue starters, gigantic jets, trolls, gnomes, pixies and ghosts.

Ground, air and space-based lightning location and detection projects and systems are described with precise attention given to the carried payload instruments and results achieved.

Then ground-based and space-based techniques for lightning detection are explained. All the systems were capable to achieve their goals. However not every technique and instrument are suitable for the CubeSat type mission.

In order to make recommendations for CubeSat payload which is capable to detect and locate TLE type lightning from space, two similar nanosatellite projects were analyzed as well. Due to limited parameters of the CubeSat structure, instruments supposed to suit the following conditions: low cost, low power, low mass, low complexity, no redundancy availability.

Through the analysis of all the described instruments it can be concluded that observations of TLE can be performed with any of free possible type of instruments or their combination that will meet the following derived requirements:

1) Optical instrument should have next parameters:
   - NUV and IFR in the ranges from 300nm till 740 nm and specifically 777.4 nm spectral bands
   - CCD or CMOS type
   - Pixel resolution range around 508x1080 pixels
   - Spatial resolution of 160x160 km
   - High ISO parameter >1200, low shutter time
   - At least 25 FPS
   - Operational temperature (0-40 C)
   - Power consumption <10 W
   - Dimensions can vary according to the number of nanosatellite Units

2) Spectrometer, Photometer or DUV detector should have next parameters:

- Spectral ranges for these instruments are NUV, UV and Red, IR bands, to be specific 150-280 nm, 250 - 390nm, 623-750nm, 337nm, 777.4nm
- FOV of a photometer or spectrometer can repeats the FOV of an optical instrument used on satellite
- Time resolution can vary from 1 kHz till 100kHz (higher better)
- Mostly recommended component is different models of Hamamatsu PMT (R374, R1463, R5900M64, S9195, S9736, 256 PMT, H7546A)
- Energy rate of spectrometer 70 kev to 4 Mev

3) RF type instruments should have next parameters:

- Electric filed rage of devise can vary between 20 - 40 MHz and Dc - 20kHz
- Low power and weight indicators
- Number of GGB antennas 1-3
- Typical RF antenna dimensions around 2-3 m

Furthermore, the advantages and disadvantages of RF detection and optic detection like short-latency, small antennas, low power requirements, ability of lightning taxonomy, ionospheric effects and geolocation techniques are listed. Another aspect which needs to be considered in payload choice is VHF frequency preference in comparison with LF frequency, as ionosphere penetration capability of the LF radio signal is lower than of the VHF signal.

Bibliography

1. Sentman, D. D., E. M. Wescott, D. L. Osborne, D. L. Hampton, and M. J. Heavner *"Preliminary results from the Sprites94 Aircraft Campaign."*, (1995), doi.org/10.1029/95GL00583.

2. R. C. Franz, R.J. Nemzek, J.R. Winckler, *"Television image of a large upward electric discharge above a thunderstorm system."* Science 249, 48–51: 1. Red sprites, Geophys. Res. Lett., DOI: 10.1126/science.249.4964.48

3. D. Siingh, S.Kumar, A.K. Singh,*"Thunderstorms/ Lightning Generated Sprites and Associated Phenomena*", e-Journal Earth Science India, Vol 3(II), April 2010, pp 124-145, ISSN: 0974-8350

4. Martin Fullekrug, E. Mareev, M. Rycroft., *"Sprites, elves and intense lightning discharges"* (2006), ISBN : 1-4020-4627-8

5. Victor P. Pasko , Yoav Yair , Cheng-Ling Kuo, *"Lightning Related Transient Luminous Events at High Altitude in the Earth's Atmosphere: Phenomenology, Mechanisms and Effects"* , June 2012, Space Science Reviews 168(1):1-42, DOI:10.1007/s11214-011-9813-9

6. Cathet, Copenhagen Center for Health Technology, *"New knowledge about thunderstorm effects on the climate"*, https://www.cachet.dk/news/nyhed?id=2A200E6D-3BBC-41F6-82C1-EEDDBE9BE4C3

7. Torsten Neubert, Nikolai Østgaard, Victor Reglero, Elisabeth Blanc, Olivier Chanrion, Carol Anne Oxborrow, Astrid Orr, Matteo Tacconi, Ole Hartnack6, Dan D.V. Bhanderi, *"The ASIM Mission on the International Space Station"* (2019), Space Science Reviews 215(2), DOI:10.1007/s11214-019-0592-z

8. A. Kostinskiy, T.C. Marchall, M. Stolzenburg*"The Mechanism of the Origin and Development of Lightning From Initiating Event to Initial Breakdown Pulses (v.2)"*, Novermber 2020, DOI:10.1029/2020JD033191

9. Djalel Dib, Mourad Mordjaouri, Zhour Abada *, "Contribution to the study of the aggression of lightning phenomenon on the wind turbine structures"*, February 2016, Wind Engineering 40(1):100-111, DOI:10.1177/0309524X15624615

10. Rutger Boonstra *"Validation of SAFIR/FLITS lightning detection system with railway-damage reports",* November 2007 – June 2008, Intern rapport ; IR 2008-05

11. Satoru Yoshida, Manabu Akita, Takeshi Morimoto, Tomoo Ushio1and Zen Kawasaki, *"Stepped leader characteristics in developing horizontally within thunderclouds and in descending out of thunderclouds" Osaka,* Japan (2011*),* DOI:10.1109/URSIGASS.2011.6050704

12. *"How does a lightning conductor work | Pthusics | Electrostatic grade 8-12"* https://www.youtube.com/watch?v=pBLo6nB5WBs

13. Cummings K., Murphy M., *"Overview of Lightning Detection in the VLF, LF and VHF Frequency Ranges",* (2008) USA

14. Danyal Petersen, William H. Beasley *"High-speed video observations of a natural negative stepped leader and subsequent dart-stepped leader"* 20 October 2013, doi.org/10.1002/2013JD019910

15. Joseph R. Dwyer, Martin A. Uman , *"The physics of lightning*" , 2013 , Vol 534, Issue 4, Pages 147-241, doi.org/10.1016/j.physrep.2013.09.004

16. "*Lightning Types and Classifications"*, Dan Robinson https://stormhighway.com/types.php

17. "*Types of Lightning*", the Weather Club, Royal Meteorological Society https://www.theweatherclub.org.uk/node/431

18. D.Robinson, "*LightningTypes and Classifications"*, https://archive.ph/20130411214534/http://stormhighway.com/types.shtml

19. "*Main types of lightning"*, Zefirka.net https://zefirka.net/2015/06/29/osnovnye-vidy-molnij/

20. *MetMatters, Royal Meteorological Society, "Types of Lightning"*, https://www.rmets.org/metmatters/types-lightning

21. "*What types of lightning does exist?',* Discovery, Alive Planet, http://animalworld.com.ua/news/Kakie_byvajut_vidy_molnij

22. *"Types of Lightning"*, Pikabu.ru https://pikabu.ru/story/vidyi_molniy_6022503

23. "*Different types of Lightning"*, AlabamaWX, Weather BLOG, https://www.alabamawx.com/?p=173831#:~:text=There%20are%20three%20primary%20types,to%20the%20positively%20charged%20ground

24. "*High Above Storm Clouds, Lightning Powers Terrestrial Gamma-Ray Flashes and Ultraviolet 'Elves'"*, SciTechDaily, https://scitechdaily.com/high-above-storm-clouds-lightning-powers-terrestrial-gamma-ray-flashes-and-ultraviolet-elves/

25. "*Sprites, blue jets, gigantic jets, elves – Upper Atmosphere Lightning"*, Severe weather Europe https://www.severe-weather.eu/theory/sprites-blue-jets-gigantic-jets-elves-upper-atmosphere-lightning/

26. "*Blue jets, Sprites and Elves formed by electrical activity above storm clouds | Colourful Weather"*, Youtube https://www.youtube.com/watch?v=Xp-8xp_3hqU

27. "*T.L.E ("TRANSIENT LUMINOUS EVENTS")"*, Thunderstorm http://la.climatologie.free.fr/orage/thunderstorm1.htm#orage5

28. *"Red Sprites"*, Internet Archive, Wayback Mashine https://web.archive.org/web/20070320222916/http://www.spritesandjets.com/sprites.htm

29. "*Red Sprites, Blue Jets and Elves",* https://www.albany.edu/faculty/rgk/atm101/sprite.htm

30. "*Photo from Angela Hague"*, Pinterest https://www.pinterest.com/pin/485544403549632835/

31. D.R. Moudry, M.J. Heavner, D. D. Sentman, E.M. Wescott, J.S. Morrill, and C. Siefring, *"Morphology of Sprites",* (1998)

32. E. A. Bering III, J. R. Benbrook, J.A. Garrett, A.M. Paredes, E.M. Wescott, D.R. Moudry, D.D. Sentman, H.C. Stenbaek-Nielsen, W.A. Lyons, *"Sprite and elve electrodynamics"* , November 2002, Advances in Space Research 30(11):2585-2595 , DOI:10.1016/S0273-1177(02)80350-7

33. Christopher P. Barrington-Leigh, U. S. Inan, *"Elves Triggered By Positive and Negative Lightning Discharges"* April (1999), DOI: 10.1029/1999GL900059, ISBN: 1944-8007

34. G. M. McHarg, R.K.Haaland, D.Moudry, H.C. Stenbaek-Nielsen "*Altitude-time development of sprites",* 15 November 2002, doi.org/10.1029/2001JA000283

35. Matt Heavner, *"Optical Spectroscopic Observations of Sprites, Blue Jets, and Elves: Inferred Microphysical Processes and their Macrophysical Implications"* May (2000), Physics, Environmental Science, Corpus ID: 117845103

36. "*Red sprites and blue jets",* THE EUROPEAN SPACE AGENCY http://www.esa.int/ESA_Multimedia/Videos/2016/04/Red_sprites_and_blue_jets

37. "*Facts about lightning",* Environment & Health Issues https://enviromentandhealthissuesworldwide.wordpress.com/2019/08/21/facts-about-lightning/

38. "*50 Awesome Natural Phenomena That Will Blow Your Mind",* Fact Republic, https://factrepublic.com/50-awesome-natural-phenomena-that-will-blow-your-mind/

39. "*What's up in space",* Space Weather, https://www.spaceweather.com/archive.php?day=17&month=08&year=1915&view=view&PHPSESSID=d6kcp0t22h4ijgei605ed08vv2

40. Water Science School "*Satellite view of cumulonimbus cloud over Africa",* February 5, 2008 https://www.usgs.gov/media/images/satellite-view-cumulonimbus-cloud-over-africa

41. "*Red Sprites and Blue JetsExplained – New Discovery!",* Youtube https://www.youtube.com/watch?v=tGPQ5kzJ9Tg

42. "*Introducing, the Green Ghost",* Space Weather Archive https://spaceweatherarchive.com/2020/05/31/introducing-the-green-ghost/

43. "*ASIM background information, facts and partners"*, DTU Space, National Space Institute, https://www.space.dtu.dk/english/research/projects/project-descriptions/asim/background-on-asim

44. "*Atmosphere-Space Interactions Monitor" (ASIM),* Birkeland Center For Space Science, https://birkeland.uib.no/atmosphere-space-interactions-monitor-asim/

45. Torsten Neubert, Victor Reglero, Nikolai Ostgaard, Elisabeth Blanc, *"The ASIM Mission on the International Space Station"* , March (2019), Space Science Reviews 215(2), DOI:10.1007/s11214-019-0592-z

46. "*ISS Utilization ASIM"*, Sharing Earth Obseration Resource, https://directory.eoportal.org/web/eoportal/satellite-missions/i/iss-asim

47. Signs Of The Times, *"Thor experiment captures rare footage of electric 'blue jets' in the space"*, 10 February 2017, https://www.sott.net/article/342221-THOR-experiment-captures-rare-footage-of-electrical-blue-jets-in-space

48. Alice Michel, Carla Jacobs, Geraldine Mariën, Olivier Chanrion, Torsten Neubert, *"What Happens Above Thunderstorms: First Operational Concept and Lessons Learned from the THOR Experiment during the Short Duration Mission on-board the International Space Station"*, (2017), 68th International Astronautical Congress (IAC), Australia, 25-29 September 2017, IAC-17,B6,3,9,x41029

49. "*THOR - What Happens Above Thunderstorms? (National Contribution)"*, Erasmus Experiment Archive, http://eea.spaceflight.esa.int/portal/exp/?id=9501

50. Olivier Chanrion, Torsten Neubert, Andreas Morgensen, Yoav Yair, Martin Stendel, Rajesh Singh, and Devendraa Siingh, *"Profuse activity of blue electrical discharges at the tops of thunderstorm"*, 23 December 2016, doi.org/10.1002/2016GL071311

51. Cheng-Chien Liu, *"Processing of FORMOSAT-2 imagery for site surveillance"*, December 2006, IEEE Transactions on Geosience and remote Sencing, 44(11):3206-3214, DOI:10.1109/TGRS.2006.880625

52. Kun-Shan Chen, An-Ming Wu, Jeng-Shing Chern, Liang-Chien Chen, and Wen-Yen Chang, *"FORMOSAT-2 Mission: Current Status and Contribution to Earth Observations"*, (June 2010), DOI:10.1109/JPROC.2009.2035355

53. Yein-An Lion, An-Ming Wu, Hsuan-Yu Lin, *"Formosat -2 Quick Imaging"*, (January 2015), DOI: 10.1002/9781118945179.ch17

54. "*FormoSat-2 / ROCSat-2 (Republic of China Satellite-2*)", Sharing Earth Obseration Resource, https://directory.eoportal.org/web/eoportal/satellite-missions/f/formosat-2#launch

55. CNES Projects Library, "*TARANIS"*, ONES Centre National Detudes Spatiales, https://taranis.cnes.fr/en/TARANIS/index.htm

56. Pierre Spizzi, "TARANIS : *"Myriade small satellite for TLE observation, 8 instruments challenge"* , France, (32th Annual AIAA/USU Conference on Small Satellites) , published 2018, Environment Science , Corpus ID: 54579485

57. F. Lefeuvre, E. Blanc , J.L. Pincon and TARANIS Team, "*TARANIS- a Satellite Dedicated to the Physics of the TLEs and TGFs"*, 05 May 2009, doi.org/10.1063/1.3137711

58. *"TARANIS" (Tool for the Analysis of RAdiations from lightNIngs and Sprites)*, Sharing Earth Obseration Resource, https://earth.esa.int/web/eoportal/satellite-missions/t/taranis

59. *"TARANIS"*, LPC2E, https://www.lpc2e.cnrs.fr/en/scientific-activities/plasmas-spatiaux/projects/space-missions/taranis/

60. Elisabeth Blanc, P. L. Blelly, E.Seran, *"TARANIS — Scientific payload and mission strategy"*, (September 2011), DOI:10.1109/URSIGASS.2011.6050938

61. Carl L, Jeff S. Morrill, David D., Sentman and Mattew J. Heavner. *"Simultaneous near-infrared and visible observations of sprites and acoustic – gravity waves during, the EX-98 campaign."*, 09 October 2010, doi.org/10.1029/2009JA014862

62. *"Balloon Experiments Reveal New Information About Sprites"*, Moon Daily, the discovery, exploration and application of luna https://www.moondaily.com/reports/Balloon_Experiments_Reveal_New_Information_About_Sprites_.html

63. Wescott, E. M., et al., *"Triangulation of sprites, associated halos and their possible relation to causative lightning and micrometeors",* Journal of Geophysical Research Atmospheres, 106(A6):10467-10477, (June 2001), DOI:10.1029/2000JA000182

64. *"The Sprites 99 Balloon Campaign",* https://uh.edu/research/spg/agu98eab/index.htm

65. E. A. Bering III, J. R. Benbrook, J. A. Garrett, A. M. Paredes, E. M. Wescott, D. R. Moudry, D. D. Sentman, H. C. Stenbaek-Nielsen, W. A. Lyons *"The electrodynamics of sprites"* , (March 2002), Geophysical Research Letters 29(5), DOI:10.1029/2001GL013267

66. Jeremy Thomas, *"A New High-Voltage Electric Field Instrument for Studying Sprites"* (2004) IEEE Transactions on Geoscience and Remote Sensing 42(7):1399-1404, DOI:10.1109/TGRS.2004.826806

67. "*UW Sprite Balloon Experiment 2002",* https://earthweb.ess.washington.edu/space/AtmosElec/project.html

68. *"Sprite detection, development by University of Washington*" (UW)/ INPE/ Utah State Univerasity, Balloon launched on 3/6/2003, from Balloon Launch Sector, Cachoeira Paulista, Brazil: http://stratocat.com.ar/fichas-e/2003/CAP-20030306.htm

69. M. J. Taylor, P.-D. Pautet, M. Bailey, Logan, Utah R. H. Holzworth, J. N. Thomas, M. C. McCarthy, F. Sao Sabbas, O. Pinto Jr INPE, M. Sato, H. Fukunishi and K. Yamamoto, *"Coordinated investigations of sprite characteristics and energetics over Brazil"*

70. Hayakawa, M., T. Nakamura, Y. Hobara, and E. Williams (2004), *"Observation of sprites over the Sea of Japan and conditions for lightning induced sprites in winter"*, December 2003, DOI:10.1109/CEEM.2003.1282387

71. Yoav Yair, Colin Price b, Michal Ganot b, Eran Greenberg b, Roy Yaniv a,b, Baruch Ziv a, Yosef Sherez b, Adam Devir a, Jo'zsef Bór c, Gabriella Sátori, *"Optical observations of TLE associated with winter thunderstorm near the coast of Israel"* , (February 2009), Atmospheric Research 91(2-4):529-537, DOI:10.1016/j.atmosres.2008.06.018

72. Michal Ganot, Yoav, Yair, Baruch Ziv, Yosef Sherez , *"First detection of transient luminous events associated with winter thunderstorms in the eastern Mediterranean"* , (June 2007), Geophysical Research letters 34(12), DOI:10.1029/2007GL029258

73. David Applbaum, Gil Averbuch, Colin Price, Yoav Yair, Yochai Ben-Horin, *"Infrasound observations of sprites associated with winter thunderstorms in the eastern"*, Atmospheric Research, Vol 235, 1 May 2020, 104770, doi.org/10.1016/j.atmosres.2019.104770

74. J. Montanyà, O. van der Velde, D. Romero, V. March, G. Solà, N. Pineda, M. Arrayas, J. L. Trueba, V. Reglero, and S. Soula *"High-speed intensified video recordings of sprites and elves over the western Mediterranean Sea during winter thunderstorms"*, April 2010, Journal of Geophysical Research Atmospheres 115(A4), DOI:10.1029/2009JA014508

75. Bracewell, R. N., and T. W. Straker (1949), *"The study of solar flares by means of very long radio waves"*, Monthly Notices of the Royal Astronomical Society, Volume 109, Issue 1, February 1949, Pages 28–45, doi.org/10.1093/mnras/109.1.28

76. Moore, C. R., C. P. Barrington-Leigh, U. S. Inan, and T. F. Bell, *"Early/fast VLF events produced by electron density changes associated with sprite halos",* (October 2003), Journal of Geophysical Research Atmospheres 108(A10), DOI:10.1029/2002JA009816

77. Johnson 2000 Johnson, M. P., and U. S. Inan (2000), *"Sferic clusters associated with early/fast VLF events",* Geophysical. Research Letters, Vol. 27(Issue 9), p. 1391 – 1394, doi.org/10.1029/1999GL010757

78. S. Soula, J. Montanya, D. Romero, O. Chanrion, T. Neubert, N. Pineda, F. Gangneron, Y. Meyerfeld *"TLEs Observations during the summer and fall Eurosprite 2007 campaign in South-Western France and North-Eastern Spain"* (2008)

79. *"Tatiana-2/Universitetsky-2",* EO Sharing Earth Observation Resources https://directory.eoportal.org/web/eoportal/satellite-missions/t/tatiana-2#:~:text=The%20Tatiana%2D2%20spacecraft%20finished,attitude%20failure%20of%20the%20spacecraft.&text=Tatiana%2D2%20has%20measured%20more,3%20months%20of%20its%20operation.&text=%2D%20The%20total%20and%20peak%20UV,%E2%80%9Ctrigger%20effect%E2%80%9D%20was%20analyzed.

80. G.K. Garipov, B.A. Khrenov, P.A. Klimov, V.S. Morozenko, *"Program of transient UV event research at Tatiana2 satellite"*, (May 2010), Journal of Geophysical Reserch Atmospheres 115(5), DOI:10.1029/2009JA014765

81. G.K. Garipov, B.A. Khrenov, P.A. Klimov, V.S. Morozenko, M.I. Panasyuk, V.I. Tulupov, V.M. Shahparonov, S.A. Sharakin, S.I. Svertilov, N.N. Vedenkin, I.V. Yashin, H.I Salazar, O.B. Martinez, E.L. Ponce, J.P. Cotsomi, I.H. Park *"UV And Red-IR Radiation Flashes Energy Characteristics Measured by UV&IR Detector On-Board "Universitetsky-Tatiana-2" Satellite." (2010)*

82. *"Chibis-M Microsatellite Mission"*, EO Sharing Earth Observation Resources, https://directory.eoportal.org/web/eoportal/satellite-missions/c-missions/chibis-m

83. L. M. Zelenyia , A. V. Gurevichb , S. I. Klimova , V. N. Angarova , O. V. Batanova , A. V. Bogomolovc , V. V. Bogomolovc , L. Bodnare, † , D. I. Vavilova

, G. A. Vladimirovaa , G. K. Garipovc , V. M. Gotliba , M. B. Dobriyana , M. S. Dolgonosova , N. A. Ivlevg , A. V. Kalyuzhnyia , V. N. Karedina , S. O. Karpenkog , V. M. Kozlova , I. V. Kozlova , V. E. Korepanovd , A. A. Lizunovh , A. A. Ledkova , V. N. Nazarova , M. I. Panasyukc , A. P. Papkovf , V. G. Rodina , P. Segedie , S. I. Svertilovc , A. A. Sukhanova , Ch. Ferenze , N. A. Eysmonta , and I. V. Yashina *"The Academic Chibis-M Microsatellite"* (2013) , (March 2014), Cosmic Research 52(2):87-98, DOI:10.1134/S0010952514010110

84. B.A. Khrenov, P.A. Klimov, M.I. Panasyuk, S.A. Sharakin, L.G. Tkachev, M.Yu. Zotov, S.V. Biktemerova, A.A. Botvinko, N.P. Chirskaya, V.E. Eremeev, G.K. Garipov, V.M. Grebenyuk, A.A. Grinyuk, S. Jeong, N.N. Kalmykov, M. Kim, M.V. Lavrova, J. Lee, O. Martinez, I.H. Park, V.L. Petrov, E. Ponce, A.E.Puchkov, H. Salazar, O.A. Saprykin, A.N. Senkovsky, A.V. Shirokov, A.V. Tkachenko, I.V. Yashina, *"First results from the TUS orbital detector in the extensive air shower mode"*, (April 2017), Journal of Cosmology and Austroparticle Physics 2017(09), doi:10.1088/1475-7516/2017/09/006

85. Ji Eun Kim, Jik Lee, A.H. Park, G. K. Garipov, B. A. Khenov & M. I. Panasyuk, *"Development of TUS pinhole cameras for observing transient luminous events from space and establishing role of those events as a background for ultra-high-energy cosmic-ray measurements."* Journal of the Korean Physical Society 64, 672-678, (February 2014), DOI:10.3938/jkps.64.672

86. E. Ponce, G. Garipov, B. Khrenov, P. Klimov, H. Salazar, *"Pinhole camera for study of atmospheric UV flashes as a source of background in the TUS experiment"*, (May 2011), Nuclear Instruments and Methodsin Physics Research A Accelerators Spectrometers Detectors and Associated Equipment 639(1):77-78, DOI:10.1016/j.nima.2010.10.100

87. D.V. Skobeltsyn Institute of Nuclear Physics of M.V. Lomonosov Moscow State University *"Experiment RELEC onboard the Vernov spacecraft"* The results of scientific research on completed space missions obtained by Russian scientists in 2014-2015, bibcode: 2015EGUGA..17.5122S

88. M.I. Panasyuk, S.I. Svertilov, V.V. Bogomolov, G.K. Garipov, E.A. A.V. Bogomolov, I.N. Myagkova, P.A. Klimov, A.V. Prokhorov; S.I. Klimov, T.V. Grechko, V.A. Grushin, D.I. Vavilov, V.E. Korepanov, S.V. Belyaev, A.N. Demidov ,Cs. Ferencz ; L. Bodnár, P. Szegedi ,H. Rothkaehl, M. Moravski , *"Observation of TGFs and Relativistic Electron Precipitation in RELEC experiment on-board Vernov Mission"* (2015) 5-th International TEPA Symposium, INIS Volume 47, INIS Issue 45, Reference number 47111656

89. , M. I. Panasyuk, V. V. Bogomolov, G. K. Garipov, O. R. Grigoryan, Y. I. Denisov, B. A. Khrenov, P. A. Klimov, L. L. Lazutin, S. I. Svertilov, N. N. Vedenkin,I. V. Yashin, S. I. Klimov, L. M. Zeleny, V. S. Makhmutov, Y. I. Stozkov,N. S. Svirzhevsky, V. V. Klimenko,E. A. Mareev,Y. V. Shlyugaev,V. E. Korepanov, I. H. Park, H. I. Salazar, and H. Rothkaehl, *"Transient luminous event phenomena and energetic particles impacting the upper atmosphere: Russian space experiment programs"* (2010) Journal of Geophysical Researche, Vol. 115, A00E33, doi:10.1029/2009JA014763

90. Svertilov, *"The Results of TGFs and TLEs Observations in RELEC Experiment on board Vernov Space Mission"* Skobel'tsyn Institute of Nuclear Physics of Lomonosov, S.A. Lavochkin, Scientific and Production Association., Russia

91. J. Nash, N.C. Atkinson, E. Hibbett, G. Callaghan, P.L. Taylor, P. Odams, D. Jenkins, S. Keogh, C. Gaffard and E. Walker Met Office, Exeter, UK *"The new Met office ATDNET lightning for detection system"*, (January 2006)

92. "Swati Sharma, Shoba Krishnan, Ajay Khandare, *"Orthogonal Magnetic Loop Antenna for Lightning Detection"* (2014), International Journal of Application or Innovation in Engineering & Management, ISSN 2319-4847

93. Ushio, T., Z. Kawasaki, Y. Ohta, and K. Matsuura, *"Broadband interferometric measurement of rocket triggered lightning in Japan",* Geophys. Res. Lett., Vol. 24(Issue 22), pp. 2769–2772, (15 November 1997), doi.org/10.1029/97GL02953

94. Kawasaki, Z-I., R. Mardiana, T. Ushio, *"Broadband and narrow band RF interferometers for lightning observation",* Geophysical Research Letters, Vol. 27(Issue 19), pp. 3189-3193, (1 October 2000), doi.org/10.1029/1999GL011058

95. Takeshi Morimoto, Zen Kawasaki, *"VHF Broadband Digital Interferometer"* IEEJ Trans 2006; 1: 140–144, ISBN:0-7803-8404-0, DOI: 10.1109/APRASC.2004.1422589

96. T. Ushio, Z -I. Kawasaki, M. Akita, S. Yoshida, T. Morimoto, Y. Nakamura, *"A VHF broadband interferometer for lightning observation"*, (20 October 2011), DOI: 10.1109/URSIGASS.2011.6050771

97. Takeshi Morimoto, Hiroshi Kikuchi, Mitsuteru Sato, Tomoo Ushio, Atsushi Yamazaki, Makoto Suzuki, Ryohei Ishida, Yuji Sakamoto, Kazuya Yoshida, Yasuhide Hobara, Takuki Sano, Takumi Abe and Zen-Ichiro Kawasaki, *"An overview of VHF lightning observations by digital interferometry from ISS/ JEM-GLIMS"* Morimoto et al. Earth, Planets and Space 68(1) (December 2016), DOI:10.1186/s40623-016-0522-1

98. E. Philip Krider, Carl Noggle, Martin A.Uman, *"A Gate , Wideband Magnetic Direction Finder for Lightning Return Strokes"* (April 1976), Journal of Applied Meteorology15(3), DOI:10.1175/1520-0450(1976)015<0301:AGWMDF>2.0.CO;2

99. *"Lightning strikes detection methods"* Osclar, http://193.2.45.87/en/sistem/metode-zaznavanja-strel/

100. Ammar Al-Ammari, Ammar Ahmed Alkahtani, Mohd Riduan Ahmad, Fuad Numan, *"Lightning Mapping: Techniques, Challenges, and Opportunities"*, (October 2020), DOI:10.1109/ACCESS.2020.3031810

101. Gerhard Diendorfer *"Lightning location systems (LLS)".* OVE-ALDIS Vienna, Austria (30th November 2007) For do Iguacu , Brazil , IX International Symposium on the Lightning Protection

102. *"Satellite: OrbView-1/MicroLab"* OSCAR, Observing Systems Capability Analysis and Review Toll, http://www.wmo-sat.info/oscar/satellites/view/309

103. *"ISS Utilization: LIS (Lightning Imaging Sensor)"* EO Sharing Earth Observation Resources.https://directory.eoportal.org/web/eoportal/satellite-missions/content/-/article/iss-utilization-lis

104. *"Instruments: Geostationary Lightning Mapper"*, Goes-R https://www.goes-r.gov/spacesegment/glm.html

105. S.J. Goodman, R. Blakeslee, M. Douglas, W. Koshak *"The Geostationary Lightning Mapper (GLM) for the GOES_R Series of Geostationary Satellitres"*, 30 April 2012, Document ID 20120015474

106. A.Rakov, *"Lightning electric and magnetic fields"* University of Florida, Gainesville, FL, USA, January 1999, Physics, Corpus ID: 35660902

107. *"FireFly CubeSat"* Spaceflight101.com Space News and Beyond https://spaceflight101.com/spacecraft/firefly/

108. *"Firefly - Space Science on a Nanosatellite"*, Missions database https://directory.eoportal.org/web/eoportal/satellite-missions/f/firefly

109. D.E. Rowland, J. Hill, P. Uribe, J. Klenzing, F. Hunsaker , M. Fowle, T. Cameron, K. Simms, H. Hancock, M. Saulino, D. Guzman, S. Kholdebarin, L. Ramsey, A. Willingham, *"The NSF Firefly CubeSat mission: Rideshare mission*

to study energetic electrons produced by lightning", NASA Goddard Space Flight Center , 5-12 March 2011, ISBN: 978-1-4244-7351-9, DOI: 10.1109/AERO.2011.5747231

110. Ghulam Jaffer, Hans U. Eichelberger, Konrad Schwingenschuh and Otto Koudelka, "*A LEO Nano-Satellite Mission for the Detection of Lightning VHF Sferics*", Institute of Communication Networks and Satellite Communications Graz University of Technology, Graz Space Research Institute, Austrian Academy of Sciences, Graz Austria, (June 2011), DOI:10.5772/16677

111. Ghulam Jaffer, M.Sc., *"Study of an Austrian Lightning Nano-Satellite (LiNSAT): Space and Ground Segments."* Graz, Austria, 2011

112. Suszcynsky, D. M., M. W. Kirkland, et al. (2000), *"FORTE observations of simultaneous VHF and optical emissions from lightning: Basic phenomenology.*" Journal of Geophysical Research-Atmospheres 105(D2): pp 2191-2201, DOI:10.1029/1999JD900993

113. Rock Jeng-Shing Chen, Shin-Fa Lin, An-Ming Wu, *"Ten-year transient luminous events and Earth observations of FORMOSAT-2"* , Vol. 112, July–August 2015, Pages 37-47 , DOI:10.1016/j.actaastro.2015.02.030

114. Alfred B Chen, Cheng-Ling Kuo, Yi-Jen Lee, Han-Tzong Su , *"Global distributions and occurrence rates of transient luminous events"*, August 2008 , Journal of Geophysical Research Atmospheres 113(A8) , DOI: 10.1029/2008JA013101

115. RocketGyan, *"[Launch 30:59] Vega Rocket Failed | Arianespace & ESA VV17 Mission| SEOSAT-Ingenio & Taranis" ,* https://www.youtube.com/watch?v=zH6Ni9QKufM&ab_channel=RocketGyan

116. Stephen Clark, "SpaceFlight Now" news, *"Arianespace traces cause of Vega launch failure to 'human error"*, November 12, 2020, *https://spaceflightnow.com/2020/11/17/arianespace-traces-cause-of-vega-launch-failure-to-human-error/#:~:text=Engineers%20concluded%20that%20cables%20leading,Lagier%2C%20Arianespace's%20chief%20technical%20officer.*

117. P.A. Klimov, G.K. Garipov, A.A. Grinyuk, B.A. Khrenov, M.I. Panasyuk, V.S. Morozenko, S.A. Sharakin, A.V. Shirokov, L.G. Tkachev, A.V. Tkachenko, I.V. Yashin, *"Analysis of UV flashes measured by Universitetsky-Tatiana-2 satellite as signifi- cant factor of TUS detector operation"*, 33rd International Cosmic Ray

Conference , Rio De Janeiro 2013, The Astroparticle Physics Conference, Physics, Environment Science, Corpus ID: 165152656

118. G. K. Garipov, B.A. Khrenov, P.A. Klimov, V.V. Klimenko, E.A. Mareev, O. Martines, V.S. Morozenko, M.I. Panasyuk, I.H. Park, E. Ponce, H. Salazar, V.I. Tulupov, N.N. Vedenkin, I.V. Yashin , *"Global Transients in ultraviolet and red-infrared ranges from data of the "Universitetsky- Tatiana-2" satellite",* 25 January 2013, doi.org/10.1029/2012JD017501

119. S.I. Klimov, Cs. Ferencs, L.Bodnar, P. Szegedi, P. Steinbach, V.M. Gotlib, , D.I. Novikov, S. Belyayev, A. Morusenkov, O. Ferencs, V. Korepanov, J. Lichtenberger, D. Hamar, *"First results of MWC SAS3 electromagnetic wave experiment on board of the CHIBIS-M satellite"*, Vol 54, Issue 9, November 2014, Pages 1717-1731, doi.org/10.1016/j.asr.2014.06.044

120. S.I. Klimov, L.M. Zelenyi, V.N. Angarov, V.M. Gotlib, N.A. Elismont, M.S. Dolgonosov, V.N. Karedin, D.I. Novikov, D.I. Vavilov, M.I. Panasyuk, V.E. Korepanov, D.F. Dudkin, Cs. Ferencs, P. Szegedi, *"Microsatellite "Chibis-M" (25.01.2012 – 15.10.2014) Results, lessons and prospects"* , April 2015, Conference: 10th IAA Symposium on Small Satellites for Earth Observation, 20-24 April 2015 , Berlin, Germany

121. A.J.Bedard, Jr., W.A.Lyons, R.A.Armstrong, T.E.Nelson, B.Hill, and S. Gallagher *"A search for low-frequency atmospheric acoustic waves associated with sprites, blue jets, elves, and storm electrical activity"* AGU, 80(46), Fall Meeting (1999)

122. L. Liszka and Y. Hobara, *"Sprite-attributed infrasonic chirps-their detection, occurrence and properties between 1994 and 2004,"* J. Atmos. Solar-Terrestrial Phys., vol. 68, no. 11, pp. 1179–1188, 2006, DOI: 10.1016/j.jastp.2006.02.016

123. Mohamed Khalaf-Allah , "*Time of Arrival (TOA)-Based Direct Location Method",* published in: 2015 16th International Radar Symposium (IRS), Dresden, Germany, doi: 10.1109/IRS.2015.7226229, ISBN:978-3-9540-4853-3

124. P. Klimov, *"Recent results from the TUS/LOMONOSOV Space Mission",* Frascati Physics Series Vol. 66 (2018), ISBN 978-88-86409-67-4

125. M.I. Panasyuk, S.I. Svertilov, V.V. Bogomolov, G.K. Garipov, E.A. Balan, V.O. Barinova, A.V. Bogomolov, I.A. Golovanov, A.F. Iyudin, V.V. Kalegaev, B.A. Khrenov, P.A. Klim, A.S. Kovtyukh, E.A. Kuznetsova, V.S. Morozenko, O.V. Morozov, I.N. Myagkova, V.I. Osedlo, V.L. Petrov, A.V. Prokhorov, G.V. Rozhkov, K.Yu. Saleev, E.A. Sigaeva, N.N. Veden'kin, I.V. Yashin, S.I.

Klimov, T.V. Grechko, V.A. Grushin, D.I. Vavilov, V.E. Korepanov, S.V. Belyaev, A.N. Demidov, Cs. Ferencz, L. Bodna´r, P. Szegedi, H. Rothkaehl, M. Moravski f, I.H. Park g, J. Lee g, J. Kim g, J. Jeon g, S. Jeong g, A.H. Park g, A.P. Papkov, S.V. Krasnopejev, V.V. Khartov, V.A. Kudrjashov, S.V. Bortnikov, P.V. Mzhelskii, *"RELEC mission: Relativistic electron precipitation and TLE study on-board small spacecraft"*, Advances in Space Research, 2016, DOI: 10.1016/j.asr.2015.11.033, WOSUID: WOS:000369456400011

126. Global Hydrometeorology Resource Center, Lightning Space Search and Observations, *"Optical Transient Detector (OTD)"* - https://ghrc.nsstc.nasa.gov/lightning/overview_otd.html

127. H.J. Christian, R.J. Blakeslee, S.J. Goodman, D.A. Mach, M.F. Stewart, D.E. Buechler, W.J. Koshak, J.M. Hall, W.L. Boeck, K.T. Driscoll, D.J. Boccippio, *"The lightning imaging sensor"*, July 1999, Document ID 19990108789

128. Global Hydrometeorology Resource Center, Lightning Space Search and Observations, "Lightning Imaging Sensor (LIS)", https://ghrc.nsstc.nasa.gov/lightning/overview_lis_instrument.html#:~:text=The%20Lightning%20Imaging%20Sensor%20(LIS,during%20both%20day%20and%20night.

129. Nanosats Database, Firefly, https://www.nanosats.eu/sat/firefly

130. Mohamed Kameche, Haider Benzeniar, Ayhane Bey Benbouzid, Redha Amri, Nadir Bouanani , *"Disaster Monitoring Constellation Using Nanosatellites"*, February 2014 , doi: 10.5028/jatm.v6i1.281